Title
Mechanisms of Ubiquitin-Driven Cell Cycle Control

Author
Williamson, Adam

Publication Date
2012

Peer reviewed|Thesis/dissertation

Mechanisms of Ubiquitin-Driven Cell Cycle Control

By Adam Williamson

A dissertation submitted in partial satisfaction of the

requirements for the degree of

Doctor of Philosophy

in

Molecular and Cell Biology

in the

GRADUATE DIVISION

of the

UNIVERSITY OF CALIFORNIA, BERKELEY

Committee in charge:

Professor Michael Rape, Chair
Professor Kathleen Collins
Professor Rebecca Heald
Professor Arash Komeili

Abstract

Mechanisms of Ubiquitin-Driven Cell Cycle Control

by

Adam Williamson

Doctor of Philosophy in Molecular and Cell Biology

University of California, Berkeley

Professor Michael Rape, Chair

Posttranslational modification of proteins with ubiquitin, ubiquitylation, is essential in all eukaryotes. Ubiquitylation is accomplished by an enzymatic cascade: E1 activates ubiquitin and transfers it to E2, which works with E3 to transfer ubiquitin to substrate residues, usually lysines. Once attachment of the first ubiquitins to substrate, chain initiation, has occurred, E2 and E3 modify one of the seven lysine residues in ubiquitin itself, resulting in formation of polymeric ubiquitin chains, chain elongation. Ubiquitylation is involved in nearly every cellular process, and is central to cell cycle control. Ubiquitin-dependent protein degradation is especially important during mitosis, as cells must turn over many proteins within a short time-window. The anaphase-promoting complex (APC/C) is an essential E3 that targets cell cycle regulators for degradation during mitosis. The APC/C must degrade many substrates within a short period of time, and likely acts under saturation. Furthermore, APC/C substrates are required at different times during mitosis. Therefore, the APC/C cannot degrade all substrate at once, but rather must order substrate degradation so that substrate proteins can accomplish their functions. The balance between efficiency and regulated degradation is the APC/C's major challenge as it orchestrates mitotic exit.

In this dissertation I address how human APC/C targets its many substrates for degradation. First, I report our finding that APC/C functions by decorating its substrates with Lys11-linked ubiquitin chains. Lys11-linked chains target substrates to the 26S proteasome and are essential for cell division in human cells, *Drosophila* cells, and *Xenopus tropicalis* embryos. The human APC/C uses a dedicated E2, Ube2C/UbcH10, to perform chain initiation while a second E2, Ube2S, elongates these first modifications using exclusively Lys11 on ubiquitin. Ube2C and Ube2S likely function simultaneously, thus allowing APC/C to overcome its massive substrate workload. Efficient chain initiation by Ube2C is made possible by conserved initiation motifs in substrates. Initiation motifs do not regulate substrate binding to APC/C, but instead control the efficiency with which Ube2C and APC/C attach the first ubiquitin moieties to substrates. I will show that chain initiation by Ube2C is the rate-limiting, regulated step during Lys11-linked chain formation by the APC/C. Once Ube2C has initiated chains on APC/C substrates, Ube2S takes over, rapidly elongating Lys11-linked ubiquitin chains that target substrates to the 26S proteasome. Finally, I address how use of two E2 enzymes

performing different functions allows APC/C to overcome its major challenge: rapid yet regulated turnover of essential cell cycle regulators. The separation of ubiquitin chain formation by the APC/C into initiation and elongation steps, with initiation being rate-limiting and tightly regulated, draws parallels between ubiquitylation and other processive reactions such as transcription and translation.

For Levelt, may you now find peace

Table of Contents

Acknowledgments

I consider myself incredibly lucky to have performed by dissertation research in the MCB department at Berkeley. I have been part of a very special community here, the wonderful qualities of which will only become more clear as I have a chance to reflect on my time here.

I thank Professor Michael Rape for his mentorship during the past years. Michael, you possess a rare combination of enthusiasm, rigor, and brilliance that makes being in your lab truly a joy. I thank my dissertation committee, Professor Kathleen Collins, Professor Rebecca Heald, and Professor Arash Komeili for excellent guidance. I looked forward very much to my yearly meetings.

Watching the lab grow from just a few of us to nearly a dozen has been great fun, and I thank my lab-mates for teaching me so much and creating a positive, energetic, forward-looking scientific environment where the scientific discourse is never-ending and we work together to arrive at the best solutions and models. In particular, I have been lucky to work closely alongside the talented scientists Sudeep Banerjee, Kate Wickliffe, Lingyan Jin, Allison Craney, Hermann-Josef Meyer, Ling Song and Aileen Kelly.

I thank Indro Fedrigo for his time, collaborative spirit, energy, and patience in developing the computational platforms that make the current work we are doing in the lab possible.

Support and wisdom from friends collected over countless trips to Peets has been a gift. In particular, this run would have been a dull one without the companionship of Mike Bond, Brock Roberts, Nadine Jahchan, Malik Francis, Mary Matyskiela, Ann Fischer, and Pete Dillon.

Jody Lewen, Amy Roza, Maureen Lahiff, Jun Hamamoto, Sonal Singhal, Sarah Tahamont, and the Prison University Project at San Quentin: you allowed me to teach a wonderful group of motivated men Biology and Mathematics. I cherish the opportunities you have given me to develop as an instructor and as an individual. To the PUP students: You taught me more from you than I ever could have imparted, I wish you all the best of luck.

Ellen, thank you for your love and support. Building a life with you has been a joy and I look forward to discovering what our future holds. Anne, Eleanor and Patrick, I love you so very much.

Chapter 1

Introduction

The Ubiquitin System

Ubiquitin is essential in all eukaryotes and ubiquitylation is required for nearly every cellular process. Functions of ubiquitylation in the cell include clearing and degrading misfolded proteins in the endoplasmic reticulum, DNA repair, apoptotic signaling and cell cycle progression. Lesions in the ubiquitin system are found in a multitude human diseases including cancer, neurodegeneration, and developmental disorders (Amir et al., 2001).

Ubiquitylation is the attachment of a small protein, ubiquitin, to substrate proteins via an isopeptide linkage During repeated rounds of ubiquitylation proteins are modified with polymeric ubiquitin chains. Ubiquitylation requires an enzymatic cascade composed of E1s – ubiquitin-activating enzymes, E2s – ubiquitin-conjugating enzymes, and E3s – ubiquitin ligase enzymes (Dye and Schulman, 2007; Pickart, 2001; Schulman and Harper, 2009; Ye and Rape, 2009). These enzymes first catalyze formation of an isopeptide bond between the C-terminus of ubiquitin and a substrate residue, usually a lysine. Attachment of the first ubiquitin to substrate is called monoubiquitylation. One or more lysines on a substrate may be modified with ubiquitin and modification may occur at a defined single residue on the substrate – this is seen for the DNA-damage dependent modification of proliferating cell nuclear antigen (PCNA) (Hoege et al., 2002) or at many residues along a substrate's length, as seen for epidermal growth factor (EGFR) (Haglund et al., 2003).

After attachment of the first ubiquitin to substrate, one of the seven lysine residues on ubiquitin itself is modified, resulting in ubiquitin chains. The attachment of the first ubiquitin to substrate is chain initiation (chain nucleation) and attachment of further ubiquitins to these first modifications is chain elongation. Ubiquitin chains are recognized by factors associated with the 26S proteasome and targeted for degradation – the classical function of protein ubiquitylation (Finley, 2009). Alternatively, ubiquitin chains or ubiquitins on substrates may be recognized and cleaved by deubiquitylating enzymes (DUBs) therefore requiring the reactions be repeated for the desired outcome to occur (Reyes-Turcu et al., 2009).

Ubiquitin Chains Have Distinct Topologies that Determine Substrate Fate

Ubiquitin chains may be formed using only a single lysine residue resulting in ubiquitin chains of a single linkage (Lys11-, Lys48-, or Lys63-linked chains) or chains may have a mixed topology resulting from use of different lysine residues in ubiquitin to make the chain. A third option is that two or more lysine residues on ubiquitin may be used for chain elongation, resulting in a branched ubiquitin chain. All ubiquitin linkages have been detected in human cells (Peng et al., 2003; Xu et al., 2009). Lys48-linked ubiquitin chains are the canonical proteasome targeting signal while Lys63-linked ubiquitin chains are essential for signaling and are thought to be non-proteolytic (Dikic et al., 2009).

Results presented and discussed in the following chapters will cover the discovery of the Lys11-linked ubiquitin chain and its importance in cell cycle regulation in human cells. At the time this work was undertaken functions had only been described for Lys48- and Lys63-linked ubiquitin chains. While adding to the ubiquitin code is exciting, little is known about the function Lys6-, Lys27-, Lys29-, and Lys33-linked ubiquitin chains or

their substrates (Komander and Rape, 2012). While discussion in my dissertation will be limited to the mechanism of Lys11-linked chain formation in the context of cell cycle control, it will be fascinating to address questions of other linkages in the future and important to keep in mind as we move forward.

Advantages of Ubiquitin-Dependent Signaling

Ubiquitin-driven control of signaling systems is powerful for a number of reasons. First, degradation of a substrate by the proteasome is irreversible. In the context of cell cycle regulation or apoptosis this is important: though each reaction itself is reversible the outcome desired must be unidirectional. For instance once a cell has replicated its DNA in S-phase, mitosis should occur without fail since slipping back into a G1-like state and then proceeding through a second round of replication would result in polyploidy. Second, ubiquitin dependent signaling does not necessarily require transcription or translation of new factors. Therefore ubiquitin-dependent processes occur rapidly. Ubiquitin can be attached to substrates on the millisecond scale, and processive ubiquitylation enzymes can attach up to 13 ubiquitins in a chain in a single binding event (Pierce et al., 2009; Wickliffe et al., 2011). This signal is sufficient for proteasomal targeting and attached rapidly in processive fashion: repeated rounds of ubiquitylation on a substrate in a single binding event. This is essential for pathways including but not limited to cell cycle regulation, since transitions must occur within tight time windows.

Ubiquitylation and the Cell Cycle

The precise and controlled delivery of genetic material to daughter cells is essential in all organisms. Eukaryotic cells divide genetic material into two daughter cells during mitosis, orchestrated by a complex and carefully regulated program. Though cell cycle regulation may take place at any stage of the cell cycle, much of the regulatory focus is on mitosis, during which cells divide duplicated genetic material into daughter cells through a process characterized by dramatic structural rearrangements for the cell: namely nuclear envelope breakdown and condensation of chromosomes into a compressed form capable of transfer by the mitotic spindle. Many pathways control mitosis – including phosphorylation dependent activation pathways, checkpoints that ensure that only healthy cells divide, but protein degradation pathways are essential for control of the cell cycle. Consistent with the importance of the ubiquitin pathway and ubiquitin chain formation and degradation for division, interference with the 26S proteasome or inhibition of formation of Lys48- or Lys11-linked ubiquitin chains interferes with cell division in multiple organisms (Jin et al., 2008; Rodrigo-Brenni and Morgan, 2007).

Ubiquitylation enzymes and the cell cycle regulators have an intertwined history. Many essential regulators of cell division uncovered in saturating screens for cell cycle regulators are components of the ubiquitin system or regulated by these components (Hartwell et al., 1974). Components of Skp-Cullin-F-box (SCF) E3 ubiquitin ligases and subunits of the anaphase-promoting complex (APC/C) were discovered in these screens. Discovered factors that are subunits of ubiquitin ligases important for cell division include Cdc4 and Cdc34 (components of Skp-Cullin-F-box ligases, SCF) and Cdc16,

Cdc20, and Cdc27 (subunits of the anaphase-promoting complex, APC/C). The anaphase-promoting complex is essential in all eukaryotes and orchestrates mitotic progression. The human anaphase-promoting complex (APC/C) will be the focus of my dissertation.

The Anaphase-Promoting Complex (APC/C)

The anaphase-promoting complex (APC/C) is essential for establishing the timing of mitosis. The human APC/C is a 1.5 mDa E3 ubiquitin ligase comprised of at least 14 subunits, not counting its cognate E2s or inhibitors (Barford, 2011b). The APC/C is directly inhibited by the mitotic checkpoint complex (MCC) until all kinetochores are attached (Peters, 2006). The human APC/C targets substrates for degradation with the help of two co-activators, Cdc20 and Cdh1 (Peters, 2006). The APC/C is estimated to have more than 100 substrates (Meyer and Rape, 2011).

APC/C substrates cannot be degraded randomly during mitosis. Instead, the APC/C must accomplish ordered substrate degradation as its many substrates perform different functions. The APC/C substrate securin, for instance, must be degraded early in mitosis for sister chromatid separation to occur while factors such as Tpx2, Plk1, and Aurora B have functions later in mitosis, and therefore must be degraded much later. Therefore, while protein degradation an essential process in cell division it must be tightly regulated. Additionally, the APC/C targets its own E2s for degradation and given that these E2s are required for substrate degradation they must be stable until substrate degradation is accomplished. How substrate degradation by the human APC/C is accomplished and regulated will be the focus of my dissertation.

Substrate Binding and Ubiquitylation by APC/C

Substrates bind to E3 ubiquitin ligases via recognition motifs, or degrons. These degrons can be dynamic, as is the case for many SCF ubiquitin ligases. The substrate degron is created by phosphorylation (Ang and Harper, 2005). However, this process does not regulate binding of APC/C substrates - the recognition motifs depend on amino acid sequence, so are always present in the substrates. However, motifs may vary in their ability to support processive APC/C-dependent ubiquitylation (Rape et al., 2006; Williamson et al., 2011) or not always be accessible to the APC/C (Song and Rape, 2010). Consistent with the fact that its substrates that perform a wide-array of functions during different times of the cell cycle, there is no single mode of APC/C substrate binding and ubiquitylation (Barford, 2011a). Instead, APC/C substrates possess different motifs in varying combinations and properties that allow substrates to perform their functions while maintaining proteolytic control.

The classical APC/C recognition motif is the destruction box (D-box), RxxLxxI/VxN, a motif first characterized in cyclin B (Glotzer et al., 1991; King et al., 1996). A second APC/C motif, the KEN-box, KEN with a P close by, is present in many APC/C substrates, usually in addition to the D-box (Pfleger and Kirschner, 2000). The processivity of ubiquitylation of APC/C substrates varies - some substrates are ubiquitylated and targeted for degradation in a single binding event, while some come on and off the complex and are therefore ubiquitylated in distributive fashion (Rape et al.,

2006). Differences in the processivity of ubiquitylation is one mechanism by which the human APC/C accomplishes ordered degradation of its substrates and in large part is determined by the sequence of substrate recognition motifs. The APC/C also uses regulated chain initiation (nucleation) to regulate the timing of substrate degradation.

For full activity, the APC/C requires two E2 enzymes. Ube2C/UbcH10 is a traditional RING-finger binding E2 that works with the APC/C subunit Apc11 to transfer the first ubiquitins to substrates and forms short ubiquitin chains - chain initiation or nucleation (Jin et al., 2008; Rape and Kirschner, 2004; Williamson et al., 2011). Following addition of the first ubiquitin moieties to the substrate, human APC/C depends on a dedicated chain elongating E2, Ube2S, to modify ubiquitins on the substrate itself and target the substrate to the 26S proteasome (Wickliffe et al., 2011; Williamson et al., 2009; Wu et al., 2010). Efficient chain elongation by Ube2S is one of the mechanisms by which APC/C handles its enormous substrate workload.

Three outstanding problems are addressed in my dissertation. 1. How does APC/C form ubiquitin chains on its substrates? In Chapter 2, we use extracts from synchronized human cells and cultured cells to determine the mechanism of ubiquitin chain formation by the human anaphase-promoting complex. 2. How does APC/C regulate the timing of substrate degradation? In Chapter 3, we separate initiation from elongation and show that initiation is the regulated, rate-limiting step in substrate degradation. 3. How does APC/C handle its immense substrate workload? In Chapter 4, we report and characterize the dedicated chain elongation E2 Ube2S. Efficient elongation of initiated chains is an important mechanism by which APC/C targets its many substrates for degradation.

Chapter 2

Mechanism of Ubiquitin Chain Formation by the Human Anaphase-Promoting Complex

Lingyan Jin*, Adam Williamson*, Sudeep Banerjee, Isabelle Philipp, and Michael Rape
Cell (2008) *133*, 653-665

* equal contribution

Summary

The anaphase-promoting complex (APC/C) orchestrates progression through mitosis by decorating cell-cycle regulators with ubiquitin chains. To nucleate chains, the APC/C links ubiquitin to a lysine in substrates, but to elongate chains it modifies lysine residues in attached ubiquitin moieties. The mechanism enabling the switch from lysine residues in substrates to specific ones in ubiquitin remains poorly understood. Here, we determine the topology and the mechanism of assembly for the ubiquitin chains mediating functions of the human APC/C. We find that the APC/C triggers substrate degradation by assembling K11-linked ubiquitin chains, the efficient formation of which depends on a surface of ubiquitin, the TEK-box. Strikingly, homologous TEK-boxes are found in APC/C substrates, where they facilitate chain nucleation. We propose that recognition of similar motifs in substrates and ubiquitin enables the APC/C to assembly ubiquitin chains with the specificity and efficiency required for tight cell-cycle control.

Introduction

In eukaryotes, the posttranslational modification of key regulators with ubiquitin plays a crucial role in almost every process (Kerscher et al., 2006). Ubiquitylation can trigger the reorganization of protein complexes, changes in localization, or degradation. The fate of ubiquitylated proteins is determined by adaptors, which recognize ubiquitin chains and deliver the modified substrates to effectors, such as the 26S proteasome (Hicke et al., 2005). To understand how ubiquitylation gains its versatility in signaling, it is pivotal to dissect the mechanisms underlying ubiquitin chain assembly.

The formation of ubiquitin chains is carried out by an enzymatic cascade (Dye and Schulman, 2007). It is initiated by the generation of a thioester between the carboxyl terminus (C terminus) of ubiquitin and a cysteine in ubiquitin-activating enzymes (E1). This ubiquitin is transferred to the active site of ubiquitin-conjugating enzymes (E2), which deliver it to ubiquitin ligases (E3). E3s are classified depending on their catalytic domain: HECT-E3s possess an active-site cysteine and receive ubiquitin from E2s before modifying the substrate. By contrast, RING-E3s simultaneously bind to E2s and substrates and facilitate ubiquitin transfer directly from E2.

All E3s nucleate chain formation by attaching the C terminus of the first ubiquitin to the ε-amino group of a substrate lysine. The subsequent chain elongation requires the modification of specific lysine residues in consecutive ubiquitin moieties. In yeast, all seven lysine residues of ubiquitin are used for chain assembly, resulting in chains of different topology (Peng et al., 2003). However, only the functions of chains linked through K48 or K63 of ubiquitin have been firmly established. While K48-linked chains trigger proteasomal degradation, K63-linked chains recruit binding partners during inflammation or DNA repair (Kerscher et al., 2006). Several E3s can assemble specific ubiquitylation chains in a single substrate binding event (Petroski and Deshaies, 2005b; Rape et al., 2006). It is not understood how this is accomplished, as lysine residues in substrates and ubiquitin are in different chemical environments and at different positions within the growing chain.

The anaphase-promoting complex (APC/C) has served as a model or the analysis of RING-finger-dependent chain formation (Rape et al., 2006; Rodrigo-Brenni and

Morgan, 2007; Thornton et al., 2006). Ubiquitin chain formation by the APC/C can trigger protein degradation to control cell cycle progression (Peters, 2006), quiescence (Wirth et al., 2004), and differentiation (Lasorella et al., 2006), but it can also induce the nonproteolytic disassembly of spindle checkpoint complexes (Reddy et al., 2007). The APC/C can assemble chains on substrates, such as securin and cyclin B1, rapidly and with high processivity (Carroll and Morgan, 2002; Rape et al., 2006). An in vitro study using from APC/C suggested that these chains can be linked through K11, K48, or K63 of ubiquitin (Kirkpatrick et al., 2006). However, the topology of the ubiquitin chains mediating the diverse functions of the APC/C has remained unknown, complicating the analysis of APC/C-dependent chain formation and cell cycle control.

Here, we determine the topology of the ubiquitin chains that mediate functions of the human APC/C. We find that the APC/C and its E2 UbcH10 trigger protein degradation preferentially by assembling K11-linked rather than K48-linked chains. K11-linked ubiquitin chains act as efficient proteasomal targeting signals in vitro and in vivo. We identify a surface of ubiquitin, the TEK-box, which is necessary for the elongation of K11-linked chains. Strikingly, similar TEK-boxes are found in APC/C substrates, where they facilitate the transfer of the first ubiquitin to a substrate lysine. We propose a mechanism in which recognition of a TEK-box first aligns a substrate lysine and later K11 of ubiquitin with the active site of UbcH10 to allow a rapid formation of a K11-linked chain by the APC/C.

Results

The APC/C Functions by Assembling K11-Linked Ubiquitin Chains

To determine the topology of the ubiquitin chains that mediate functions of the human APC/C, we tested recombinant ubiquitin mutants in in vitro assays recapitulating APC/C activity. We employed mutants that had a single lysine replaced with arginine, such as ubiquitin-K48R (ubi-R48). Alternatively, all lysine residues were mutated except for one, as in ubiquitin K48 as its only lysine (ubi-K48). Together, these mutants allowed us to assess whether chains of a specific topology are required or sufficient for APC/C functions.

We first assayed the ubiquitin mutants for their capacity to support the degradation of a mitotic APC/C substrate, cyclin B1. Addition of UbcH10 and $p31^{comet}$ to extracts of mitotic cells with an activated spindle checkpoint (CP extracts) triggers the APC/C-dependent disassembly of Cdc20/Mad2 complexes (Reddy et al., 2007; Stegmeier et al., 2007). This leads to full activation of APC/C^{Cdc20}, and consequently, cyclin B1 ubiqitination and degradation. As reported previously, cyclin B1 is efficiently degraded in UbcH10/p31comet-treated CP extracts containing wild-type (WT) ubiquitin (Figure 1A). Strikingly, cyclin B1 is turned over in a proteasome-dependent manner, when CP extracts are supplemented with a ubiquitin mutant that has K11 as its only lysine (ubiquitin K11; Figures 1A and 1B). By contrast, mutation of K11 of ubiquitin (ubi-R11) interferes with cyclin B1 degradation and also with disassembly of Cdc20/Mad2 complexes (Figure 1C and Figure S1A). No single-lysine mutant other than ubi-K11, including ubi-K48, supports degradation of cyclin B1, while no mutation other

than that of K11 stabilizes cyclin B1. These results suggest that in CP extracts APC/C^{Cdc20} achieves cyclin B1 degradation by decorating it with K11-linked chains.

From anaphase until late G1, Cdc20 is replaced by a homologous coactivator, Cdh1 (Peters, 2006). To determine whether the coactivator or cell-cycle stage influence the topology of APC/C-dependent chains, we tested our ubiquitin mutants in degradation assays using extracts with active APC/C^{Cdh1}. Consistent with our experiments in mitotic extracts, the APC/C substrate securin is rapidly degraded by the 26S proteasome in G1 extracts supplemented with ubi-K11, but it is stabilized if K11 of ubiquitin absent, such as in ubi-R11 or methylubiquitin (Figures 1D and S1B). No single-lysine mutant other than ubi-K11 fully supports the degradation of securin in G1 extracts. Ubi-K11 allows the degradation of multiple ACP/C substrates (Figure S1C) in extracts prepared from cells in G1 or in quiescence, when APC/C^{Cdh1} is also active (Figure S1D). By contrast, inhibiting the formation of K11-linked chains does not impair the ubiquitylation or degradation of the SCF substrate Emi1 (Figure S1E). These findings provide evidence that in extracts both APC/C^{Cdc20} and APC/C^{Cdh1} function by decorating substrates with K11-linked chains.

To determine the importance of K11-linked chains in mediating APC/C functions in vivo, we overexpressed ubi-R11 in human cells or injected recombinant ubi-R11 into *Xenopus tropicalis* embryos at the two cell stage. The overexpression of ubi-R11 in 293T cells impedes the Cdh1-dependent degradation of the APC/C substrates geminin, Plk1, and securinΔD (Figure 1E). Moreover, injection of ubi-R11 into *X. tropicalis* embryos delays early cell division and results in death of injected embryos before gastrulation (Figures 1F and 1G). These phenotypes are less dramatic but similar to those observed after injection of a dominant-negative mutant of the APC/C-specific E2, UbcH10C114S. By contrast, overexpression or injection of WT ubiquitin does not affect the degradation of APC/C substrates, progression through the cell cycle, or development of embryos. Thus, interfering with the formation of K11-linked chains stabilizes APC/C substrates and impairs cell-cycle progression and development in vivo, attesting to the importance of K11-linked chains for APC/C activity.

UbcH10 provides Specificity for the Assembly of K11-Linked Chains

E2s often contribute to the specificity of ubiquitin chain formation (Dye and Schulman, 2007). The human APC/C has been reported to cooperate with three E2s: the specific UbcH10 and the more promiscuous UbcH5c and E2-25K. To dissect the mechanism underlying the formation K11-linked chains, we purified these E2s and tested their specificity in APC/C^{Cdh1}-dependent chain assembly. Strikingly, APC/C^{Cdh1} and its specific E2 UbcH10 form long ubiquitin chains only in the presence of ubi-K11 but not with other single-lysine mutants. The same strong preference for formation of K11-linked chains is observed with the distributive substrate cyclin A (Figure 2A), with the processive substrate securin (Figure 2B), and for UbcH10 autoubiquitylation (Figure 2C). The mutation of K11 in ubiquitin delays chain formation by APC/C^{Cdh1} and UbcH10 (Figure 2D). Furthermore, as shown below, ubiquitin chains assembled by APC/C^{Cdh1} and UbcH10 using ubi-R11 are not efficiently recognized by proteasomal receptors. These results indicate that UbcH10 endows the APC/C with specificity for assembling functional K11-linked chains.

In contrast to UbcH10, UbcH5a and UbcH5c can use ubi-K11, ubi-K48, and ubi-K63 to catalyze the ubiquitylation of APC/C^{Cdh1} substrates (Figure 2E) and, thus, allow the formation of chains linked through lysine residues other than K11. E2-25K assembles chains very inefficiently, and earlier experiments indicated that these chains are linked through K48 (Figures S2A and S2B; (Rodrigo-Brenni and Morgan, 2007). Consistent with the importance of K11-linked chains for APC/C activity, the specific UbcH10 is more potent in promoting the degradation of the APC/C^{Cdh1} substrate securinΔD in G1 extracts than UbcH5 or E2-25K, as observed over a wide range of E2 concentrations (Figures 2F and 2G). These results further suggest that Ubch10, but not UbcH5 or E2-25K, provide the APC/C with specificity for assembling functional K11-linked chains.

To determine the molecular basis underlying the specificity of UbcH10, we compared mutants of UbcH10 and UbcH5 in APC/C-dependent assays. The interaction of E2s with the RING finger of E3s requires an aromatic side chain in loop 1 of the E2 (Zheng et al., 2000). As expected, mutation of the respective residues in UbcH10 and UbcH5, UbcH10Y91D and UbcH5F62D, inactivates both E2s in degradation and ubiquitylation assays dependent on APC/C^{Cdh1} (Figures S2C-S2E). When added to G1 extracts, UbcH10Y91D and UbcH10Y91, but not UbcH5cF62D, impair degradation of the APC/C substrate securin and thus behave and dominant-negative mutants (Figure S2D). Consistent with this observation in extracts, injection of UbcH10Y9D into *X. tropicalis* embryos delays cell-cycle progression (Figure S2F). UbcH10Y91D does not interfere with proteasomal degradation, as the SCF substrate Emi1 is ubiquitylated and degraded in its presence (Figure S2G). Therefore, despite a defective RING finger interaction, UbcH10Y91D can bind the APC/C and compete with endogenous E2s in the extracts, suggesting that UbcH10 contains additional APC/C binding motifs.

A likely candidate for a second APC/C-binding site in UbcH10 is helix 1 of its UBC domain, which in other E2s participates in E3 binding (Reverter and Lima, 2004; Zheng et al., 2000) and is not conserved between UbcH10 and UbcH5. Indeed, mutations in or close to helix 1 (UbcH10K33D and UbcH10D47K) significantly reduce the activity of UbcH10 in degradation and ubiquitylation assays (Figures 2H and 2SI). In contrast to UbcH10Y91D, UbcH10K33D and UbcH10D47K do not act as dominant negatives, indicating that their binding to the APC/C is disturbed. UbcH10K33D is also less efficiently charged by E1, which is consistent with findings that E1- and E3-binding sites in E2s overlap (Eletr et al., 2005). These results imply that residues in or close to helix 1 constitute part of a second PAC/C-binding motif in UbcH10. We suggest that the simultaneous engagement of two binding motifs stabilizes UbcH10 binding to the APC/C to orient UbcH10 in the optimal position for assembling K11-linked chains.

Importantly, the assembly of homogenous K11-linked chains by the APC/C and UbcH10 allowed us to determine whether these chains function as proteasomal targeting signals. Indeed, APC/C substrates decorated with K11-linked chains are recognized by the proteasomal substrate receptors Rad23 (Figure 3A) and S5a in vitro (Figure 3B). Consequently, they are efficiently degraded by 26S proteasomes that copurify with the APC/C (Figure 3E; (Verma et al., 2000)). APC/C substrates modified with K11-linked chains are also rapidly turned over by purified 26S proteasomes from human embryonic kidney cells that were added subsequent to the ubiquitylation (Figure 3F). Securin can be modified with K11-linked chains and captured by Rad23 in 293T cells as well (Figures

3C and 3D). These findings provide strong evidence that K11-linked ubiquitin chains function as efficient proteasomal targeting signals.

As described above, the APC/C and UbcH10 are able to modify substrates with ubiquitin chains also in the absence of K11, but this occurs with delayed kinetics. In addition, the affinity of APC/C substrates to Rad23 is reduced, if chains are assembled by UbcH10 using ubi-R11 (Figure 3A), and these chains are less sensitive to proteasome activity in cells (Figure S3A). K11 is not part of the surface of ubiquitin that is recognized by Rad23, as determined by structural analysis (Varadan et al., 2005), and substrates modified with ubi-R1 by E2s other than UbcH10 are efficiently retained by Rad23 (Figure S3B). This indicates that mutation of K11 alters the structure of ubiquitin chains, which are formed by APC/C^{Cdh1} and UbCH10, thereby impeding recognition by Rad23. We conclude that the APC/C and UbcH10 function by preferentially assembling K11-linked chains, which, as shown here, are efficient proteasomal targeting signals.

The TEK-Box in Ubiquitin Is Required for Assembly of K11-Linked Chains

In addition to the proper orientation of UbcH10, formation of K11-linked chains by the APC/C requires the alignment f K11 in the acceptor ubiquitin relative to the active site of UbcH10. To identify residues in ubiquitin that help present K11, we mutated surface-exposed amino acids to alanine and monitored the capacity of these mutants to support APC/C activity in extracts.

Out of a total of 17 ubiquitin mutants, substituting K6, L8, T9, E34, and I36 with alanine strongly stabilizes securin in extracts (Figure 4A). Accordingly, overexpression of ubi-K6A and ubi-L8A in 293T cells interferes with the degradation of the APC/C^{Cdh1} substrate securinΔD to a similar extent as overexpression of ubi-R11 (Figure 4B). Ubiquitylation reactions using purified APC/C^{Cdh1} and UbcH10 revealed that the stabilization of APC/C substrates is a consequence of impaired chain formation in the presence of these mutants (Figures 4C-4E). Overexpression of ubi-L8A reduced the modification of securin in cells as well (Figure 3C). Interestingly, if the positive charge at position 6 is maintained, as in ubi-R6, neither degradation nor ubiquitylation of APC/C substrates is strongly affected (Figure 1D). This suggests that K6 contributes to binding but is unlikely to be ubiquitylated itself. These experiments identify the ubiquitin residues K6, L8, T9, E34, and I36 to be required for the efficient formation of K11-linked chains by the APC/C and UbcH10. Importantly, these residues form a cluster surrounding K11, which we refer to as the TEK-box of ubiquitin (4F).

In contrast to mutating the TEK-box, altering several other positions of ubiquitin does not affect ubiquitylation or degradation of APC/C substrates. This includes residues shown to support the formation of LK29 linkages by a HECT-E3 (E16A/E18A), the formation of K48 and K63 linkages by several E3s (I44A; K48R; Y59A; K63A/E64A), and ubiquitin recognition (I44A, D58A). Moreover, when UbcH5c is used as E2, mutations in the TEK-box inhibit APC/C-dependent chain formation less severely (Figure S4A). Only ubi-L8A, and to a lesser extend ubi-I36A, are deficient in supporting chain formation by APC/C^{Cdh1} and UbcH5c. None of the TEK-box residues of ubiquitin is important for the monoubiquitylation of an unrelated protein (UEV1A) or for formation of K63-linked ubiquitin dimers by Ube2N/UEV1A (Figure S4B). All ubiquitin mutants are soluble at high concentrations and, with the exception of the slightly impaired E34A

mutant, efficiently loaded onto the active site of UbcH10 (data not shown). These experiments underscore the specific importance of the TEK-box of ubiquitin for UbcH10-dependent chain formation. We conclude that a cluster of residues surrounding K11 of ubiquitin, the TEK-box, is required for the efficient formation of K11-linked chains by the APC/C and UbcH10.

The TEK-Box is Found in APC/C Substrates

Strikingly, we found sequences closely related to the TEK-box of ubiquitin in the APC/C substrate securin. The two TEK-boxes in securin are located immediately downstream of its D-box, which is an APC/C-binding motif responsible for its processive ubiquitylation (Figure 5A; (Burton and Solomon, 2001; Kraft et al., 2005; Rape et al., 2006)). The second TEK-box of securin is especially well conserved (Figure S5A). In analogy to the TEK-box in ubiquitin, TEK-boxes in substrates could facilitate the modification of a substrate lysine, thereby nucleating ubiquitin chain formation.

To test this hypothesis, we first determined whether the TEK-boxes in securin contribute to APC/C binding. We used a competition assay, in which the ubiquitylation and degradation of a radiolabeled APC/C substrate is competitively inhibited by addition of recombinant securin mutants. As expected, WT securin is an efficient competitor of APC/C-dependent degradation in G1 extracts, i.e., it binds well to the APC/C (Figures 5B, S5B, and S5C). Even if both the D-box and a redundant motif, the KEN-box, are deleted (securinΔDΔK), the securin inhibits the APC/C, albeit with reduced efficiency. The same is observed if the D-box, KEN-box, and the first TEK-box of securin are removed by deleting the amino-terminal 78 amino acids (securinΔN78), suggesting that the remaining TEK-box in securinΔN78 is able to mediate APC/C inhibition. Indeed, the deletion (securinΔN78ΔTEK) or mutation (securinΔN78/K91A/K92A) of this TEK-box abolishes competition of securinΔN78. Moreover, when both TEK boxes are deleted in the securinΔDΔKEN, the competition for degradation of an APC/C^{Cdh1} substrate is markedly reduced (Figure 5C). If more than 78 residues are deleted at the amino terminus, binding of securin to APC/C^{Cdh1} is also lost. Together these experiments strongly suggest that the TEK-box is essential for productive operation of the human APC/C.

To test whether the APC/C recognizes D-boxes and TEK-boxes by using distinct sites, we employed D-box and TEK-box peptides in our competition assay. As expected, the addition of a D-box peptide to G1 extracts stabilizes the labeled APC/C substrate (Figure 5D). This competition can be overcome by increasing the concentration of UbcH10 in the extracts, which allows that APC/C to ubiquitinate weakly bound substrates ((Rape et al., 2006); Figure 5D). In a similar manner, competition by the TEK-box peptide securinΔ78 is overcome by the addition of UbcH10 (Figures 5D and S5D). In striking contrast, when both the D-box- and TEK-box-binding sites are saturation by the simultaneous addition of the two peptides, even high concentrations are unable to bypass the competitive inhibition of the APC/C. If the labeled substrate itself does not contain the TEK-boxes (securinΔTEK1/ΔTEK2), the D-box peptide alone inhibits the APC/C in the presence of high UbcH10 concentrations (Figure 5E). These results indicate that D-boxes and TEK-boxes are recognizes by two non-identical sites on the APC/C and/or UbcH10.

Substrate TEK-Boxes Promote the Initiation of Ubiquitin Chains

To determine how TEK-box binding affects the UbcH10-dependent degradation of securin, we monitored securin turnover in extracts of quiescent T24 cells (G0 extracts). These extracts have very low levels of UbcH10, and APC/C substrates are degraded rapidly only after recombinant UbcH10 has been added. As expected, WT securin is degraded in G0 extracts supplemented with UbcH10 (Figure 6A). The deletion of both TEK-boxes (securinΔTEK1/ΔTEK2), but not of each TEK-box alone, strongly stabilizes securin under these conditions. If the first TEK-box is deleted, mutation of K91/K92 in the second TEK-box to alanine (securinΔTEK1/K91A/K92A) is sufficient to stabilize securin in G0 extracts. If K91/K92 are replaced by arginine, securin degradation is not affected, indicating that, reminiscent of K6 of ubiquitin, K91/K92 of securin serve as binding but not ubiquitylation sites for APC/C and UbcH10. A similar dependency on TEK-boxes is observed in G1 extracts, when we measured the degradation of securinΔD after addition of UbcH10. Again, simultaneous deletion of both TEK-boxes results in stabilization of the substrate in the presence of UbcH10 (Figure 6B). Finally, deletion of both the D-box and the TEK-boxes, but not deletion of either motif alone, strongly stabilizes securin against APC/C^{Cdh1}-dependent degradation in intact cells (Figure 6C). The TEK-boxes in securin are therefore important for its APC/C-dependent degradation in extracts and cells.

Since the similarity to the TEK-box in ubiquitin implied that the TEK-boxes in securin promote the modification of a securin lysine, we monitored ubiquitylation kinetics in the presence of methylubiquitin, which is unable to form chains. As reported previously (Rape et al., 2006), APC/C^{Cdh1} and UbcH10 rapidly modify WT securin on several lysine residues (Figure 6D). By contrast, the deletion of both TEK-boxes strongly delays the monoubiquitylation of securin and reduces the number of modified lysine residues. A similar reduction in the number of modified lysine residues is observed, when the TEK-box peptide securinΔN78 is added to block the TEK-box-binding site (Figure S6A). We conclude that the TEK-boxes in securin are required for efficient modification of substrate lysine residues.

As expected from the impaired monoubiquitylation of securinΔTEK1/ΔTEK2, the onset of UbcH10-dependent multiubiquitylation of securinΔTEK1/ΔTEK2 is strongly delayed (Figure 6E). However, following the initial delay, ubiquitin chains approaching full length are rapidly assembled. The same delayed onset of ubiquitin chain formation is observed upon mutation of K91/K92 in securinΔTEK1 to alanine (securinΔTEK1/K91A/K92A) but not when these residues are replaced by arginine (securinΔTEK1/K91R/K92R). By contrast, the deletion of the D-box of securin does not delay chain formation but results in reduced chain length. Consistent with the cooperation between D-box and TEK-boxes, the deletion of both motifs almost completely abrogates securin ubiquitylation. The deletion of the TEK-boxes in securin has less sever effects on chain formation by APC/C^{Cdh1} and UbcH5c (Figures S6B and S6C). These findings all suggest that the TEK-boxes in securin promote the initiation of ubiquitin chains by the APC/C's specific E2 UbcH10.

If the sole function of TEK-boxes in substrates is to promote ubiquitin chain initiation, they should be required only for the addition of the first ubiquitin. By contrast, the D-box of substrates should remain important throughout the reaction. To test this hypothesis, we bypassed chain initiation in D-box and TEK-box mutants by fusing ubiquitin to securinΔD/ΔTEK1/2_UbiΔGG) or by replacing the C terminus of securinΔD, including both TEK boxes, with ubiquitin (ΔD/70-Ub). Intriguingly, despite the lack of TEK-boxes, both ubiquitin fusions are degraded in G1 extracts in an APC/C-dependent manner (Figures 7A and 7F) and ubiquitylated by purified APC/C^{Cdh1} (Figure 7B). The fused ubiquitin is only functional if neither its TEK-box nor its K11 are mutated (Figure 7D). The degradation of the ubiquitin fusions is inhibited by the TEK-box peptide securinΔN78, indicating that the TEK-box in the fused ubiquitin recognizes the same site as the TEK-box in securin (Figure 7F). All fusions are degraded only after the extracts are supplemented with UbcH10, which suggests that addition of the first ubiquitin overcomes the lack of TEK-boxes but not the lack of a D-box in securin. These findings can be reproduced in cells, where the fusion ΔD/70-Ub, but not securinΔDΔTEK1/2, is degraded in an APC/C^{Cdh1}-dependent manner (Figure 7C). As in extracts, mutation of the TEK-box in ubiquitin interferes with the APC/C-dependent degradation of the fusion in cells (Figure 7E). Thus, both in extracts and cells, addition of the first ubiquitin eliminates the requirement for TEK-boxes but not for the D-box in securin. We conclude that the TEK-boxes in securin function primarily in ubiquitin chain nucleation, while the D-box is recognized throughout the ubiquitylation reaction.

Several APC/C substrates, including cyclin B1 and geminin, contain TEK-box-like sequences downstream of their D-box (Figure S6D). To test whether TEK-boxes are recognized during the modification of other APC/C substrates, we monitored their ubiquitylation after the TEK-box-binding site had been saturated with the TEK-box peptide securinΔN78 (Figure 7G). With the exception of cyclin A, the monoubiquitylation of all APC/C substrates analyzed in this assay is impaired by securinΔN78 but not by securinΔN78ΔTEK. In addition, the multiubiquitylation of all APC/C substrates tested, including cyclin A, is inhibited by securinΔN78 but not by securinΔN78ΔTEK. Accordingly, addition of securinΔN78 to G1 extracts stabilizes all examined APC/C substrates, including cyclin A (Figure S6E). Thus, saturation of the TEK-box-binding site interferes with the ubiquitylation and degradation of several APC/C substrates. Based on the results presented in this study, we propose that TEK-boxes in substrates facilitate the nucleation of ubiquitin chains, while the TEK-box in ubiquitin promotes the elongation of the K11-linked chains mediating APC/C-dependent reactions.

Discussion

The modification of proteins with ubiquitin chains is a crucial regulatory event in eukaryotes. This process is nucleated by the modification of a substrate lysine, but it proceeds by targeting of lysine residues in each following ubiquitin. Often, specific lysine residues in ubiquitin are preferred for chain formation, resulting in chains of distinct topology and function. Despite the importance of ubiquitin for signaling, little is known about how lysine residues are selected in substrates and ubiquitin, nor is it understood how E3s can both nucleate and elongate ubiquitin chains of specific topologies.

Here, we have determined the topology of the ubiquitin chains that mediate functions of the human APC/C and have dissected the mechanism underlying their assembly. Surprisingly, we find that the APC/C and its E2 UbcH10 target substrates for degradation by decorating them with K11-linked instead of canonical K48-linked ubiquitin chains. The assembly of K11-linked chains depends on a cluster of amino acids, the TEK-box, which is present in substrates and ubiquitin. In substrates, the TEK-box facilitates the transfer of the first ubiquitin to a substrate lysine and, thus, chain nucleation. The TEK-box of ubiquitin is required for the modification of K11 in ubiquitin and, thus, chain elongation. The recognition of similar sequences in substrates and ubiquitin empowers the APC/C to rapidly decorate substrates with K11-linked chains, which is critical for its central regulatory role in mitosis.

K11-Linked Ubiquitin Chains as a Signaling Entity in Cell-Cycle Control

In yeast, linkages involving all lysine residues of ubiquitin, including K11, have been observed, but no function has been attributed to the modification of cellular substrates with K11-linked chains (Peng et al., 2003). The *Xenopus laevis* APC/C is able to catalyze the formation of K11, K48, and K63 linkages, but the relevance of the different linkages for the functions of the APC/C has not been addressed (Kirkpatrick et al., 2006). By using the degradation of cell-cycle regulators as a readout, we show that the human APC/C and UbcH10 preferentially function by assembling K11-linked chains. APC/C substrates modified with K11-linked chains are recognized by proteasomal receptors and, consequently, degraded by the 26S proteasome. This strongly suggests that K11-linked ubiquitin chains serve as proteasomal targeting signals and thus represent a novel signaling entity important for cell-cycle regulation.

Our analysis revealed the APC/C-specific E2 UbcH10 as a key player conveying specificity for K11-linked chains. UbcH10 can use ubi-K11, but no other single-lysine mutant, for efficient chain formation. If K11 is mutated, but other lysine residues are still present (ubi-R11), UbcH10 is able to assemble chains, but these are formed slowly and recognized less efficiently by proteasomal acceptors. We suspect that when K11 is missing, the APC/C modifies the remaining lysine residues nonspecifically, which is likely to result in the formation of short, branched, and nonfunctional ubiquitin chains.

In contrast to UbcH10, the E2 UbcH5 is less specific and promotes APC/C-dependent chain formation in the presence of ubi-K11, ubi-K48, and ubi-K63. This is consistent with a previous study showing that ubiquitin conjugates formed by the APC/C and UbcH5 contain equal amounts of K11, K48, and K63 linkages (Kirkpatrick et al., 2006). Being more promiscuous coincides with the reduced activity of UbcH5 in several E2-dependent assays. Our findings are reminiscent of the lower activity of UbcH5 compared to UbcH10 in promoting the degradation of cyclin A in G1 (Rape and Kirschner, 2004). Consistent with this, APC/C inactivation in G1 involves the degradation of its specific E2 UbcH10, which assembles K11-linked chains, whereas the levels of UbcH5 are not altered (Rape and Kirschner, 2004)

Why do the APC/C and UbcH10 assemble K11-linked chains rather than canonical K48-linked chains? We suspect that this is related to the regulation of the APC/C by deubiquitylating enzymes (DUBs). DUBs regulate the timing of APC/C substrate ubiquitylation and protect cells against premature APC/C-dependent

inactivation of the spindle checkpoint (Rape and Kirschner, 2004; Stegmeier et al., 2007). Many DUBs recognize substrates based on their ubiquitin chains and display a preference for chains of a certain topology (Nijman et al., 2005). K11-linked chains could identify substrates ubiquitylated by the APC/C, and DUBs could play their role in cell-cycle regulation without interfering with the degradation of substrates ubiquitylated by other E3s in mitosis.

Nucleation and Elongation of Ubiquitin Chains by the APC/C

Ubiquitin chain formation requires E3s to nucleate chains by modifying a substrate lysine but to elongate chains by targeting lysine residues in ubiquitin. E3s have evolved distinct strategies to accomplish this difficult reaction, the transition from chain nucleation to chain initiation. The SCF can nucleate and elongate ubiquitin chains using a single E2, Cdc34, but these reactions occur with strikingly different kinetics (Petroski and Deshaies, 2005a; Pierce et al., 2009). In the UFT pathway, two distinct enzymes, the E3 Ufd4 and the E4 Ufd2 act in succession to mediate chain nucleation and elongation (Koegl et al., 1999). The yeast APC/C employs one E2, Ubc4, to modify a substrate lysine, whereas a second E2, Ubc1, elongates K48-linked chains (Rodrigo-Brenni and Morgan, 2007). Some of these mechanistic differences could be related to the observation that some E2s transfer preformed ubiquitin chains (Li et al., 2007; Ravid and Hochstrasser, 2007), but they could also reflect complex mechanisms of regulation.

In contrast to the aforementioned enzymes, the human APC/C and its E2 UbcH10 are able to nucleate and elongate chains in a single binding event (Rape et al., 2006). This processive multiubiquitylation is critical for the rapid degradation of securing and cyclin B1 at the transition from metaphase to anaphase. As we show here, ubiquitin chain formation by the APC/C relies on a sequence motif, the TEK-box, which is present in substrates and ubiquitin (Figure S7). TEK-boxes in substrates promote the modification of a substrate lysine with ubiquitin, while the TEK-box in ubiquitin supports chain elongation of the K11-linked chain.

Our data show that TEK-boxes promote the association of substrates with the APC/C. In mediating substrate binding, TEK-boxes collaborate with the D-box, an APC/C-binding motif that determines the processivity of ubiquitylation (Burton et al., 2005; Kraft et al., 2005). The simultaneous recognition of the D-box by Cdh1 and the TEK-box by the APC/C or UbcH10 could explain the increased stability of the complex between the APC/C, Cdh1, and substrate compared to dimeric subcomplexes (Burton et al., 2005). Following the transfer of ubiquitin to a lysine within or in proximity to the TEK-box, the substrate-TEK-box is likely to be replaced by the TEK-box of the attached ubiquitin. Importantly, as substrates remain bound to the APC/C by their D-box, elongation of K11-linked ubiquitin chains still occurs only on APC/C substrates. It is tempting to speculate that the recognition of the D-box is a prerequisite for the engagement of the TEK-box with its cognate site on the APC/C or UbcH10. In fact, it may be coupled to conformational changes that were observed on the APC/C following substrate binding (Dube et al., 2005).

In addition, TEK-boxes may play a pivotal role during catalysis by aligning the acceptor lysine with the thioester of UbcH10 and by providing an electrostatic environment that allows the acceptor lysine to act as nucleophile. This hypothesis is

supported by the observation that a cluster of charged amino acids surrounds the active site of UbcH10, but not UbcH5 (Lin et al., 2002; Tolbert et al., 2005).

TEK-boxes are present in several substrates, but we could not detect them in all APC/C substrates. However, the TEK-box is not necessarily a linear sequence motif and could be generated by the three-dimensional orientation of charged amino acids. If substrates do not contain TEK-boxes, their APC/C-dependent degradation might depend on a combination of E2s, as suggested for yeast APC/C, or on an E2 different from UbcH10 that recognizes different surfaces in substrates or ubiquitin. As noted previously (Kirkpatrick et al., 2006), a combination of different E2s might result in several nucleation events before chains are formed. Such a mechanism could increase the probability of deubiquitylating enzymes acting on these substrates, thereby delaying their degradation and improving substrate discrimination by kinetic proofreading.

TEK-boxes are not found in budding yeast, but the yeast APC/C assembles conventional K48-linked instead of K11-linked chains. Strikingly, the yeast APC/C cannot form chains by using a single E2 but rather employs a nucleating E2 (Ubc4) and an elongating E2 (Ubc1; (Rodrigo-Brenni and Morgan, 2007)). As budding yeast also does not have a UbcH10 homolog, these observations suggest that TEK-boxes and cognate E2s such as UbcH10 coevolved to cope with the increased demands of regulating in cell-cycle progression in multicellular organisms. It is possible that TEK-boxes in substrates were selected for because they allow rapid coupling of nucleation and elongation on cell-cycle regulators, and thus tighter cell-cycle control. It will be important to determine whether similar surfaces in substrates and ubiquitin are a specific feature of APC/C, or whether they are a more general hallmark of ubiquitin chain formation in humans.

In this chapter, we show that the human anaphase-promoting complex forms K11-linked ubiquitin chains on its substrates. K11-linkages were essential for degradation of all APC/C substrates tested, while canonical K48-linkages did not support degradation of APC/C substrates. The human APC/C uses a novel motif we report here, the TEK-box, for chain initiation on its substrate securin. After modification of substrate residues, APC/C uses a similar TEK-motif in ubiquitin for chain formation, allowing APC/C to make the transition to chain nucleation (initiation) to elongation. While we only characterized the TEK-box in the substrate securin, a peptide comprising securin's TEK-motif competed for ubiquitylation and degradation of other APC/C substrates, implying its general importance. Unfortunately, in this chapter we were not able to determine the precise residues that make up the TEK-box of securin because while the TEK-boxes of securin were important for degradation, they were not essential. Therefore we sought a substrate that depends on its TEK-box to describe the motif's function in detail.

We named the TEK-box as such because of the conserved Thr-Glu-Lys repeat downstream of its D-box. While we knew the TEK-box was essential for efficient chain initiation on securin. Because motifs functionally similar to the TEK-box have now been characterized on other APC/C substrates (Williamson et al., 2011), and the important residues are not always Thr-Glu-Lys, we refer to TEK-box motifs as "chain initiation motifs." We define chain initiation motifs as conserved basic stretches of amino acids near APC/C degradation motifs that promote efficient chain initiation by the human APC/C and Ubd2C/UbcH10.

In Chapter 3, we show that the APC/C substrate geminin depends on its initiation motif for degradation. Deletion of the chain initiation motif in geminin stabilizes geminin against degradation by APC/C and Ube2C/UbcH10. Determining a consensus amino acid sequence for the chain initiation motif allowed us to characterize the motif in other APC/C substrates and discover a novel APC/C substrate, PCNA-Associated Factor of 15 kDa (PAF15). Furthermore we discovered that the chain initiation motif does not serve as a high-affinity APC/C binding site and in fact chain initiation is regulated independently of substrate binding. The interpretation of our results in Chapter 2 is consistent with the importance of the TEK-box for substrate degradation, but in fact the TEK-box in securin is not a canonical APC/C binding motif. Instead, mutation or saturation of TEK-box binding site interferes with Ubc2C/UbcH10's ability to drive APC/C-dependent chain initiation, but not substrate binding.

The development of new tools to study APC/C substrate ubiquitylation has allowed us to separate binding and chain initiation and show that regulated chain initiation is a novel mechanism that allows APC/C to precisely time the degradation of its many substrates and that, as seen in other processive reactions, chain initiation is the rate-limiting and regulated step of degradation of APC/C substrate degradation. These findings are presented in Chapter 3.

Methods

Plasmids and Antibodies

Human securin, geminin, cyclin A, cyclin B1, Plk1, and Cdc20 were cloned into pCS2 for IVT/T and into pET28 for purification. Deletions of the TEK-boxes in securin encompassed R^{79}ATEKSVK (TEK1) or K^{91}KMTEKVK (TEK2). The securin-ubiquitin fusions contained securin$^{\Delta D,\Delta TEK1/2}$ or the first 70 amino acids of securin$^{\Delta D}$, followed by a Gly/Ser-rich linker, and ubiquitin$^{\Delta GG}$. Rad23, S5a, and hPlic2 were cloned into pGEX4T1 for purification and into pCS2-HA for immunoprecipitations. His_6-tagged ubiquitin was cloned into pET28 for purification. Ubiquitin was cloned into pCS2 for expression in cells. Antibodies ere purchased for detection of Cdc27, Mad2, securin, geminin, and cyclin B1 (Santa Cruz), Plk1 (Upstate), securin (MBL), and β-actin (Abcam).

Peptides and Proteins

His_6-tagged proteins were expressed in BL21 (RIL) cells and purified by NiNTA-agarose. Human ^{His}E1 was purified from baculovirus-infected SF9 cells by NiNTA-purification. The securin D-box peptide (aa 51-70) was purchased from Elim. Rad23, its UBA domains, S5a, and hPlic2 were purified as GST fusions using glutathione sepharose. Purified human 26S proteasomes were purchased from Boston Biochem.

Degradation Assays

Degradation assays were performed as described (Rape et al., 2006). Concentrated extracts of mitotic HeLa S3 cells arrested by nocodazole were supplemented with UbcH10 (5 μM) and p31^{comet} (1 μM) to activate the APC/C.

Recombinant ubiquitin or mutants (~50 μM) were added. Reactions were analyzed for degradation of endogenous cyclin B1 by western blotting

Extracts of HeLa S3 cells in G1 or T24 and T98G cells in quiescence were prepared as described (Rape and Kirschner, 2004). Degradation assays were supplemented with recombinant ubiquitin mutants (~50 μM) and radiolabeled securin mutants. The radiolabeled substrates were synthesized by IVT/T using TnT-system (Promega). Reactions were analyzed for substrate degradation by autoradiography.

Competition Assays

Competition assays were performed in G1 extracts. The degradation of radiolabeled securin after 60 min at 23ºC was monitored by autoradiography. Increasing concentrations of recombinant competitors were added, and the effect on degradation of securin was measured.

In Vitro Ubiquitylation Reactions

In vitro ubiquitylation reactions were performed as described (Rape et al., 2006). The APC/C was purified from 1.5 ml G1 extracts using 75 μl monoclonal αCdc27 antibodies and 100 μl Protein G-agarose (Roche). Washed beads were incubated with 50 nM E1, 100 nM E2, 1 mg/ml ubiquitin, energy mix (20 mM ATP, 15 mM creatine phosphate, creatine phoshpokinase), 1 mM DTT at 23ºC. Reactions were analyzed by autoradiography.

Purification of Ubiquitin Conjugates from Cells

293T cells expressing securin and ^{His}ubiquitin mutants were lysed by TCA. Precipitates were resuspended in 6M GdHCl and purified using NiNTA agarose. Ubiquitylated securin was detected by western blotting using securin antibodies. For binding assays, 293T cells expressing securin, ubi, and ^{HA}Rad23 were lysed by detergent. Cleared lysates were added to anti-HA agarose (Roche), incubated at 4ºC, and probed for copurifying securin by western blotting.

In Vivo Degradation Assays

In vivo degradation assays were performed in 293T cells. APC/C substrates and Cdh1 were coexpressed for 20-24 hr in the presence of ^{His}ubiquitin or respective mutants. Cells were lysed and probed for the levels of the APC/C substrates by western blotting.

In Vitro Fertilization and Injection of *Xenopus tropicalis* Embryos

Females were primed with 10 U hGC and males boosted with 100 U hGC. The next day, females were boosted with 100 U hGC. Males were anesthetized in 0.05% benzocaine and testes were isolated. Sperm and eggs were gently mixed. Thirty minutes after activation, media are changed to 3% cysteine for 15 min and then to 1/9 MR solution containing 3% ficoll. One cell of a two-cell stage embryo is injected with 32 ng

of protein premixed with miniRed tracer. Injected embryos were selected by fluorescence, and the phenotypes at different developmental stages were analyzed and quantified.

Supplemental Data

Supplemental Data include seven figures and can be found at http://www.cell.com/cgi/content/full/133/4/653/DC1/

Acknowledgments

We thank Julia Schaletzky, Ling Song, Hermann-Josef Meyer, and James Walker for help and advice and Julia Schaletzky for also critically reading the manuscript. We are indebted to Michelle Yasukawa and Ann Fischer for tissue culture support and to Tao Wu and Marc Kirschner for sharing results prior to publication. Lingyan Jin is funded in part by a Tang scholarship. This work was funded by NIH Director's New Innovator Award and the Pew Scholar Award.

Figure Legends

Figure 1: K11-Linked Ubiquitin Chains Mediate APC/C Functions

(A) K11-linked chains are sufficient for degradation of cyclin B1 in mitotic extracts. CP extracts were supplemented with WT-ubi or single-lysine mutants. The APC/C was activated by addition of UbcH10 and $p31^{comet}$, and degradation of cyclin B1 was monitored by western blotting. **(B)** Degradation of APC/C substrates by K11-linked chains is proteasome dependent. Degradation of radiolabeled cyclin B1 is CP extracts was triggered by addition of p31comet/UbcH10 is the presence of WT-ubi or ubi-K11. The proteasome inhibitor MG132 was added when indicated. **(C)** K11 is required for rapid degradation of cyclin B1 in mitotic extracts. CP extracts were supplemented with ubiquitin mutants and treated as described above. Degradation of cyclin B1 was monitored by western blotting. **(D)** K11 linkages are required for full activity of APC/C^{Cdh1} in G1. The degradation of radiolabeled securin was monitored by autoradiography in G1 extracts in the presence of ubiquitin mutants. **(E)** K11-linked chains target APC/C^{Cdh1} substrates for degradation in vivo. The APC/C-dependent degradation of geminin, Plk1, and securinΔD was triggered in 293T cells in the presence of indicated ubiquitin mutants (WT-ubi, ubi-R11, ubi-R48) by coexpression of Cdh1. The expression levels were analyzed by western blotting. **(F)** K11 linkages are required for rapid cell-cycle progression in embryos of *Xenopus tropicalis*. One cell of *X. tropicalis* embryos at the two-cell stage was injected with recombinant WT-ubi or ubi-R11 and a fluorescent tracer. Injected cells were followed by fluorescence microscopy, and cell division was monitored by phase microscopy. **(G)** K11 linkages are required for *X. tropicalis* development. Injected embryos were allowed to develop to the tadpole stage. The percentage of embryos without developmental aberrations ("normal") and that of viable embryos was determined. Error bars represent error from three independent experiments.

Figure 2: APC/C^{Cdh1} and UbcH10 Preferentially Assemble K11-Linked Chains In Vitro

(A) APC/C^{Cdh1} and UbcH10 assemble chains on cyclin A using ubi-K11 but no other single-lysine mutant. APC/C^{Cdh1} and UbcH10 were incubated with E1 and ubiquitin mutants. **(B)** APC/C^{Cdh1} and UbcH10 assemble chains on the processive substrate securin using ubi-K11 but no other tested single lysine mutant. **(C)** UbcH10 autoubiquitylation by APC/C^{Cdh1} is supported by ubi-K11 while other single-lysine mutants are much less efficient. **(D)** The formation of ubiquitin chains by APC/C^{Cdh1} and UbcH10 on cyclin A is delayed, if K11 is mutated. The kinetics of chain formation on cyclin A by APC/C^{Cdh1} and UbcH10 in the presence of WT-ubi and ubi-K11A was analyzed by autoradiography. **(E)** APC/C^{Cdh1} and UbcH5c form ubiquitin chains on cyclin A linked through K11, K48, and K63. APC/C^{Cdh1} and UbcH5c were incubated with E1 and ubiquitin mutants. Similar results were obtained with UbcH5a. **(F)** UbcH5 is less efficient in promoting the degradation of securinΔD in G1 extracts. G1 extracts were supplemented with ubiquitin mutants and UbcH10 (upper panel), UbcH5c (lower panel), and a combination of UbcH10 and E2-25K (lower panel). Degradation of radiolabeled securinΔD was

monitored by autoradiography. **(G)** UbcH10 is more potent in triggering degradation of securinΔD in G1 extracts over a wide range of concentrations. Three E2s, UbcH10, UbcH5c, and E2-25K, were titrated in G1 extracts. Reactions were analyzed after 60 min for securinΔD levels by autoradiography.

Figure 3: K11-Linked Ubiquitin Chains are a Proteasomal Targeting Signal

(A) K11-linked chains are recognized by the proteasomal receptor Rad23. The UBA domains of Rad23 were immobilized on beads and incubated with cyclin A that was ubiquitylated in the presence of wt-ubi, ubi-K11, and ubi-R11. Proteins retained by the UBA domains are shown by the letter "B" (bound). **(B)** APC/C substrates modified with K11-linked chains are recognized by proteasomal receptors. Cyclin A was ubiquitylated by APC/C^{Cdh1} and UbcH10 in the presence of ubi-K11 and tested for binding to Gst (negative control), Gst-S5a, and hPlic2. Bound proteins were analyzed by autoradiography. **(C)** APC/C substrates can be modified with K11-linked chains in cells. Securin was coexpressed in 293T cells with His_6-ubiquitin mutants. Conjugates were purified on NiNTA-agarose under denaturing conditions. Ubiquitin without lysine residues ("noK") is not incorporated into chains, showing that ubi-K11 expression leads to the decoration of securin with K11-linked chains. **(D)** K11-linked chains are recognized by proteasomal receptors in vivo. HARad23 was purified from 293T cells expressing securin and ubi-K11 by anti-HA affinity chromatography. Ubiquitylated securin coeluted with Rad23, but not control immunoprecipitations, as detected by western blotting. **(E)** K11-linked chains target an APC/C substrate for proteasomal degradation in a semipurified system. The APC/C was purified under conditions allowing the copurification of active proteasomes (Verma et al., 2000) and used for ubiquitylation/degradation of securin. When indicated, MG132 or ATPγS (which inhibits the proteasome and deubiquitylation by Rpn11) was added. **(F)** K11-linked chains target APC/C substrates for degradation. Cyclin A was ubiquitylated by APC/C^{Cdh1} and UbcH10 and subsequently incubated with purified human 26S proteasomes. MG132 was added wen indicated.

Figure 4: The TEK-Box in Ubiquitylation Is Required for UbcH10-Dependent Chain Formation

(A) Degradation of the APC/C substrate securin in G1 extracts in the presence of ubiquitin mutants, as monitored by autoradiography. **(B)** Degradation of the APC/C^{Cdh1} substrate securinΔD in 293T cells is inhibited by overexpression of ubi-R11, ubi-K6A, and ubi-L8A. Cdh1 was coexpressed where indicated (●), and the levels of securinΔD and β-actin were monitored by western blotting. **(C)** In vitro ubiquitylation of cyclin A by purified APC/C^{Cdh1} and UbcH10 is impaired by mutation of K6, L8, T9, K11, and I36. Other ubiquitin mutants had less severe effects on cyclin A ubiquitylation. **(D)** Mutation of K6, L8, T9, and I36 in ubi-K11 impairs the assembly of K11-linked chains on cyclin A. Ubiquitylation was catalyzed by APC/C^{Cdh1} and UbcH10. **(E)** Mutation of K6, L8, T9, K11, I36, and E34 interferes with autoubiquitylation of radiolabeled UbcH10 by APC/C^{Cdh1}. **(F)** Localization of mutations that affect APC/C activity in G1 on the surface

of ubiquitin. K11 is marked in red; mutants of ubiquitin interfering with APC/C activity are labeled orange; mutants that didn't affect APC/C activity are marked in green.

Figure 5: TEK-Boxes in Securin Contribute to APC/C-Dependent Degradation

(A) Identification of a motif in securin, which is highly related to the TEK-box in ubiquitin. **(B)** The TEK-boxes in securin contribute to APC/C-dependent degradation. The degradation of a radiolabeled APC/C substrate in G1 extracts was monitored in the presence of increasing concentrations of recombinant securin mutants. **(C)** Deletion of TEK-boxes in securinΔDΔK reduces substrate competition for degradation. The degradation of a radiolabeled APC/C substrate in G1 extracts was monitored in the presence of increasing concentrations of securinΔDΔK or securinΔDΔKΔTEK1/2. **(D)** The D-box and the TEK-boxes are recognized by two independent binding sites on the APC/C and/or UbcH10. Degradation of radiolabeled securin in early G1 extracts was monitored by autoradiography. Addition of a D-box or a TEK-box peptide (securinΔN78) stabilized securin in early G1 extracts (upper panel). Addition of recombinant UbcH10 could overcome this competition (lower panel). If both the D-box- and the TEK-box-binding sites are blocked by addition of both peptides, UbcH10 is unable to overcome the competitive inhibition. **(E)** The saturation of the D-box-binding site is sufficient to stabilize a TEK-box mutant of securin. The degradation of securinΔTEK1/2 was monitored in G1 extracts in the presence of a D-box peptide.

Figure 6: The TEK-Box in Securin is Required for Efficient UbcH10-Dependent Ubiquitylation and Degradation

(A) Deletion of both TEK-boxes stabilizes securin in a UbcH10-dependent degradation assay. Degradation of indicated securin mutants in extracts of quiescent T24 cells supplemented with UbcH10 was monitored by autoradiography. **(B)** Deletion of both TEK-boxes impairs the UbcH10-dependent degradation of securinΔD. Degradation of securinΔD mutants in G1 extracts supplemented with UbcH10, as monitored by autoradiography, is shown. **(C)** Deletion of both TEK0boxes stabilizes the APC/C^{Cdh1} substrate securinΔD in cells. The APC/C dependent degradation of the indicated securin mutants was triggered in 293T cells by overexpression of Cdh1, ^{myc}UbcH10, or both (●). Expression levels were analyzed by western blotting. **(D)** Deletion of both TEK-boxes delays modification of securin lysine residues. The kinetics of monoubiquitylation of radiolabeled securin or securinΔTEK1/2 by APC/C^{Cdh1} and UbcH10 was monitored in the presence of methylubiquitin by autoradiography. **(E)** Deletion of both TEK-boxes delays the onset of chain formation on securin by APC/C^{Cdh1} and UbcH10. Radiolabeled securin and the indicated mutants were incubated with APC/C^{Cdh1} and UbcH10 in the presence of ubiquitin and analyzed by autoradiography.

Figure 7: The TEK-Boxes in Securin Function in Ubiquitin Chain Nucleation

(A) APC/C-independent addition of the first ubiquitin to securin obviates the requirement for TEK-boxes. Degradation of securin mutants in G1 extracts with or without additional UbcH10 was analyzed by autoradiography. Chain nucleation was bypassed by fusing

ubiquitin to securinΔDΔTEK1/2 or by replacing the C terminus of securin with ubiquitin (ΔD/70-Ub). **(B)** Addition of the first ubiquitin restores APC/C-dependent ubiquitylation. Ubiquitylation of ΔD/70-Ub by APC/C^{Cdh1} and UbcH10 was monitored by autoradiography. **(C)** Bypassing chain nucleation rescues APC/C^{Cdh1}-dependent degradation of TEK-box mutants in cells. SecurinΔDΔTEK1/2 and ΔD/70-Ub were coexpressed with Cdh1 and ^{myc}UbcH10 in 293T cells as indicated. Expression levels were determined by western blotting. **(D)** Bypassing chain nucleation rescues degradation of TEK-box-deleted securin only if the fused ubiquitin contains a TEK-box and K11. Mutants of ΔD/70-Ub were analyzed for degradation in G1 extracts supplemented with UbcH10. **(E)** Ubiquitin fusions are degraded in cells only if the fused ubiquitin contains a TEK-box. The respective mutants were coexpressed with Cdh1 where indicated (●) and expression levels were determined by western blotting. **(F)** Bypassing chain nucleation does not obviate the requirement of a D-box, the APC/C, or TEK-box recognition. Degradation of ΔD/70-Ub was analyzed by autoradiography in G1 extracts supplemented with UbcH10, the APC/C inhibitor Emi1, an excess of the APC/C substrate securin, the TEK-box peptide securinΔN78, or mutant securinΔN78ΔTEK. **(G)** The TEK-box-binding site on APC/C^{Cdh1} is required for the ubiquitylation of several APC/C substrates. The APC/C^{Cdh1} substrates Cdc20, cyclin B1, cyclin A, Plk1, and geminin were incubated with APC/C^{Cdh1} and UbcH10 and the presence of methylubiquitin (to measure nucleation) and ubiquitin (to monitor elongation). Reactions were challenged with the TEK-box peptide securinΔN78 or the securinΔN78ΔTEK mutant, and ubiquitylated species were visualized by autoradiography.

Figure S1: K11-linked ubiquitin chains mediate APC/C-functions

(A) K11-linked chains are involved in spindle checkpoint complex disassembly. APC/C was purified from CP-extracts and treated with UbcH10, p31comet and wt-ubi or ubi-R11. The "Input" lane shows the checkpoint complex disassembly reaction in the presence of ATPγS, which inhibits dissociation of Mad2 from Cdc20. The amount of ubiquitylated Cdc20 and co-purifying Mad2 are visualized by Western blotting. B. K11-linked chains are an efficient proteasomal targeting signal in G1. Degradation of radiolabeled securin in G1-extracts was monitored in the presence of the indicated ubiquitin mutants. Where indicated, MG132 was added. C. K11-linked chains mediate cyclin A degradation in G1-extracts. Radiolabeled cyclin A was added to early G1-extracts, which have UbcH10, in the presence of indicated single-lysine ubiquitin mutants. The degradation of cyclin A was analyzed by autoradiography. D. Degradation of securin in extracts of quiescent T98G-cells supplemented with UbcH10 is dependent on K11-linked chains. The degradation of radiolabeled securin in the presence of the indicated ubiquitin mutants was monitored by autoradiography. E. K11-linkages are not required for degradation of the SCF-substrate Emi1 in extracts. CP-extracts were supplemented with human Cdc34 and ubiquitin mutants, and radiolabeled Emi1 was analyzed by autoradiography.

Figure S2: The role of different E2-domains in supporting APC/C-activity

(A) E2-25K is less active than UbcH10 and UbcH5c in promoting ubiquitylation by

human APC/C^{Cdh1}. E2-25K attaches few ubiquitin molecules and does not cooperate with UbcH10. **(B)** E2-25K does not extent pre-nucleated ubiquitin chains. Ubiquitin chains were nucleated on cyclin A by APC/C^{Cdh1} and UbcH10 in the presence of ubi-K48. UbcH10 is not able to extend ubiquitin chains on ubi-K48, but E2-25K is able to synthesize K48-linked ubiquitin chains. However, no additional activity is detected when UbcH10 and E2-25K are added compared to the reaction containing only UbcH10. **(C)** RING-finger binding by UbcH10 and UbcH5c is required for E2 activity in ubiquitylation assays. Purified APC/C^{Cdh1} was tested for its ability to ubiquitinate cyclin A in the presence of wt-UbcH10 and UbcH5, E2-mutants disrupting a non-covalent ubiquitin binding site in UbcH5c (UbcH5cS21R, UbcH10S51R), and E2-mutants which based on structural data are predicted to interfere with binding to the RING-finger APC11 (UbcH5cF62D, UbcH10Y91D). D. Mutation of the RING-finger binding site in UbcH10, but not in UbcH5c, generates dominant negative E2s. The indicated E2s were added to G1-extracts to test for their effects on the degradation of radiolabeled securin. Mutation of Y91 in UbcH10 and F62 in UbcH5c alters the residue predicted to interact with the RING-finger APC11. Mutation of K33 and D47 interferes with UbcH10 activity, but does not generate a dominant-negative mutant. Mutation of C114 in UbcH10 and C85 in UbcH5c abrogates catalytic activity and leads to dominant negative effects. E. UbcH10Y91D does not induce degradation of radiolabeled securinΔD, as observed by autoradiography. F. UbcH10Y91D behaves as a dominant-negative mutant in embryos of *Xenopus tropicalis*. Recombinant UbcH10Y91D was injected into X. tropicalis embryos at the two cell stage together with a fluorescent marker. Cell cycle progression was analyzed by phase microscopy. G. UbcH10Y91D does not generally inhibit ubiquitylation in extracts. The Cdc34-dependent ubiquitylation and degradation of the SCF-substrate Emi1 was monitored in mitotic extracts in the absence or presence of UbcH10Y91D. H. Helix-1 mutants of UbcH10 are inactive in extracts. The degradation of radiolabeled securinΔD in G1-extracts was monitored after addition of the indicated UbcH10-mutants by autoradiography. UbcH10K33D and UbcH10D47K, both mutants in or close by helix-1, are inactive. UbcH10K33D is also inefficiently charged by E1. I. UbcH10D47K is less active in supporting the ubiquitylation of cyclin A by purified APC/C^{Cdh1}. The ubiquitylation of radiolabeled cyclin A is monitored by autoradiography.

Figure S3: The role of K11-linked chains in proteasome recognition

A. K11-linked chains are degraded in vivo. His-tagged ubiquitin or ubi-R11 and securin were expressed in HeLa cells synchronized in G1. MG132 was added where indicated. Ubiquitin conjugates were purified under denaturing conditions on NiNTA-agarose. Ubiquitylated securin was detected by Western blotting. Securin modified with wt-ubi is detected only in the presence of MG132, whereas securin modified with ubi-R11 is detected both in the presence and absence of MG132 to a similar extent, suggesting that the ubi-R11 chains are inefficient proteasome targeting signals in vivo. The right panel shows a lower exposure of the Western blot of the experiment performed in the presence of MG132 to indicate the decreased efficiency of substrate modification in the presence of ubi-R11. B. Rad23 binds proteins modified with ubi-R11 by E2s other than UbcH10. APC11 was subjected to autoubiquitylation by E1 and UbcH5c in the presence of ubi-R11 and analyzed for binding to immobilized UBA-domains as described in Figure 3A.

APC11 ubiquitylated by ubi-R11 is recognized as efficiently as if modified with wt ubiquitin, indicating the mutation of K11 of ubiquitin by itself does not explain the reduced efficiency of APC/C-substrates to Rad23, when they were modified by UbcH10.

Figure S4: The TEK-box in ubiquitin is specifically important for UbcH10-dependent chain formation

A. Mutation of the TEK-box in ubiquitin affects UbcH5c-dependent chain formation to a lesser extent than UbcH10-dependent chain formation. Only mutation of L8 and, to a lesser extent, I36 in ubiquitin affects ubiquitylation of cyclin A by purified APC/C^{Cdh1} and UbcH5c. Mutation of K6, T9, and K11 has much less severe effects on the UbcH5c-dependent ubiquitylation of cyclin A. B. Mutation of ubiquitin residues required for the UbcH10-dependent chain assembly does not impair formation of K63-linked ubiquitin dimers or monoubiquitylation of UEV1A, as catalyzed by human Ube2N/UEV1A complexes.

Figure S5: TEK-boxes are found in APC/C-substrates

A. Two TEK-boxes are found in the APC/C-substrate securin immediately downstream of its D-box. Securin sequences from different species were aligned using ClutalW. Perfect sequence conservation is marked by an "*" below the alignment. B. Competitive inhibition of APC/C-dependent degradation by a securin mutant lacking the D-box and KEN-box. Degradation of radiolabeled securin was monitored in extracts of cells in G1, quiescence, and mitosis by autoradiography. Recombinant securin, securinΔD, or securinΔDΔK were added as competitors. C. The competition by securinΔDΔK is observed in the purified system. APC/C^{Cdc20} or APC/C^{Cdh1} were used to catalyze the ubiquitylation of wild-type securin in the presence of recombinant competitors securin or securinΔDΔK. The competition is observed both in the presence of UbcH10 and UbcH5c. D. UbcH10, but not UbcH5c, can overcome competition by the TEK-box peptide. Degradation of radiolabeled securin in G1-extract was competitively inhibited by addition of the TEK-box peptide securinΔN78. Increasing concentrations of radiolabeled UbcH10 or UbcH5c were added. Only higher concentrations of UbcH10, but not UbcH5c, overcome the inhibition.

Figure S6: The TEK-box in securin is important for chain nucleation

A. Mutation of the TEK-boxes in securin or saturation of the TEK-box-binding site on APC/C^{Cdh1} reduces the number of modified lysine residues. APC/C^{Cdh1} was used to catalyze the monoubiquitylation (using methylubiquitin) of securin or securinΔTEK1/ΔTEK2. The circle marks the reaction where recombinant securinΔN78 was added to saturate the TEK-box binding site. Ubiquitylated species were detected by autoradiography. B. Deletion of the TEK-boxes has weak effects on securin ubiquitylation by APC/C^{Cdh1} and UbcH5. Radiolabeled securin and securinΔTEK1/2 were ubiquitylated by APC/C^{Cdh1} and UbcH5c and analyzed by autoradiography. C. Deletion of the TEK-boxes abrogates ubiquitylation of radiolabeled securinΔDΔKEN by APC/C^{Cdh1}

and UbcH10, but not by UbcH5c, as analyzed by autoradiography. D. Sequences downstream of the D-boxes of the human APC/C-substrates cyclin B1, geminin, and securin are shown. Highly conserved residues are in bold. E. Degradation of radiolabeled securin, geminin, and cyclin A in extracts was monitored over time. Extracts were supplemented with recombinant securin, securinΔDΔK, or the TEK-box peptide securinΔN78 as indicated.

Figure S7: Model of ubiquitin chain nucleation and elongation by the human APC/C and its E2 UbcH10

Substrates bind to the co-factor Cdh1 via their D-box, which subsequently allows a secondary binding motif, the TEK-box, to interact with either APC/C or UbcH10. The recognition of the TEK-box facilitates the transfer of the first ubiquitin to a substrate lysine residue. Subsequently, the TEK-box of the substrate is replaced by the TEK-box of ubiquitin, aligning K11 of ubiquitin with the thioester of UbcH10. If repeated, this leads to elongation of K11-linked ubiquitin chains.

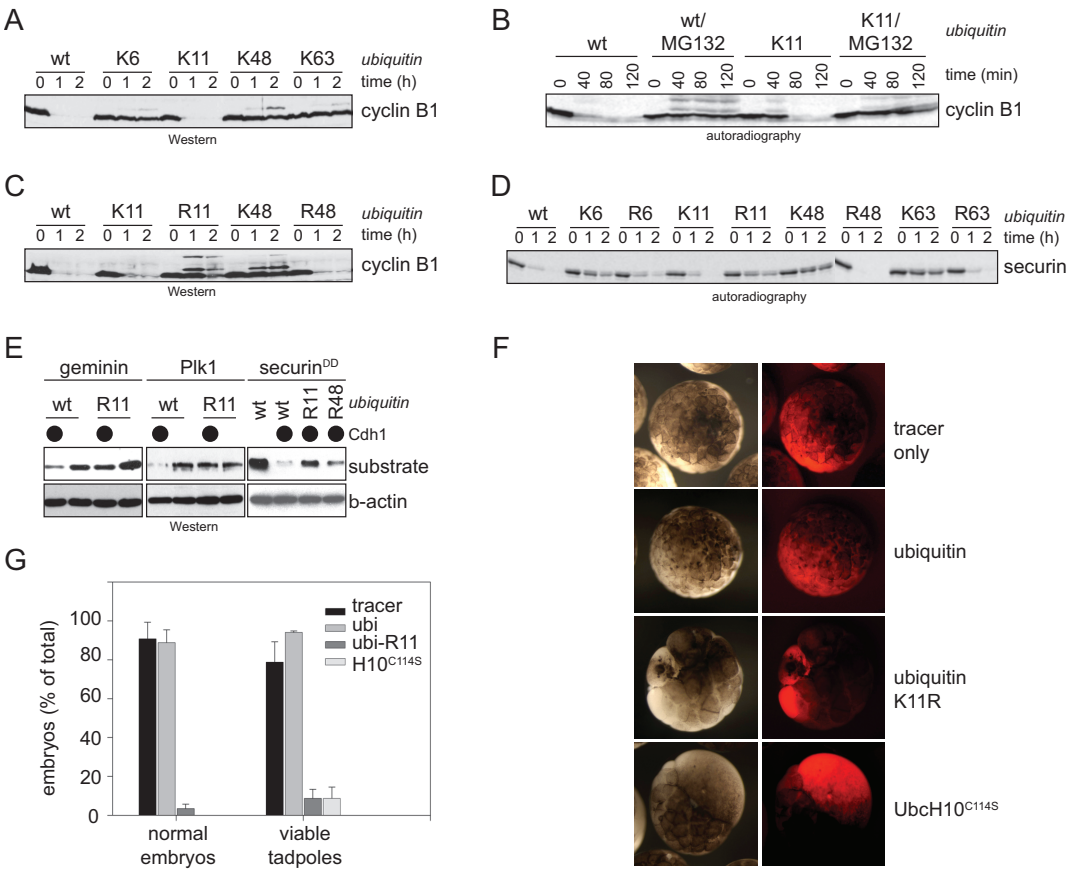
A
wt
K6
K11
K48
K63
ubiquitin
0 1 2
time (h)
cyclin B1
Western
B
wt
wt/ MG132
K11
K11/ MG132
ubiquitin
0 40 80 120
time (min)
cyclin B1
autoradiography
C
wt
K11
R11
K48
R48
ubiquitin
time (h)
cyclin B1
Western
D
wt
K6
R6
K11
R11
K48
R48
K63
R63
ubiquitin
time (h)
securin
autoradiography
E
geminin
Plk1
securinDD
wt
R11
R48
ubiquitin
Cdh1
substrate
b-actin
Western
F
tracer only
ubiquitin
ubiquitin K11R
UbcH10C114S
G
embryos (% of total)
100
80
60
40
20
0
tracer
ubi
ubi-R11
H10C114S
normal embryos
viable tadpoles

Figure 1

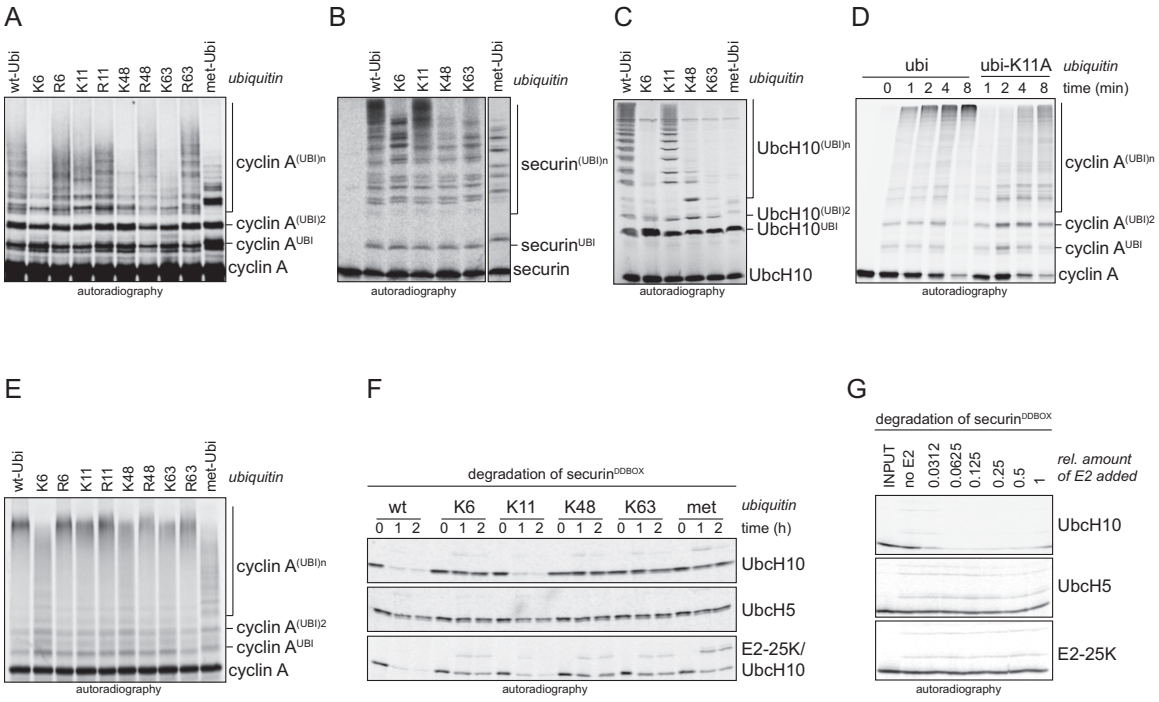
A
wt-Ubi
K6
R6
K11
R11
K48
R48
K63
R63
met-Ubi
ubiquitin
cyclin A(UBI)n
cyclin A(UBI)2
cyclin AUBI
cyclin A
autoradiography
B
wt-Ubi
K6
K11
K48
K63
met-Ubi
ubiquitin
securin(UBI)n
securinUBI
securin
autoradiography
C
wt-Ubi
K6
K11
K48
K63
met-Ubi
ubiquitin
UbcH10(UBI)n
UbcH10(UBI)2
UbcH10UBI
UbcH10
autoradiography
D
ubi
ubi-K11A
ubiquitin
0 1 2 4 8 1 2 4 8
time (min)
cyclin A(UBI)n
cyclin A(UBI)2
cyclin AUBI
cyclin A
autoradiography
E
wt-Ubi
K6
R6
K11
R11
K48
R48
K63
R63
met-Ubi
ubiquitin
cyclin A(UBI)n
cyclin A(UBI)2
cyclin AUBI
cyclin A
autoradiography
F
degradation of securinDDBOX
wt
K6
K11
K48
K63
met
ubiquitin
0 1 2 0 1 2 0 1 2 0 1 2 0 1 2 0 1 2
time (h)
UbcH10
UbcH5
E2-25K/
UbcH10
autoradiography
G
degradation of securinDDBOX
INPUT
no E2
0.0312
0.0625
0.125
0.25
0.5
1
rel. amount
of E2 added
UbcH10
UbcH5
E2-25K
autoradiography

Figure 2

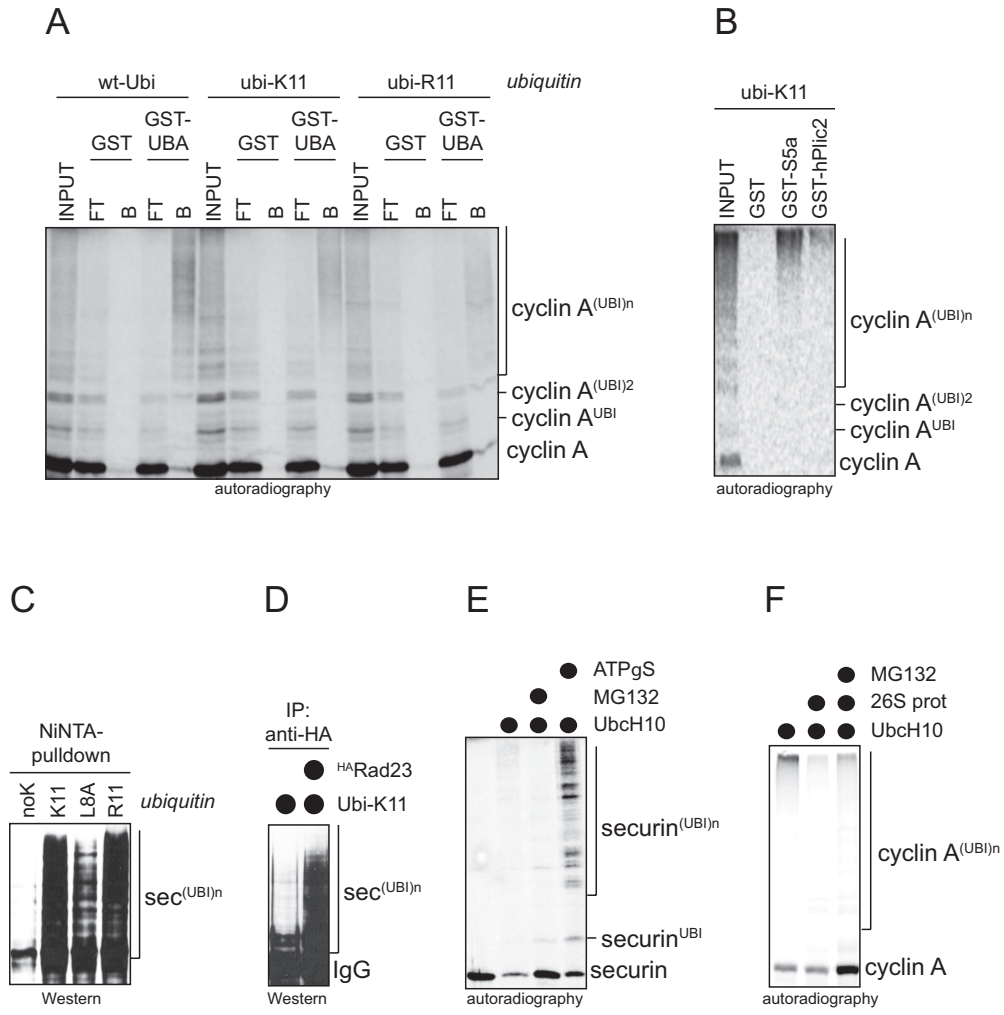
A
wt-Ubi
ubi-K11
ubi-R11
ubiquitin
GST
GST-UBA
INPUT
FT
B
cyclin A(UBI)n
cyclin A(UBI)2
cyclin A UBI
cyclin A
autoradiography
B
ubi-K11
INPUT
GST
GST-S5a
GST-hPlic2
cyclin A(UBI)n
cyclin A(UBI)2
cyclin A UBI
cyclin A
autoradiography
C
NiNTA-pulldown
noK
K11
L8A
R11
ubiquitin
sec(UBI)n
Western
D
IP: anti-HA
HARad23
Ubi-K11
sec(UBI)n
IgG
Western
E
ATPgS
MG132
UbcH10
securin(UBI)n
securin UBI
securin
autoradiography
F
MG132
26S prot
UbcH10
cyclin A(UBI)n
cyclin A
autoradiography

Figure 3

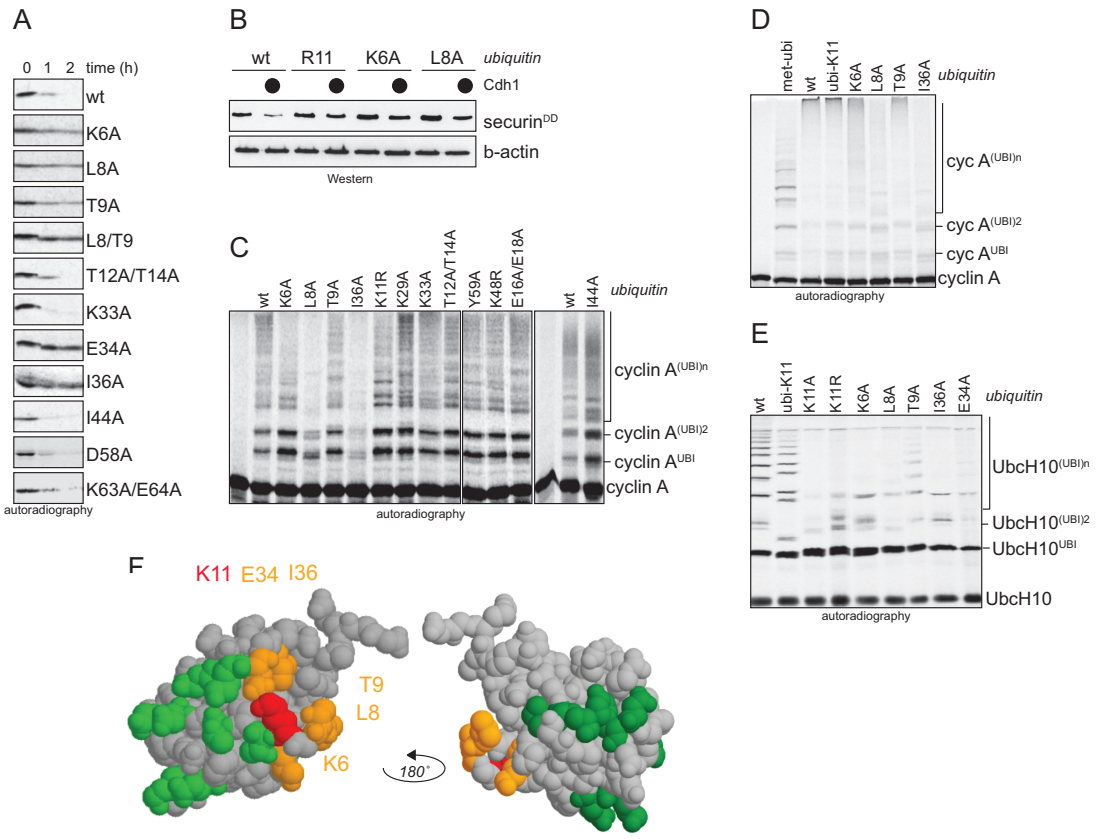
A
0 1 2 time (h)
wt
K6A
L8A
T9A
L8/T9
T12A/T14A
K33A
E34A
I36A
I44A
D58A
K63A/E64A
autoradiography
B
wt R11 K6A L8A ubiquitin
Cdh1
securin^DD
b-actin
Western
C
wt K6A L8A T9A I36A K11R K29A K33A T12A/T14A Y59A K48R E16A/E18A wt I44A ubiquitin
cyclin A(UBI)n
cyclin A(UBI)2
cyclin A UBI
cyclin A
autoradiography
D
met-ubi wt ubi-K11 K6A L8A T9A I36A ubiquitin
cyc A(UBI)n
cyc A(UBI)2
cyc A UBI
cyclin A
autoradiography
E
wt ubi-K11 K11A K11R K6A L8A T9A I36A E34A ubiquitin
UbcH10(UBI)n
UbcH10(UBI)2
UbcH10UBI
UbcH10
autoradiography
F
K11 E34 I36
T9
L8
K6
180°

Figure 4

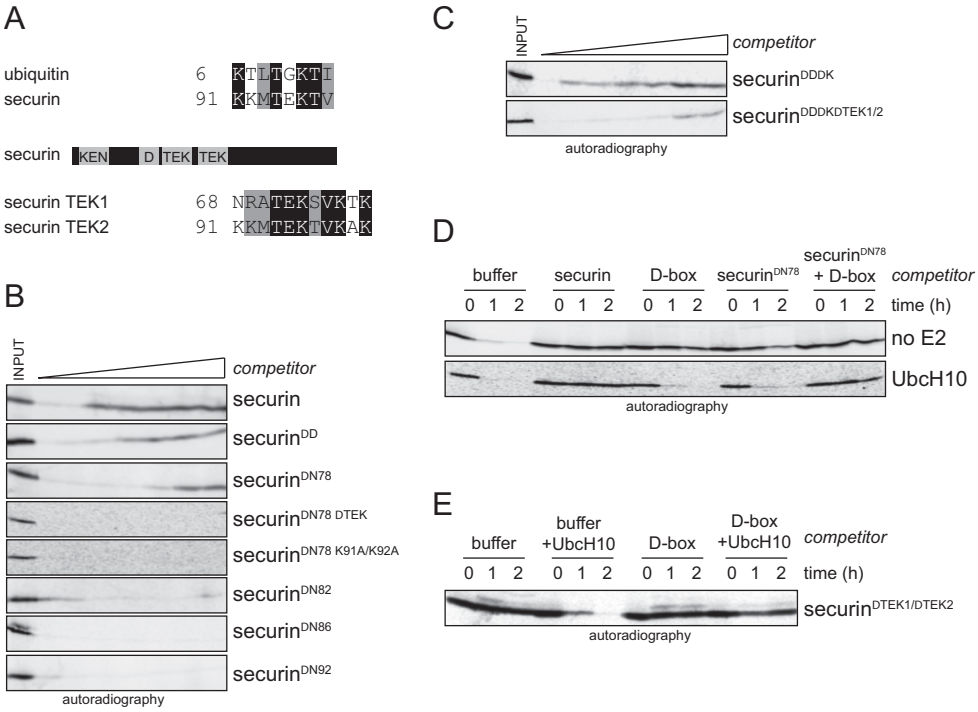
A
ubiquitin 6 KTLTGKTI
securin 91 KKMTEKTV
securin KEN D TEK TEK
securin TEK1 68 NRATEKSVKTK
securin TEK2 91 KKMTEKTVKAK
B
INPUT
competitor
securin
securinDD
securinDN78
securinDN78 DTEK
securinDN78 K91A/K92A
securinDN82
securinDN86
securinDN92
autoradiography
C
INPUT
competitor
securinDDDK
securinDDDKDTEK1/2
autoradiography
D
buffer
securin
D-box
securinDN78
securinDN78 + D-box
competitor
0 1 2 0 1 2 0 1 2 0 1 2 0 1 2
time (h)
no E2
UbcH10
autoradiography
E
buffer
buffer +UbcH10
D-box
D-box +UbcH10
competitor
0 1 2 0 1 2 0 1 2 0 1 2
time (h)
securinDTEK1/DTEK2
autoradiography

Figure 5

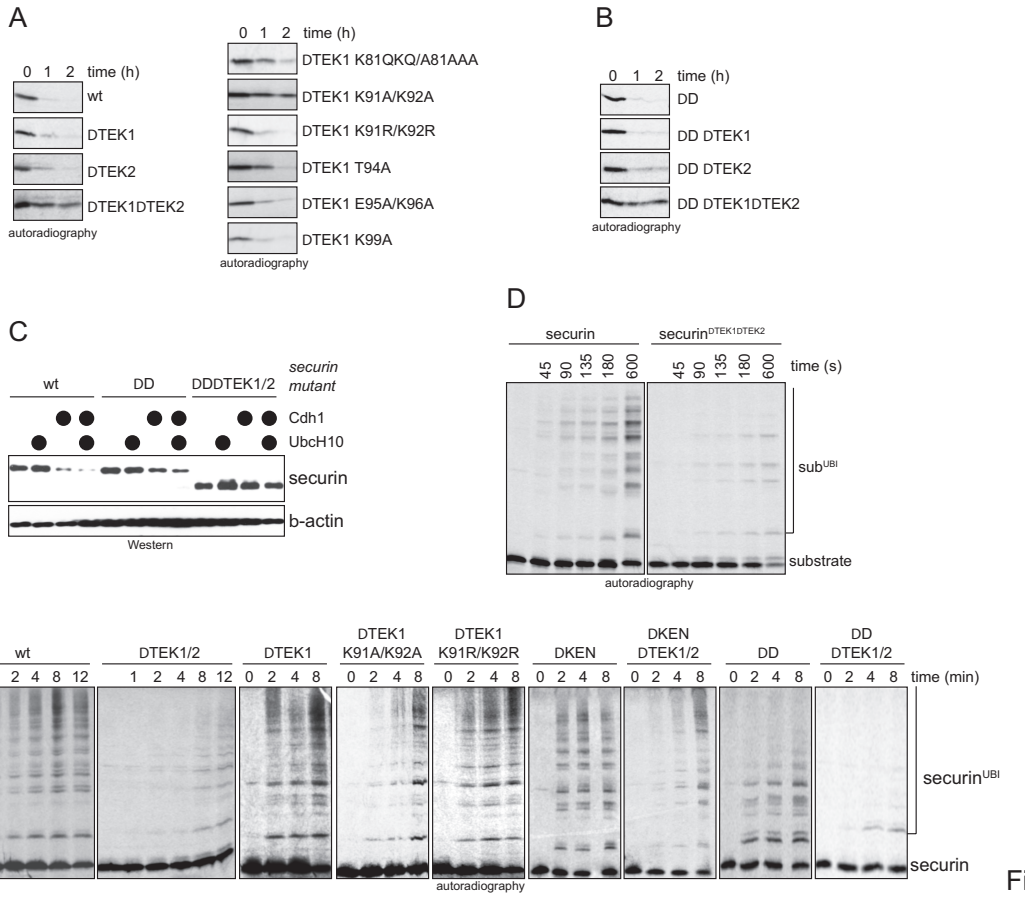
A
0 1 2 time (h)
wt
DTEK1
DTEK2
DTEK1DTEK2
autoradiography
0 1 2 time (h)
DTEK1 K81QKQ/A81AAA
DTEK1 K91A/K92A
DTEK1 K91R/K92R
DTEK1 T94A
DTEK1 E95A/K96A
DTEK1 K99A
autoradiography
B
0 1 2 time (h)
DD
DD DTEK1
DD DTEK2
DD DTEK1DTEK2
autoradiography
C
wt
DD
DDDTEK1/2
securin mutant
Cdh1
UbcH10
securin
b-actin
Western
D
securin
securinDTEK1DTEK2
45 90 135 180 600
45 90 135 180 600
time (s)
subUBI
substrate
autoradiography
E
wt
DTEK1/2
DTEK1
DTEK1 K91A/K92A
DTEK1 K91R/K92R
DKEN
DKEN DTEK1/2
DD
DD DTEK1/2
1 2 4 8 12
1 2 4 8 12
0 2 4 8
0 2 4 8
0 2 4 8
0 2 4 8
0 2 4 8
0 2 4 8
0 2 4 8
0 2 4 8
time (min)
securinUBI
securin
autoradiography

Figure 6

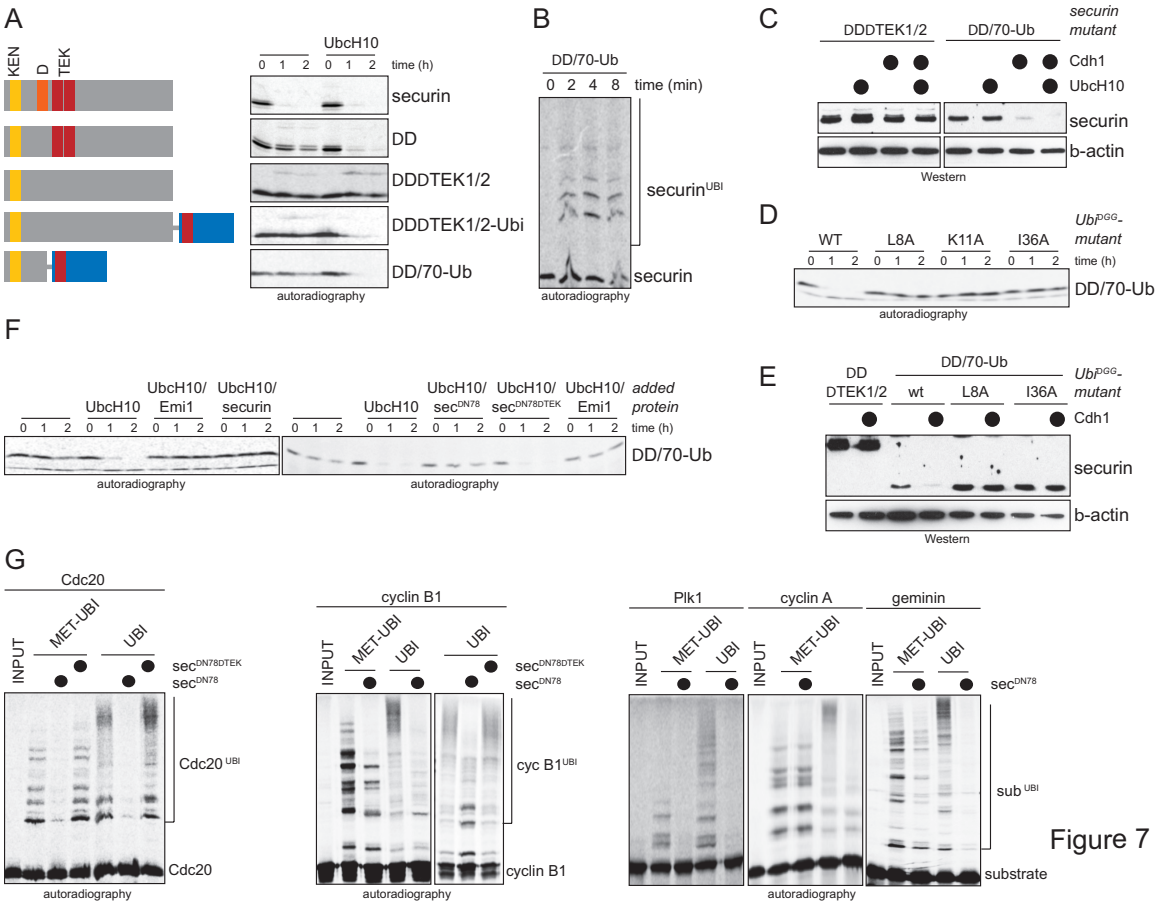
A
KEN
D
TEK
UbcH10
0 1 2 0 1 2 time (h)
securin
DD
DDDTEK1/2
DDDTEK1/2-Ubi
DD/70-Ub
autoradiography
B
DD/70-Ub
0 2 4 8 time (min)
securin^UBI
securin
autoradiography
C
DDDTEK1/2
DD/70-Ub
securin mutant
Cdh1
UbcH10
securin
b-actin
Western
D
WT
L8A
K11A
I36A
Ubi^DGG-mutant
0 1 2 0 1 2 0 1 2 0 1 2 time (h)
DD/70-Ub
autoradiography
E
DD
DTEK1/2
DD/70-Ub
wt
L8A
I36A
Ubi^DGG-mutant
Cdh1
securin
b-actin
Western
F
UbcH10
UbcH10/ Emi1
UbcH10/ securin
UbcH10
UbcH10/ sec^DN78
UbcH10/ sec^DN78DTEK
UbcH10/ Emi1
added protein
0 1 2 0 1 2 0 1 2 0 1 2 0 1 2 0 1 2 0 1 2 0 1 2 time (h)
DD/70-Ub
autoradiography
autoradiography
G
Cdc20
cyclin B1
Plk1
cyclin A
geminin
INPUT
MET-UBI
UBI
sec^DN78DTEK
sec^DN78
Cdc20^UBI
Cdc20
cyc B1^UBI
cyclin B1
sub^UBI
substrate
autoradiography
autoradiography
autoradiography

Figure 7

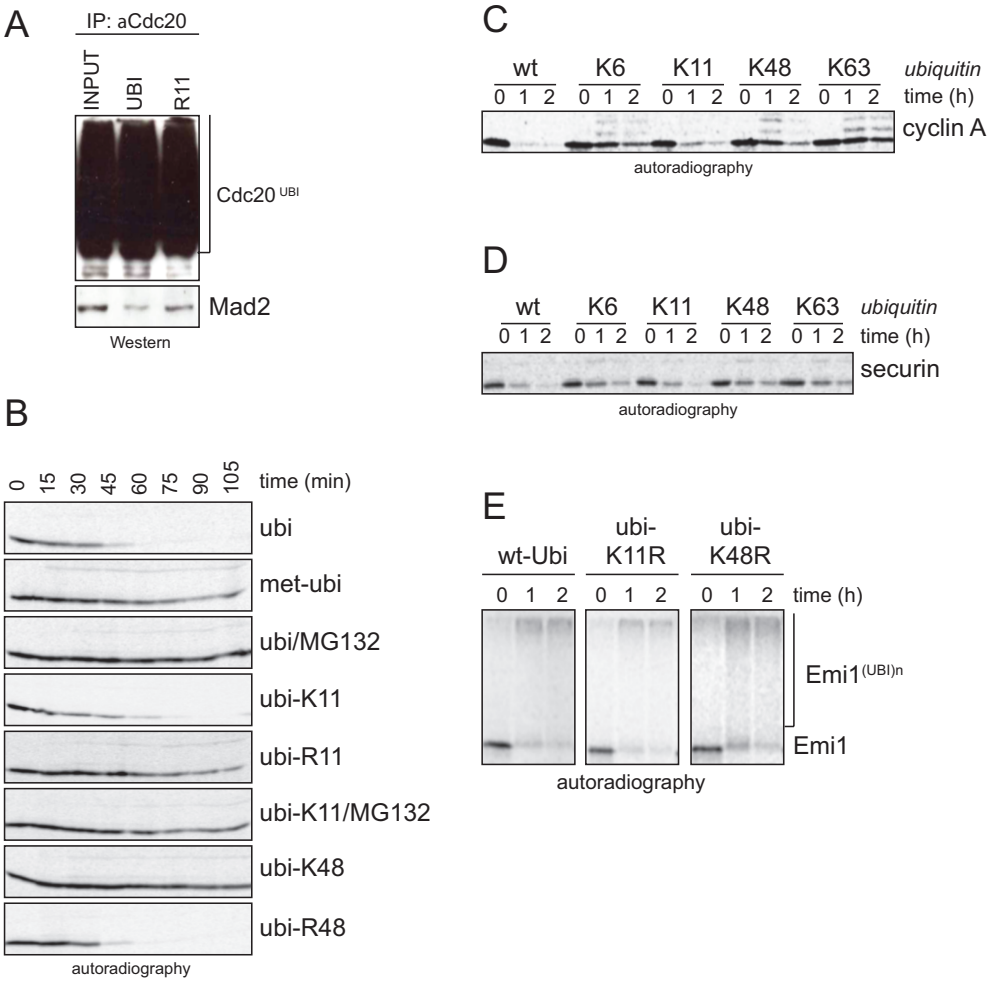

Supplementary Figure 1

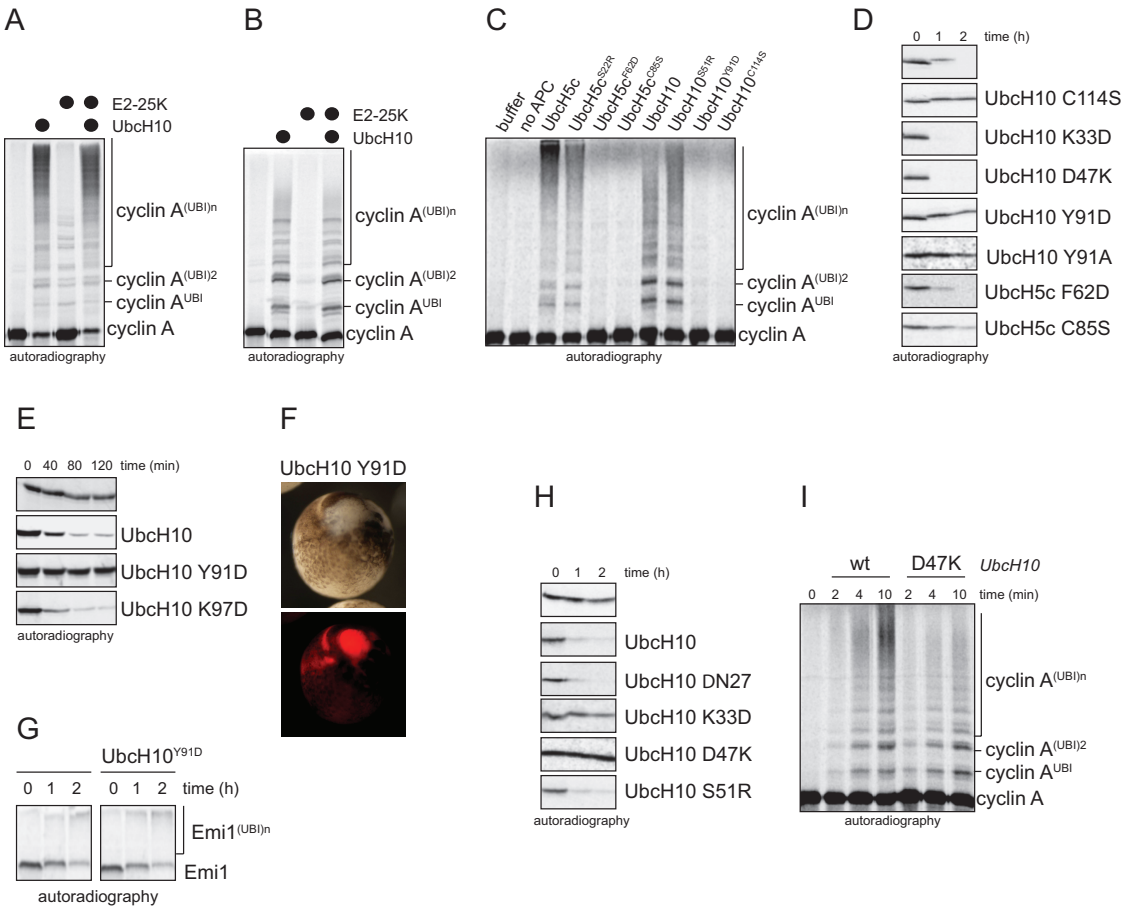

Supplementary Figure 2

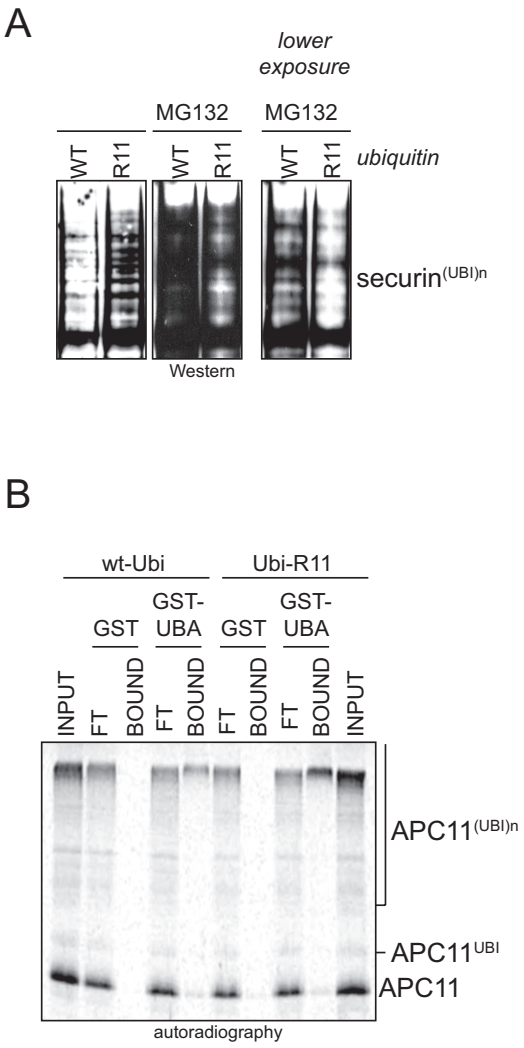

Supplementary Figure 3

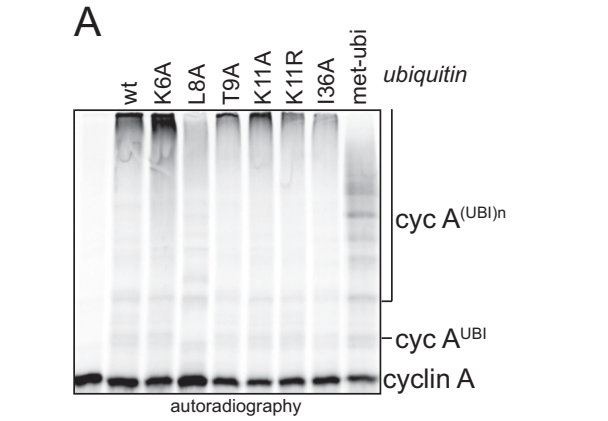

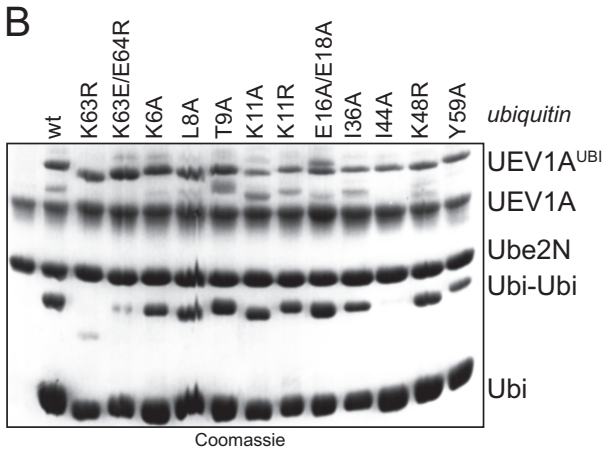

Supplementary Figure 4

A

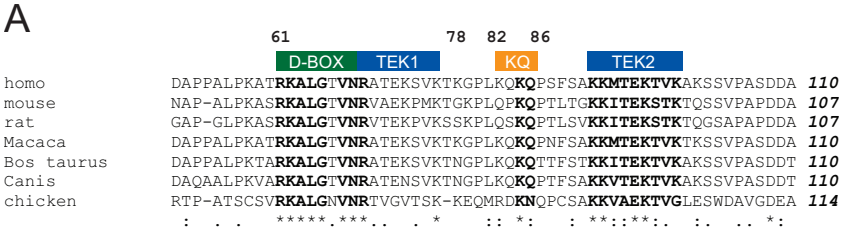

B

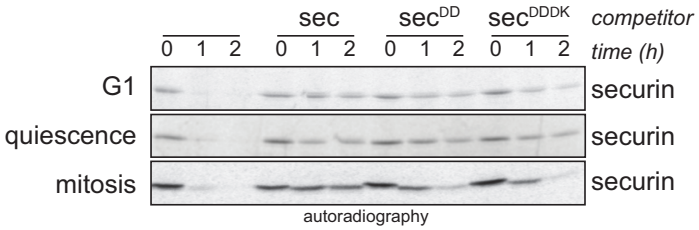

C

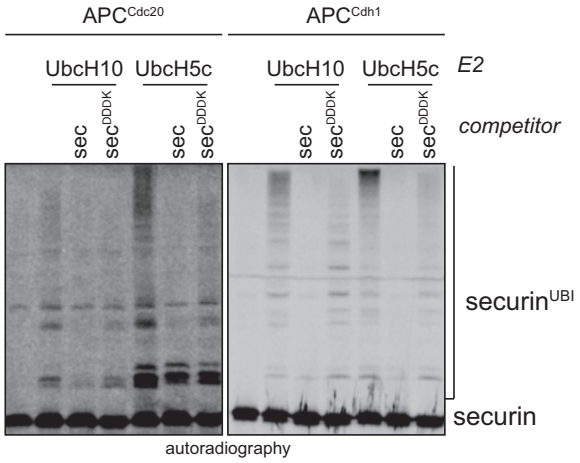

D

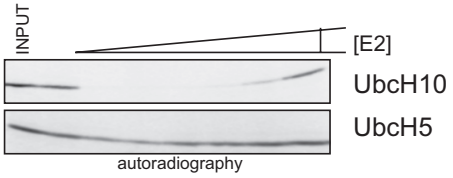

Supplementary Figure 5

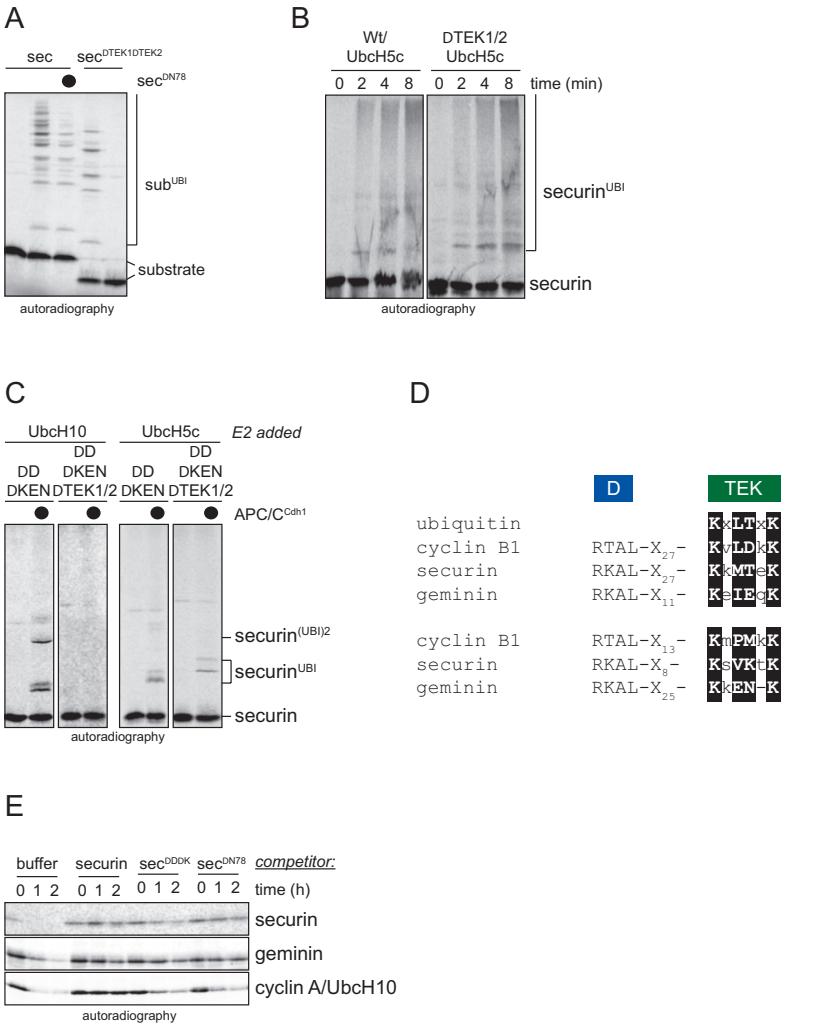

Supplementary Figure 6

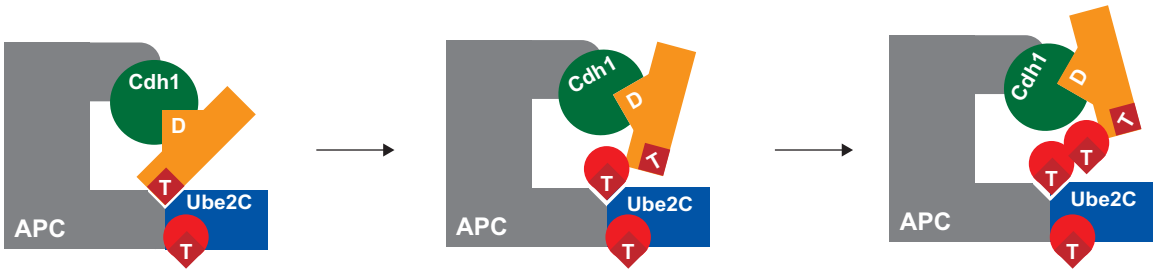

Supplementary Figure 7

Chapter 3

Regulation of Ubiquitin Chain Initiation to Control the Timing of Substrate Degradation

Adam Williamson*, Sudeep Banerjee*, Xining Zhu, Isabelle Phillip, Anthony T. Iavarone, and Michael Rape

Molecular Cell (2011) *42*, 744-757

* equal contribution

Summary

Processive reactions, such as transcription or translation, often proceed through distinct initiation and elongation phases. The processive formation of polymeric ubiquitin chains can accordingly be catalyzed by specialized initiating and elongating E2 enzymes, but the functional significance for this division of labor has remained unclear. Here, we have identified sequence motifs in several substrates of the anaphase-promoting complex (APC/C) that are required for efficient chain initiation by its E2 Ube2C. Differences in the quality and accessibility of these motifs can determine the rate of a substrate's degradation without affecting its affinity for the APC/C, a mechanism used by the APC/C to control the timing of substrate proteolysis during the cell cycle. Based on our results, we propose that initiation motifs and their cognate E2s allow E3 enzymes to exert precise temporal control over substrate degradation.

Introduction

Processive reactions including transcription and translation proceed through distinct initiation, elongation, and termination phases. Each of these steps requires specialized proteins, such as translation initiation or elongation factors, which are often regulated independently of each other. For example, regulation of translation initiation provides a means to rapidly change protein synthesis in response to stress (Sonenberg and Hinnebusch, 2009).

Reminiscent of translation, the formation of ubiquitin chains can be a highly processive reaction (Pierce et al., 2009; Rape et al., 2006), which is catalyzed by a cascade of E1, E2, and E3 enzymes (Ye and Rape, 2009). Dedicated factors are able to bring about initiation, the attachment of ubiquitin to a substrate lysine, or elongation, the formation of chains linked through Lys resides on ubiquitin. For example, the assembly of ubiquitin chains on PCNA requires the E3s Rad18 for initiation and Rad5 for elongation (Hoege et al., 2002). In a similar manner, chain initiation on substrates of the UFD pathway depends on the E3 Ufd4, while elongation is catalyzed by Ufd2 (Koegl et al., 1999). Distinct E3s for initiation and elongation allow cells to produce either mono- or multiubiquitylated substrates, which results in different consequences for the modified protein (Ye and Rape, 2009).

In a variation on this theme, several E3 enzymes employ distinct E2s to catalyze chain initiation or elongation, respectively. This phenomenon was first described for the E3 Brca1-Bard1, which can utilize the E2s Ube2D, Ube2E, or Ube2W for initiation but Ube2K or Ube2N-Uev1A for elongation (Christensen et al., 2007). In human cells, the E3 SCF appears to cooperate with Ube2D or Ube2R (Cdc34) for initiation, while it relies on Ube2R to elongate K48-linked ubiquitin chains (Petroski and Deshaies, 2005b; Wu et al., 2010). A similar division of labor is observed for the human E3 APC/C, which employs Ub2C (UbcH10) for initiation but Ube2S for the elongation of K11-linked ubiquitin chains (Garnett et al., 2009; Jin et al., 2008; Williamson et al., 2009; Wu et al., 2010). Both the APC/C and the SCF are able to promote chain formation with high processivity (Carroll and Morgan, 2002; Petroski and Deshaies, 2005b; Pierce et al., 2009; Rape et al., 2006), but distinct functions for monoubiquitylated substrates of these

E3s have not been reported. This strongly suggests that specialized E2s provide regulatory advantages that remain to be discovered.

The initiating E2s select Lys residues in substrates as acceptors for ubiquitin. Much of our knowledge about substrate lysine selection comes from studies of the E2 Ubc9, which transfers the ubiquitin-like modifier SUMO to hundreds of cellular proteins. Ubc9 directly binds substrate residues of the consensus SUMOylation motif, ΨKxE/D (Bernier-Villamor et al., 2002). Charged amino acids close to this motif can enhance nearby Ser or Thr residues allows for regulation (Mohideen et al., 2009). Lysine selection by Ubc9, therefore, is strongly influenced by degenerate sequence motifs in the substrate.

In contrast to SUMOylation, little is known about how ubiquitin-initiating E2s decide on substrate lysine residues for modification. Global analyses of ubiquitylation sites did not reveal strong preferences for specific sequence environments (Xu et al., 2009), suggesting that E2s utilize distinct strategies to determine acceptor sites for the first ubiquitin. Consistent with this hypothesis, the APC/C-specific E2 Ube2C requires residues in the APC/C-substrate securin for efficient chain initiation (Jin et al., 2008). The respective sequence in securin contained a Thr-Glu-Lys motif, and hence was labeled TEK box, but the amino acids responsible for promoting chain initiation were not determined. In a similar manner, the SCF-specific E2 Cdc34 has been suggested to recognize residues proximal to the modified lysine of the SCF-substrate Sic1 (Sadowski et al., 2010). However, as the sequences in securin and Sic1 were not characterized in detail, the recurrence of initiation motifs in multiple substrates of the same E3, their recognition by initiating E2s, and their potential regulation remained unknown. The significance of initiation motifs and their cognate E2s for ubiquitin-dependent proteolysis is, therefore, not understood.

Here, we dissected the mechanism of ubiquitin chain initiation by the human APC/C and its E2 Ube2C. We have identified a conserved initiation motif that is found in multiple APC/C substrates. Our characterization of this motif revealed three important functions in proteolysis: 1. Initiation motifs increase the efficiency of substrate degradation to allow the APC/C to degrade its many substrates; 2. The composition of initiation motifs determines the rate of substrate degradation to help the APC/C coordinate cell cycle progression; and 3. The recognition of initiation motifs by Ube2C can be regulated to fine-tune the timing of substrate degradation. Our findings, therefore, establish initiation motifs as substrate elements with important roles in protein degradation. Together with their cognate E2s, initiation motifs increase the capacity of E3s to exert precise temporal control over substrate degradation.

Results

Identification of an Essential Initiation Motif in the APC/C-Substrate Geminin

We previously found that deletion of residues in the APC/C substrate securin, its TEK box, impaired chain initiation by the APC/C-specific E2 Ube2C (Jin et al., 2008). Due to the mild effects of these deletions on securin degradation, we were unable to determine the functionally important residues in this motif. As a consequence, initiation motifs were not identified in other APC/C substrates, and their role in regulating degradation remained unclear.

Our earlier studies had shown that the ubiquitylation of the replication inhibitor geminin by the APC/C is completed by a peptide derived from the securin TEK box, suggesting that geminin and securin use similar residues to promote initiation (Jin et al., 2008). Similar to *Xenopus* (McGarry and Kirschner, 1998), human geminin depends on a D box for degradation in extracts and cells, and for ubiquitylation by APC/C (Figures 1A – 1C). Residues in proximity to the D box shared similarity to the securin TEK box (Figure 3-S1C), and these residues (IM, for initiation motif) were required for the APC/C dependent ubiquitylation and degradation of geminin (Figures 1A-1D). As seen with stable geminin$^{\Delta D}$, injection of geminin$^{\Delta IM}$ into *Xenopus* embryos caused cell cycle arrest and death (Figure S1D). Thus, geminin contains a candidate initiation motif that is required for APC/C-dependent degradation and cell cycle progression.

Several observations suggest that the new motif in geminin specifically promotes chain initiation. First, its deletion strongly inhibited the APC/C-dependent modification of geminin Lys residues with methylubiquitin (Figure 1E). Second, a Lys residue within this motif was found to be a major initiation site for APC/C and Ube2C, as determined by mass spectrometry (Figure 1G). Third, once initiation was accomplished (Ub-L-geminin; Ub-L-geminin$^{\Delta IM}$), the APC/C was able to elongate chains independently of whether this motif was present or not (Figure 1F; Figure S1E). Fourth, deletion of this motif did not abrogate binding of geminin to Cdh1, showing that it is not required for substrate recruitment (Figure 1H). Fifth, geminin mutants lacking this motif inhibited the ubiquitylation of other APC/C substrates with comparable efficiency as WT-geminin, suggesting that it does not mediate APC/C binding (Figure 1I). Together, these findings document a central and specific role for the geminin motif in promoting chain initiation and proteasomal degradation.

Initiation Motifs Are Found in Several APC/C Substrates

As deleting its initiation motif abolished geminin degradation, we used this substrate to identify key residues required for promoting initiation. We found that mutation of charged residues (RE40/41, KRK50-52, HR53/54) to alanine interfered with the APC/C-dependent ubiquitylation and degradation of geminin (Figure 2A; Figure S2A). Assays with methylubiquitin revealed that RE40/41, KRK50-52, and HR53/54 were required for efficient chain initiation (Figure 2B). Interestingly, changing all Lys residues to arginine did not strongly affect geminin degradation or chain initiation, showing that the initiation motif has functions in addition to providing acceptor sites. As expected for a motif controlling the degradation of a key cell cycle regulator, functionally important, but not irrelevant, residues are highly conserved among geminin homologs from different organisms (Figure S2B).

The initiation motif in geminin is close to the D box, its main APC/C binding site, and the distance between the two motifs is conserved among geminin homologs (Figure S2B). This observation raised the possibility that the position of the initiation motif relative to the D-box is important for APC/C-substrate degradation. Consistent with this hypothesis, altering the distance between D box and initiation motif through insertion of Gly/Ser repeats impaired initiation by the APC/C, Ube2C, and methylubiquitin (Figure 2D), and stabilized geminin against proteasomal degradation (Figure 2C). The geminin

initiation motif is, therefore, comprised of conserved patches of charged residues that occur in proximity to its APC/C-binding motif, the D box.

Based on these results, we identified initiation motifs in the APC/C substrates cyclin B1, Plk1, and securin (Figure S2C). In securin, the motif is part of the TEK box, the deletion of which provided the first evidence for a role of substrate residues in promoting initiation (Jin et al., 2008). Mutation of these motifs impaired chain initiation without strongly affecting substrate affinity to the APC/C (Figures 2E-2G); Figures S2D-S2F). As seen before, replacing all Lys residues with arginine did not abrogate the function of the initiation motifs (Figures S2G-S2F). As seen before, replacing all Lys residues with arginine did not abrogate the function of the initiation motifs (Figures S2G and S2H). In securin, a group of Lys residues was rapidly modified despite a mutant initiation motif; we suspect that the alternative APC/C binding of securin through its KEN box, rather than its D box, leads to distinct initiation (Figure S2I). Thus, initiation motifs consist of conserved patches of charged residues close to an APC/C binding motif and are found in multiple substrates of the APC/C. The complexity of APC/C initiation motifs is similar to the consensus SUMOylation or CDK phosphorylation motifs that are also recognized by enzymes with a large number of cellular substrates. Thus, or observations imply a general role for initiation motifs in promoting APC/C-dependent degradation.

Initiation Motifs Allow Negative Feedback Regulation of the APC/C

We next set out to identify roles for initiation motifs in ubiquitin-dependent proteolysis. We hypothesized that initiation motifs could allow E3s to separate substrate binding from ubiquitylation, which is required for a poorly understood aspect of APC/C regulation: during mitosis, Ube2C, Ube2S, Cdc20, or Cdh1 binds the APC/C to trigger the ubiquitylation of APC/C substrates. However, once most substrates have been turned over, the APC/C binding of these proteins results in their own ubiquitylation and degradation, leading to APC/C inhibition. For this feedback to work, mechanisms that independently control the binding and ubiquitylation of these activators must exist.

To address this question, we focused on Ube2C. We first determined whether Ube2C contains an initiation motif that is required for its own ubiquitylation, but not for APC/C binding. Previous work had shown that the first 27 amino acids of Ube2C are pivotal for its ubiquitylation by the APC/C (Rape and Kirschner, 2004), and conserved residues within this appendix have homology to the initiation motifs described above (Figure 3A). Changing positively charged residues in this motif to alanine (R6A, R17A/K18A), but not arginine (K18R), strongly impaired the APC/C-dependent degradation in extracts and cells (Figure 3C; Figure S3B), while they had no ($Ube2C^{R6A}$) or weak effects ($Ube2C^{R17A/K18A}$) on charging by E1 (Figure S3C). Thus, Ube2C contains an initiation motif required for its degradation.

To test whether its initiation motif contributes to the binding of Ube2C to the APC/C, we monitored the E2 activity of Ube2C and $Ube2C^{R6A}$. We found that over a wide concentration range, $Ube2C^{R6A}$ catalyzed the ubiquitylation of APC/C substrates and promoted their degradation with similar efficiency as that of Ube2C (Figure 3D; Figures S3D and S3E). By contrast, mutating the RING-interaction loop, deleting an N-terminal epitope tags reduced the activity of Ube2C toward APC/C substrates (Figure 3D; Figures

S3D and S3E). By contrast, mutating the RING-interaction loop, deleting an N-terminal QNP motif (Summers et al., 2008), or appending N-terminal epitope tags reduced the activity of Ube2C toward APC/C substrates (Figures S3D and S3F). Thus the initiation motif does not appear to mediate the binding of Ube2C to the APC/C.

To validate these findings, we introduced mutations into the catalytically inactive Ube2C^{C114S}. If mutations impede APC/C binding, the inhibitory effect of Ube2C^{C114S} on degradation of APC/C substrates in extracts or on cell cycle progression in frog embryos should be lost. Consistent with our previous observations, the initiation motif mutant Ube2C$^{R6A/C114S}$ stabilized APC/C substrates as efficiently as Ube2C^{C114S} (Figure 3E). Moreover, when injected into *Xenopus* embryos, Ube2C$^{R6A/C114S}$ produced the same cell cycle arrest as Ube2C^{C114S} (Figure 3F). By contrast, mutation of the RING-interaction loop (Y91D) strongly diminished the capacity of Ube2C^{C114S} to block degradation and cell cycle progression (Figures 3E and 3F). These findings show that Ube2C mainly interacts with the APC/C by recognizing the RING domain of Apc11. Its initiation motif is, therefore, only required for Ube2C degradation, but not for APC/C binding.

As a consequence, competition between initiation motifs could explain how canonical substrates Ube2C when both are bound to APC/C. Although substrates and Ube2C are recruited to the APC/C by different means, using D boxes or a RING-interaction loop, both require initiation motifs for chain formation. Consistent with this hypothesis, a mutant of the APC/C substrate securin that only contains its initiation, but not its APC/C-binding motifs (securin$^{\Delta D \Delta KEN}$), inhibited the ubiquitylation of Ube2C by the APC/C (Figure 3-3G, Figure S3G). This competitor did not impair APC/C binding of Ube2C, as it did not block the APC/C-dependent chain elongation on Ube2C that had already undergone initiation (Figure 3G). Thus, competition by substrate initiation motifs stabilizes Ube2C that is bound to the APC/C in its role as E2; this strongly suggests that initiation motifs allow an E3, i.e., the APC/C, to regulate substrate binding and ubiquitylation independently of each other.

Initiation Motifs Can Determine the Rate of Substrate Degradation

The APC/C degrades its substrates at different times during cell division to establish the sequence of mitotic events. The timing of APC/C-substrate degradation correlates with the processivity of ubiquitin chain formation, yet mechanisms that generate differences in the processivity remain unclear (Rape et al., 2006). As initiation can be rate limiting for ubiquitylation (Pierce et al., 2009), initiation motifs could have strong effects on the processivity of chain formation and the timing of substrate degradation.

To test this hypothesis, we replaced the initiation motif of Ube2C, which is among the last proteins to be degraded by the APC/C, with that of the early substrate geminin. Strikingly, the resulting mutant IM^{gem}-Ube2C was ubiquitylated by the APC/C much more rapidly that WT-Ube2C, which was dependent on its own active site and RING-interaction loop (Figures 4A and 4B). Assays with methylubiquitin revealed that chain initiation by the APC/C occurred much more efficiently on IM^{gem}-Ube2C competed to WT-Ube2C (Figure 4C). IM^{gem}-Ube2C was degraded in extracts with active APC/C^{Cdh1} much more rapidly that WT-Ube2C (Figure 4C), which was dependent on APC/C^{Cdh1} and

the proteasome (Figure S4A and S4B). Importantly, IM^{gem}-Ube2C was also degraded much faster that WT-Ube2C upon APC/C activation in cells (Figure 4E).

Altering its initiation motif did not strongly affect binding of Ube2C to the APC/C, as Ube2C and IM^{gem}-Ube2C modified APC/C substrates with similar efficiency (Figure S4C). The small differences between IM^{gem}-Ube2C and Ube2C can be explained by a decrease in the charging IM^{gem}-Ube2C by E1, as expected from a previous report (Figure S4D; (Huang et al., 2008)). Moreover, the same levels of $Ube2C^{C114S}$ and IM^{gem}-$Ube2C^{C114S}$ inhibited APC/C-substrate degradation in extracts and produced a block in cell division in embryos. Thus replacing the initiation motif of Ube2C with that of geminin accelerated with ubiquitylation of Ube2C without significantly affecting its binding to the APC/C or its activity as an E2.

To determine whether weak initiation motifs delay degradation, we replaced the initiation motif of geminin with that of Ube2C. The resulting mutant IM^{Ube2C}-geminin was modified with methylubiquitin more slowly than WT-geminin (Figure 4G), indicating impaired initiation. This caused less efficient chain formation (Figure S4F), and IM^{Ube2C}-geminin was degraded more slowly that geminin in extracts and cells (Figure 4H, Figures S4G and S4H). Competition assays using recombinant geminin or IM^{Ube2C}-geminin showed that altering its initiation motif did not change the affinity of geminin to the APC/C (Figure 4I). The initiation motif of Ube2C was functional in geminin, as IM^{Ube2C}-geminin was modified and degraded more efficiently that $geminin^{\Delta IM}$; moreover, IM^{Ube2C}-geminin was stabilized by mutation of Arg6 in the Ube2C initiation motif (Figure 4H). These swap experiments, therefore, show that the composition of initiation motifs can determine the rate of substrate degradation without affecting their affinity for the E3.

Initiation Motifs Allow the Identification of an APC/C Substrate, PAF15

Given their role in degradation, we asked whether initiation motifs could be regulated, a control mechanism likely to occur in substrates that depend on initiation motifs for their degradation. To identify such substrates, we searched for proteins that contain D or KEN boxes in proximity to conserved sequences with similarity to the initiation motifs described above. A top hit predicted by our search was PCNA-associated factor or 15 kDa (PAF15), a protein with roles in S phase and DNA repair (Hosokawa et al., 2007; Turchi et al., 2009; Yu et al., 2001). Consistent with its bioinformatic prediction, PAF15 was rapidly degraded in an APC/C- and proteasome-dependent manner in extracts (Figure 5A). PAF15 was also turned over by the APC/C in cells, as seen by Cdh1 overexpression (Figure 5D), depletion of the APC/C inhibitor Emi1 (Figure 5SB), release of nocodazole-arrested HeLa cells (Figure S5C), or serum starvation of T24 cells (Figure S5D). Confirming its role as a substrate, PAF15 was ubiquitylated by purified APC/C, but not if APC/C was inhibited by Emi1 (Figure S5B) or an excess of competing APC/C substrate (Figure 5B). Thus, despite their degenerate nature, initiation motifs have sufficient predictive power to enable the discovery of new APC/C substrates.

We next determined whether PAF15 ubiquitylation and degradation depend on its initiation motif. Indeed, mutation of the positively charged residues in this motif to Ala, but not to Arg, inhibited chain initiation on PAF15 by APC/C and methylubiquitin (Figure 5F; Figure S5E). By contrast, the initiation motif was not required for binding of PAF15 to Cdh1 (Figure 5G), and ubiquitylation reactions with Ub-PAF15 fusions

showed that the initiation motif had no role in promoting Ube2S- and APC/C-dependent chain elongation (Figure 5H). Importantly, PAF15 mutants in the initiation motif were not polyubiquitylated by the APC/C and therefore stabilized against APC/C-dependent degradation in extracts and cells (Figures 5C-5E). Thus, the APC/C substrate PAF15 requires a functional initiation motif for degradation.

Initiation Motifs Allow Regulation of Protein Degradation

PAF15 binds the DNA polymerase processivity factor, PCNA, through a PIP box located between D box and initiation motif (Figure 6A; (Yu et al., 2001)). When we tested the interaction between PAF15 and PCNA in cells, we found that a PIP box mutation not only ablated the binding of PAF15 to PCNA but also caused a strong decrease in PAF15 levels (Figure 6B). A similar effect on PAF15 levels was observed upon depletion of PCNA by siRNA (Figure 6G). The low abundance of $PAF15^{\Delta PIP}$ was rescued by mutation of its D and KEN boxes, suggesting that PCNA stabilizes PAF15 by antagonizing the APC/C. Supporting this notion, addition of PCNA to extracts stabilized PAF15, but not $PAF15^{\Delta PIP}$, against APC/C-dependent degradation (Figure 6F).

As the PIP box in PAF15 is located between D box and initiation motif, PCNA might interfere with initiation. Indeed, when PCNA was added to reactions containing APC/C, Ube2C, and methylubiquitin, it inhibited chain initiation on PAF15 in a concentration-dependent manner (Figure 6C). As a result of the reduced initiation, PCNA impaired the modification of PAF15 with WT-ubiquitin with an identical concentration dependency (Figure 6D). PCNA had no effects on the APC/C-dependent ubiquitylation of $PAF^{\Delta PIP}$, and it did not inhibit the modification of APC/C substrates that do not interact with PCNA (Figure 6E). Thus, PCNA inhibits chain initiation on PAF15 in a substrate specific manner.

In contrast to its effect on initiation, PCNA did not inhibit binding of PAF15 to the APC/C. First, the PIP box was not required for the interaction of PAF15 with Cdh1 or for its degradation by APC/C (Figure 6F; Figure S6). Moreover, pulldown assays showed that ^{Gst}PAF15 efficiently bound Cdh1, even if it was saturated with PCNA prior to incubation with Cdh1 (Figure 7A). These experiments suggest that binding sites for Cdh1 and PCNA are far enough apart to allow PAF15 to bind both proteins at the same time. Indeed, PAF15 was able to bridge an interaction between GstPCNA and Cdh1, which provides evidence for ternary complexes between ^{Gst}PAF15, PCNA and Cdh1 (Figure 7B). To test this in vivo, we precipitated ^{FLAG}PAF15-containing complexes from HeLa cells, eluted with peptide, reprecipitated with antibodies against APC/C, and probed for PCNA. Confirming our in vitro studies, these experiments revealed the existence of ternary complexes between PAF15, PCNA, and the APC/C in cells (Figure 7C).

To test whether PCNA affects chain elongation, we studies a fusion between ubiquitin and PAF15, Ub-L-PAF15. We bound Ub-L-PAF to ^{Gst}PCNA and incubated these complexes with APC/C and either Ube2C for initiation or Ube2S for elongation. As seen previously, Ube2C was unable to ubiquitinate Ub-L-PAF15 that was stoichiometrically bound to PCNA (Figure 7D). In contrast, Ube2S efficiently elongated ubiquitin chains on PCNA-bound Ub-L-PAF15 in an APC/C-dependent manner. This experiment shows that PCNA does not block the binding of PAF15 to the APC/C nor

chain elongation by Ube2S. Instead, PCNA specifically inhibits the activity of the initiating E2 Ube2C towards PAF15.

The Initiation Efficiency Controls the Timing of Substrate Degradation

To analyze the impact of regulating chain initiation, we constructed stable cell lines that stably express from a constitutive promoter: ^{FLAG}PAF15, which is recognized by PCNA and has impaired chain initiation; ^{FLAG}PAF15$^{\Delta PIP}$, which does not PCNA and has rapid initiation; and ^{FLAG}PAF15$^{\Delta D \Delta KEN}$ or ^{FLAG}PAF15$^{\Delta D \Delta KEN/\Delta PIP}$, which should be inert against the APC/C. Expression of PAF15 mutants at low levels did not strongly affect cell cycle progression, as seen by FACS or BrdU-staining (Figures S7A and S7B). Cells synchronized in prometaphase were released into fresh medium to activate APC/C, and PAF15 levels were monitored until S phase, when APC/C is inhibited again. Three important observations were made (Figure 7E). First, PAF15 was degraded less efficiently and later than PAF15$^{\Delta PIP}$, indicating that the decreased initiation efficiency in WT-PAF15 delays substrate turnover. Second, PAF15 accumulated once Ube2C levels had dropped below a certain threshold (Figures 7E and 7F), but PAF15$^{\Delta PIP}$ was degraded throughout G1. Thus, reducing the initiation efficiency increases the dependency on the initiating E2. Third, PAF15 lacking its D and KEN boxes was stable independently of whether it was able to bind PCNA or not, showing that its degradation occurred through APC/C. These findings demonstrate that initiation motifs provide and effective means of controlling the timing of substrate degradation.

Discussion

Here, we report that efficient chain initiation by the APC/C-specific E2 Ube2C requires motifs that are present in multiple APC/C substrates. Variations in the composition of these initiation motifs can determine the rate of substrate degradation without affecting their affinity for the E3. Initiation motifs also provide and opportunity for regulation, which is used by APC/C to control the timing of substrate proteolysis during the cell cycle. On the basis of these results, we propose that initiation motifs and their cognate E2s increase the capacity of E3s to exert temporal control over substrate degradation.

Characteristics of Initiation Motifs

Studies with the ubiquitin-like modifier SUMO had shown that residues in the vicinity of a substrate lysine can affect the efficiency of modification by an E2 (Bernier-Villamor et al., 2002; Mohideen et al., 2009). Our results indicate that chain initiation by the APC/C and Ube2C can in be controlled in an analogous manner by sequence motifs in substrates that are close to our overlapping with the preferred attachment site for the first ubiquitin. As mutation of initiation motifs stabilized several APC/C, they play a key role in promoting ubiquitin-dependent degradation.

In all APC/C substrates analyzed here, charged residues were required for the function of initiation motifs. As seen with geminin, Lys residues in the initiation motif can serve as major acceptor sites for ubiquitin. However, the initiation motifs in geminin,

securin, cyclin B1, Plk1, Ube2C, and PAF15 were still functional if all lysines sere mutated to arginine, which retains the positive charge but is unable to act as ubiquitin acceptor. We conclude that initiation motifs contain modified lysines but also promote the interaction of the substrate with an initiating E2, similar to binding of the consensus SUMOylation motif by Ubc9 (Bernier-Villamor et al., 2002).

With the exception of Ube2C, initiation motifs were found close to substrate D boxes. In geminin, altering the distance between its APC/C-binding motif, the D box, and the initiation motif impaired chain initiation and degradation, underscoring the importance of the proper location of an initiation motif. This finding is in agreement with structural analyses of the APC/C, which place the RING domain subunit Apc11, and by inference Ube2C, in proximity to the D box coreceptors Apc10 and Cdh1 (da Fonseca et al., 2011). Thus situation is also reminiscent of the SCF, which ubiquitinates ß-catenin and IκBα on Lys residues in proximity to their $SCF^{ß\text{-}trCP}$-binding motifs (Wu et al., 2003). Thus, the presence of conserved patches of charged residues in proximity to an APC/C-binding motif is the main characteristic of initiation motifs recognized by Ube2C.

Functions of Initiation Motifs

The activation of the APC/C during mitosis results in the massive upregulation of K11-linked chains (Matsumoto et al., 2010), implying a large number of APC/C substrates in human cells. As the concentration of active APC/C is comparably low, the APC/C likely acts close to saturation. Indeed, increasing the concentration of a single substrate was sufficient to bring cell division to a half by overloading the APC/C (Marangos and Carroll, 2008). Kinetic studies with the SCF found that most encounters between this E3 and its substrates result in substrate dissociation before ubiquitylation can take place (Pierce et al., 2009). Due to its large number of substrates, unproductive binding events might be detrimental for APC/C-dependent ubiquitylation. Initiation motifs, however, provide an elegant means to sufficiently increase the rate of degradation to allow the APC/C to shoulder the burden of its many substrates.

Our experiments suggest that the APC/C also implements initiation motifs to fine-tune the rate of substrate degradation. Once activated, the APC/C promotes substrate turnover in a conserved sequence, ensuring that inhibitors of anaphase are degraded prior to proteins required for chromosome segregation or cytokinesis (Peters, 2006). Previous work had shown that the processivity of chain formation, but not the affinity of a substrate to the APC/C, correlates with the degradation time in cells (Rape et al., 2006). Because more rapid initiation increases the processivity of ubiquitylation (Pierce et al., 2009), it should accelerate the rate of substrate degradation. As seen in initiation motif swaps using geminin and Ube2C, and in a mutational analysis of the APC/C substrate PAF15, this is the case: improving the quality or accessibility of initiation motifs accelerated the degradation of Ube2C or PAF15, whereas reducing the quality of the initiation motif in geminin delayed its degradation. Altering initiation motifs had little effect on substrate affinity for the APC/C. These findings identify chain initiation as the rate limiting step for degradation of many APC/C substrates, in analogy to the SCF (Pierce et al., 2009). As a result, initiation motifs play a critical role in determining the timing of substrate degradation by the APC/C.

Regulation of Chain Initiation

As initiation motifs differ from APC/C-binding sites, the APC/C can separate substrate binding and ubiquitylation to establish negative feedback regulation: during mitosis, APC/C activators, such as Ube2C, bind the E3 and modify its substrates without being degraded themselves. However, when Ube2C engages the APC/C after substrates have been turned over, it undergoes APC/C-dependent ubiquitylation and degradation (Rape and Kirschner, 2004). We found that ubiquitylation of Ube2C, but not its APC/C binding, requires an N-terminal initiation motif. Increasing the quality of this initiation motif accelerated Ube2C ubiquitylation without affecting its association with the APC/C. Moreover, competition by substrate initiation motifs inhibited Ube2C degradation without affecting its APC/C binding or E2 activity. Thus, even though the initiation motif does not determine the affinity of Ube2C to the APC/C, its accessibility helps determine the timing of Ube2C degradation.

Regulating the initiation efficiency also controls the timing of degradation and reaccumulation of canonical substrates, such as PAF15. PAF15 is strongly stabilized by its binding to PCNA, which selectively inhibits chain initiation, yet has no effects on APC/C binding or chain elongation. As the PIP cox in PAF15 is located between D box and initiation motif, PCNA might sterically block access of Ube2C to the PAF15 initiation motif. The stabilization of PAF15 by PCNA might play a role during late G1 or upon DNA damage, when PAF15 has been suggested to cooperate with PCNA, yet APC/C is active (Hosokawa et al., 2007). It is also possible that PAF15 bridges an interaction between PCNA and APC/C, thereby recruiting APC/C to sites of ubiquitylation on DNA; the degradation of PAF15 upon dissociation of PCNA might then provide negative feedback.

These findings provide an unappreciated function for PCNA in cell cycle control. Initially defined as a processivity factor DNA polymerases, PCNA had recently been shown to be an important regulator of protein degradation during S phase. By binding to an extended PIP box, PCNA increases the affinity of the CDK inhibitor p21 for the E3 $Cul4^{Cdt2}$, thereby triggering p21 degradation (Havens and Walter, 2009). By contrast, PCNA stabilizes PAF15, a protein required for S phase progression. Although more work is required, this may indicate that PCNA acts as a switchboard to degrade or stabilize cell cycle regulators, depending on their function in DNA replication or repair.

In conclusion, we show that initiation motifs allow the APC/C to precisely control the timing of substrate degradation. Our observations extend the similarities between the formation of ubiquitin chains and other processive reactions, such as transcription or translation, which can be divided into distinct initiation, elongation, and termination steps. Whether we can learn more by comparing the mechanisms of ubiquitin chain initiation and those long-studied processive reactions will be an interesting avenue of future research.

The APC/C works with Ube2C for chain initiation and Ube2S for chain elongation. In Chapter 3 I presented our work showing that chain initiation on APC/C substrates by Ube2C is the regulated, rate-limiting step in APC/C substrate degradation. Initiation motifs vary between APC/C substrates and characteristics of initiation motifs determine the timing of substrate degradation during mitosis. This was most clearly shown swap experiments in which we replaced the initiation motif of a late-mitotic

substrate, Ube2C, with that of an early mitotic substrate, geminin. IM^{geminin}-Ube2C was degraded earlier in mitosis than WT Ube2C, demonstrating that initiation motifs are transferrable elements that determine the timing of APC/C substrate degradation.

How does the APC/C balance carefully regulated chain initiation to orchestrate ordered substrate degradation with its enormous number of substrates that must be degraded within a short time window? The answer lies in Ube2S, a K11-specific chain elongating E2 enzyme. Ube2S does not modify substrate lysine residues, but instead elongates ubiquitin chains that have already been initiated. Ube2S is specific for K11 on ubiquitin and performs rapid chain elongation, allowing APC/C to regulate substrate degradation while nevertheless powering rapid unidirectional substrate degradation during mitosis. In Chapter 4 I present our discovery and initial characterization of Ube2s, which works in concert with Ube2C to power APC/C-dependent substrate degradation.

Methods

A detailed description of the methods can be found in the Supplementary Information accompanying this manuscript: http://www.sciencedirect.com/science/article/pii/S1097276511003686

Plasmids and Reagents

Table S1 lists all constructs, antibodies, and siRNAs. pCS2 or pCS2-ZZ/TEV were used for IVT/T and expression in cells; pET28, pGEX, or pMAL for purification; and pCMV for generation of stable cell lines.

Degradation Assays

Degradation assays were performed as described (Rape et al., 2006). Ube2C and IM^{TEK}-Ube2C were synthesized as ZZ/TEV fusions, purified over IgG-Sepharose, and eluted by TEV cleavage, before addition to extracts.

In Vivo Degradation and siRNA Experiments

293T cells were transfected with substrate plasmid, ^{myc}Cdh1, and Emi1 using TransIT-293. Twenty-four hours posttransfection, lysates were analyzed by western blot. Release experiments were performed in HeLa cells transfected with substrate (TransIT-LT1), arrested by thymidine/nocodazole, and replated after shake-off in fresh medium. For analysis of PAF15 degradation, HeLa cells stably expressing FLAGPAF15 mutants were used.

siRNA experiments were performed in HeLa cells transfected with siRNA against the 3'UTR of PAF15 or PCNA using HiPerfect. Phenotypes were identical for different siRNAs per gene, and strong effects on cell cycle progression were excluded by FACS analysis.

Ubiquitylation Assays

Ubiquitylation assays were performed as described (Rape et al., 2006). Ub-L-geminin and Ub-L-PAF15 were synthesized in reticulocyte lysate containing 175 μM ubi^{K29R} to inhibit the UFD pathway. Ub-L-geminin, Ub-L-PAF15, PAF15, and Ube2C were synthesized as ZZ/TEV fusions, purified on IgG-Sepharose, and eluted by TEV cleavage. ^{Gst}PCNA /Ub-L-PAF15 complexes were purified by incubating Ub-L-PAF15 with ^{Gst}PCNA coupled to glutathione Sepharose 4B.

Detection of Ternary Complexes between APC/C, PAF15, and PCNA in Cells

HeLa cells stably expressing FLAGPAF15 or control cells were synchronized in prometaphase. Lysates were incubated with anti-FLAG M2 affinity resin. After washing, bound proteins were eluted with peptide. Pooled eluates were incubated with αCdc27 antibodies and protein G agarose. After washing, proteins were eluted with SDS sample buffer and analyzed by western blot.

Xenopus tropicalis Embryo Injection

Embryos collected from mating *X. tropicalis* couples were dejellied for 5 min in 3% cysteine (pH 8.0), and transferred to 3% ficoll in 1/9x Modified Ringer solution. One cell of a two-cell stage embryo was injected with 3 or 6 ng of protein (final concentration ~1 μM at the two cell stage) premixed with rhodamine-tubulin for lineage tracing. Injected embryos were evaluated by fluorescence and scored for stage and phenotype.

Determination of Ubiquitylation Sites on Geminin

Recombinant geminin was incubated with APC/C, E1, Ube2C and methylubiquitin. Monoubiquitylated geminin was excised from SDS-gels, trypsinized. and subjected to tandem mass spectrometry, as detailed in the Supplemental Information.

Supplemental Information

Supplemental Information includes seven figures, one table, and Supplemental Experimental Procedures and can be found with this article at: http://www.sciencedirect.com/science/article/pii/S1097276511003686

Acknowledgments

We thank the Rape lab for helpful discussions, the Heald lab for rhodamine-tubulin, and Julia Schaletzky for reading the manuscript and many suggestions. Mass spectrometry instrumentation was supported by the National Institutes of Health (NIH) (1S10RR022393).

Figure Legends

Figure 1: Geminin Requires an Initiation Motif for Degradation

(A) Degradation of 35S-geminin mutants in extracts with active APC/C was analyzed by autoradiography. **(B)** Geminin's initiation motif is required for degradation in 293T cells after transfection with HACdh1. **(C)** Its initiation motif is required for geminin degradation in HeLa cells synchronized in mitosis. **(D)** The initiation motif drives geminin ubiquitylation. 35S-geminin mutants were incubated with APC/C, Ube2C, and ubiquitin and analyzed by autoradiography. **(E)** The initiation motif is 35S-geminin is important for chain initiation by APC/C, Ube2C, and methylubiquitin. **(F)** The initiation motif is not required for chain elongation. Modification of 35S-Ub-L-geminin mutants by APC/C and Ube2S was analyzed by autoradiography. **(G)** The initiation motif contains a preferential modification site (Lys50), as seen upon analysis of monoubiquitylated geminin by tandem mass spectrometry. **(H)** The initiation motif is not essential for Gstgeminin-binding to 35S-Cdh1, as seen by autoradiography. **(I)** The initiation motif is not required for APC/C binding of geminin. Ubiquitylation of 35S-cyclin A by APC/C and Ube2C was analyzed in the presence of increasing concentrations of His-geminin mutants.

Figure 2: Initiation Motifs Are Found in Several APC/C Substrates

(A) Degradation of 35S-geminin mutants in extracts with active APC/C requires positively charged residues in its initiation motif. **(B)** Positively charged residues are required for chain initiation on 35S-geminin APC/C, Ube2C, and methylubiquitin. **(C)** The position of the initiation motif relative to the D box is important for function. Degradation of 35S-geminin mutants with insertions of 5 or 20 GS repeats between D box and initiation motif in extracts with active APC/C was analyzed by autoradiography. **(D)** Changing the position of the initiation motif impairs substrate Lys modification. Ubiquitylation of 35S-geminin mutants by APC/C, Ube2C, and methylubiquitin was analyzed by autoradiography. **(E)** Cyclin B1 contains a chain initiation motif. Ubiquitylation of 35S-cyclin B1 or an initiation motif mutant (K63KE/AAA; Δ73-78) by APC/C, Ube2C, and methylubiquitin was analyzed by autoradiography. **(F)** Plk1 contains a chain initiation motif. Modification of 35S-Plk1 or an initiation motif mutant (Δ354-358) with methylubiquitin was analyzed as above. **(G)** Securin contains an initiation motif. Modification of 35S-securin or an initiation motif mutant (K82QKQ/AAAA; K91K/AA) with methylubiquitin was analyzed as above.

Figure 3: Initiation Motifs Allow Negative Feedback Regulation of APC/C

(A) The N terminus of Ube2C contains a candidate initiation motif. **(B)** Its initiation motif is required for ubiquitylation: 35S-Ube2C by APC/C , E1, and ubiquitin, as seen with autoradiography. Asterisks denote ubiquitylation of K119 and K121 of Ube2C, which does not require the APC/C. **(C)** The initiation motif is required for rapid degradation of 35S-Ube2C in extracts with active APC/C and low levels of APC/C substrates. **(D)** The initiation motif in Ube2C is not required for E2 activity, as seen in

degradation assays using 35S-cyclin A as a reporter. **(E)** The RING-interaction loop is the main APC/C-binding site in Ube2C. Ube2CC114S or Ube2CR6A/C114S, and RING-binding-deficient Ube2CC114S/Y91D were tested for their capability to stabilize 35S-securin in extracts. **(F)** The initiation motif is not required for APC/C binding of Ube2C in vivo. Ube2CC114S or Ube2CR6A/C114S were injected into *Xenopus tropicalis* embryos at the two-cell stage, and cell cycle arrest was scored relative to Ube2CC114S. Error bars define the standard error derived from three independent experiments. **(G)** APC/C substrates inhibit Ube2C ubiquitylation through initiation motif competition. Recombinant securinΔDΔKEN was added to ubiquitylation reactions of 35S-Ube2C by APC/C and/or Ube2S, as indicated.

Figure 4: Initiation Motifs Can Determine the Rate of Substrate Degradation

(A) The initiation motif determines the efficiency of Ube2C-ubiquitylation. Ubiquitylation of 35S-Ube2C or IMgem-Ube2C, a mutant containing the initiation motif of geminin, by APC/C was analyzed by autoradiography. The asterisk denotes the modification of Ube2C Lys residues, which occurs without APC/C during the IVT/T. **(B)** Ubiquitylation of 35S-IMgem-Ube2C or its active site and RING-interaction mutant by the APC/C were analyzed by autoradiography. **(C)** IM^{gem}-Ube2C shows more efficient chain initiation than Ube2C, as seen in assays containing APC/C and methylubiquitin. The asterisk denotes APC/C-independent ubiquitylation of Ube2C. **(D)** Efficient chain initiation results in rapid degradation of 35S-IMgem-Ube2C in extracts with active APC/C. **(E)** Efficient chain initiation results in rapid proteolysis of IMgem-Ube2CHA in synchronized HeLa cells entering anaphase. **(F)** The initiation motif does not determine binding of Ube2C to the APC/C. Ube2CC114S or IMgem-Ube2CC114S was injected into *X. tropicalis* embryos at the two cell stage, and cell cycle arrest was scored normalized to Ube2CC114S. Error bars define the standard error derived from three independent experiments.

Figure 5: Initiation Motifs Allow Identification of the APC/C Substrate PAF15

(A) Degradation of 35S-PAF15 in extracts with active APC/C was analyzed by autoradiography. **(B)** 35S-PAF15 was ubiquitylated by APC/C, Ube2C, and ubiquitin and analyzed by autoradiography. **(C)** Degradation of 35S-PAF15 in extracts with active APC/C requires an initiation motif. **(D)** The degradation of HAPAF15 in 293T cells with ^{myc}Cdh1 requires an initiation motif. **(E)** Efficient ubiquitylation of PAF15 requires an initiation motif. Modification of 35S-PAF15 mutants by APC/C, Ube2C, and ubiquitin was analyzed by autoradiography. **(F)** The initiation motif is required for efficient PAF15 lysine modification by APC/C, Ube2C, and methylubiquitin, as analyzed by autoradiography. **(G)** The initiation motif in GstPAF15 is not required for binding to 35S-Cdh1. **(H)** The initiation motif in PAF15 is not required for ACP/C binding or chain elongation. Ubiquitylation of 35S-Ub-L-PAF15 mutants by APC/C, Ube2S, and ubiquitin was analyzed by autoradiography.

Figure 6: PCNA Inhibits Chain Initiation on PAF15

(A) PAF15 binds PCNA through a PIP box. The top shows an overview of PAF15 domains (D, D box; P, PIP box; IM, initiation motif). The bottom panel shows binding of 35S-PAF15 mutants to GstPCNA. **(B)** PAF15 binds PCNA through a PIP box in vivo. HAPAF15 mutants were precipitated from 293T lysates, and coeluting endogenous PCNA was detected by western blot. **(C)** Increasing concentrations of PCNA (0.8 nM - 3.5 μM) can inhibit chain initiation on 35S-PAF15 by APC/C, Ube2C, and methylubiquitin. **(D)** Increasing concentrations of PCNA (0.8 nM - 3.5 μM) can inhibit the modification of 35S-PAF15 by APC/C, Ube2C, and ubiquitin. **(E)** Modification of 35S-PAF15 or PAF15ΔPIP by APC/C, Ube2C, and ubiquitin was analyzed after addition of PCNA, as indicated. **(F)** Degradation of 35S-PAF15 or PAF15ΔPIP in extracts with active APC/C was analyzed in the presence of recombinant PCNA, as indicated. **(G)** PCNA stabilizes PAF15 in cells. HeLa cells were treated with siRNAs targeting PCNA or PAF15, and lysates were analyzed by western blot. The siRNAs did not result in changes in the cell cycle distribution, as analyzed by FACS.

Figure 7: Regulated Chain Initiation Controls the Timing of Substrate Degradation

(A) ^{His}PCNA does not inhibit the interaction between GstPAF15 and 35S-Cdh1 as analyzed by autoradiography. **(B)** MBPPAF15 can form ternary complexes with GstPCNA and 35S-Cdh1, as analyzed by autoradiography. **(C)** PAF15, PCNA, and APC/C form ternary complexes in vivo. FLAGPAF15 was precipitated from lysates of prometaphase HeLa cells. FLAG-peptide eluates were reprecipitated with antibodies recognizing the APC/C, and PCNA was detected by western blot. The asterisk marks a modified form of PCNA. **(D)** PCNA does not inhibit APC/C binding or chain elongation on PAF15. 35S-Ub-L-PAF15 was bound to GstPCNA and incubated with APC/C, ubiquitin, and Ubd2C (for initiation) and Ube2S (for elongation). **(E)** The initiation efficiency determines the timing of PAF15 degradation and reaccumulation. Synchronized HeLa cells stably expressing FLAGPAF15, FLAGPAF15ΔPIP, FLAGPAF15ΔDΔKEN, or FLAGPAF15ΔPIPΔDΔKEN were released into anaphase to activate the APC/C, and levels of PAF15 proteins and cell cycle markers were measured by western blot. **(F)** PCNA interacts with PAF15 during late G1, when PAF15, but not PAF15ΔPIP, is stabilized. HeLa cells expressing FLAGPAF15 were synchronized in prometaphase (t=0) or late G1 (10-14hr after nocodazole release). PAF15 was precipitated on FLAG-agarose, and coprecipitating PCNA was detected by western blot.

Figure S1: Characterization of the initiation motif in geminin.

(A) The N-terminal 83 amino acids are required and sufficient for the APC/C-dependent degradation of human geminin. 35S-geminin truncation mutants were tested for degradation in extracts with active APC/C. Emi1 was added as indicated to test for APC/C-specificity. Furthermore, mutants in the N-terminal D-box and the initiation motif of geminin were introduced into geminin1-101 and tested for degradation under the same conditions. Reaction products were analyzed by autoradiography. **(B)** The D-box of human geminin is required for ubiquitylation by the APC/C. 35S-geminin or geminin**Δ**D were incubated with APC/C^{Cdh1}, E1, Ube2C, and ubiquitin. Reaction products were analyzed by autoradiography. **(C)** Sequence alignment of the TEK-box in securin and the

candidate initiation motif in geminin. Identical residues are marked with a "+", similar residues with a "*". **(D)** Mutation of the initiation motif in geminin causes cell cycle arrest and embryonic death in *X. tropicalis*. Geminin or geminin**Δ**IM were injected into X. tropicalis embryos, and cell cycle progression (left panel) and embryonic death (right panel) of injected embryos was analyzed. The same phenotype was previously observed upon injection of stable geminin**Δ**D into Xenopus embryos (McGarry and Kirschner, 1998). **(E)** Bypassing chain initiation allows Ube2C to catalyze ubiquitylation of geminin**Δ**IM. 35S-geminin mutants were synthesized by IVT/T; 35S-labeled ZZ/TEVUb-geminin and ZZ/TEVUb-geminin**Δ**IM were synthesized by IVT/T, bound to IgG sepharose, and eluted by TEV-cleavage. The purified proteins were incubated with APC/C^{Cdh1}, E1, Ube2C and ubiquitin. In these reactions, Ube2C is able to recognize the TEK-box in ubiquitin. Reaction products were analyzed by and autoradiography.

Figure S2: Characterization of initiation motifs in multiple APC/C-substrate

(A) Mutation of initiation motif residues interferes with chain formation on geminin. 35S-geminin mutants were incubated with APC/C^{Cdh1}, E1, Ube2C, and methylubiquitin or wt ubiquitin, as indicated. Reactions were analyzed by autoradiography. **(B)** Sequence alignment of the geminin sequence comprising D-box and initiation motif. Functionally important and conserved initiation motif residues are marked in green. Identical residues are further denoted with "*", similar residues with ":" (high degree of similarity) or "." (lower degree of similarity). **(C)** A conserved initiation motif is found in Plk1. Sequence alignments of initiation motif residues (green) in Plk1 from different organisms. **(D)** The initiation motif in securin is not essential for APC/C-binding. Recombinant securin mutants were titrated into the APC/C-dependent ubiquitylation of 35S-cyclin A. Reactions were analyzed by autoradiography. **(E)** The initiation motif in cyclin B1 is not required for APC/C-binding. Recombinant cyclin B1 mutants were analyzed for APC/C-binding through competitive inhibition, as described above. **(F)** The initiation motif in Plk1 is not required for APC/C-binding. Recombinant Plk1 mutants were analyzed for APC/C binding through competitive inhibition, as described above. **(G)** Lysine residues are not required for initiation motif function in cyclin B1. 35S-cyclin B1 mutants were assayed for chain initiation by APC/C, Ube2C, and methylubiquitin. Reactions were analyzed by autoradiography. **(H)** Lysine residues are not required for initiation motif function in Plk1. 35S-Plk1 mutants were assayed for chain initiation as described above. **(I)** KEN-box deletion ablates residual chain initiation in a securin**Δ**IM-mutant. 35S-securin mutants were analyzed for chain initiation by APC/C, Ube2C, and methylubiquitin, using autoradiography.

Figure S3: Characterization of the initiation motif in Ube2C

(A) The Lys residue in the initiation motif of Ube2C is not required for function. 35S-ZZ/TEVUbe2C and indicated mutants were synthesized by IVT/T, purified on IgG-sepharose, eluted by TEV-cleavage, and incubated with APC/C, E1, and ubiquitin. Reactions were analyzed by autoradiography. **(B)** The initiation motif in Ube2C is required for the APC/C-dependent degradation of Ube2C in cells. 293T cells were transfected with Ube2CHA or Ube2CR17A/K18A-HA. As indicated, APC/C was

activated by co-transfection of Cdh1. The levels of Ube2C proteins were determined by **α**HA-Western. Mutation of the initiation motif resulted in higher steady-state levels of Ube2C and in lower sensitivity to Cdh1-overexpression, both signs that APC/C-dependent degradation was impaired. **(C)** The initiation motif residue Arg6 is not required for Ube2C-charging by the E1. Recombinant $Ube2C^{His}$, initiation motif mutants (Ube2CR6A/His and Ube2CR17A/K18A/His), or N-terminally tagged ^{His}Ube2C were incubated with E1 and ubiquitin at 14°C. Reactions were stopped with gel loading buffer missing **β**-mercaptoethanol (**β**ME) and analyzed by Coomassie staining. **(D)** The initiation motif of Ube2C is not required for Ube2C-activity as an APC/C E2. 35S-cyclin A was incubated with APC/C^{Cdh1}, E1, Ube2C or the indicated mutants, and ubiquitin. Reaction products were analyzed by autoradiography. **(E)** The initiation motif is not required for Ube2C-activity, as seen over a wide range of concentrations. Ube2C or Ube2CR6A were titrated into reactions containing, APC/C, E1, 35S-cyclin A, and ubiquitin. Reaction products were analyzed by autoradiography. **(F)** Mutations in an N-terminal QNP-motif impair Ube2C-activity, as seen in reactions containing 35S-cyclin A, Ube2C or mutants, APC/C, E1, and ubiquitin. Reactions were analyzed by autoradiography. **(G)** The autoubiquitylation of Ube2C is not competed by a securin construct, securin**Δ**N92, which lacks both D-box and initiation motif. The mutation of the initiation motif reproducibly impairs the capacity of securin to inhibit Ube2C autoubiquitylation. 35SZZ/TEVUbe2C was synthesized by IVT/T, purified on IgG-sepharose, eluted by TEV cleavage, and added to APC/C, E1, and ubiquitin. Recombinant securin proteins were added as indicated. Reactions were analyzed by autoradiography.

Figure S4: Initiation motifs can determine the rate of degradation without affecting substrate affinity for the APC/C

(A) IMgem-Ube2C is degraded in extracts in an APC/C and proteasome-dependent manner. 35S-labeled ZZ/TEVIMgem-Ube2C was synthesized by IVT/T, bound to IgG sepharose, eluted by TEV-cleavage and added to extracts with active APC/C. As indicated, APC/C was inhibited by recombinant Emi1, and the proteasome was inhibited by MG132. Degradation reactions were monitored over time and analyzed by autoradiography. **(B)** IMgem-Ube2C is not rapidly degraded in mitotic extracts, in which APC/C^{Cdc20} was activated by addition to p31comet. 35S-Ube2C, IMgem- Ube2C, and geminin were synthesized by IVT/T, purified, and analyzed for degradation as described above. **(C)** IMgem-Ube2C binds the APC/C. Increasing concentrations of recombinant Ube2C and IMgem-Ube2C were incubated with APC/C^{Cdh1}, E1, ubiquitin, and 35S-cyclin A. The ubiquitylation of cyclin A was analyzed by autoradiography. **(D)** IMgem- Ube2C is charged by E1 less efficiently than wt-Ube2C. Ube2C and IMgem-Ube2C were incubated with E1, ubiquitin and ATP, and reactions were analyzed by SDS-PAGE with loading buffer that either contained or did not contain **β**-ME. **(E)** Exchanging its initiation motif does not strongly affect APC/C-binding of Ube2C. Extracts of G1 HeLa S3 cells were supplemented with buffer, Ube2CC114S, or IMgem-Ube2CC114S. The degradation of 35S-securin was monitored over time by autoradiography. Identical results were obtained at different concentrations of Ube2CC114S and IMgem-Ube2CC114S. **(F)** Exchanging the initiation motif of geminin with that of Ube2C impairs geminin

ubiquitylation. 35S-geminin, IMUbe2C-geminin, NUbe2C-geminin (a mutant in which the complete initiation motif region was exchanged with the N-terminus of Ube2C, resulting in a **Δ**IM-phenotype), and geminin**Δ**IM were incubated with APC/C^{Cdh1}, E1, Ube2C, and ubiquitin. Reaction products were analyzed by autoradiography. **(G)** IMUbe2C-geminin is degraded more slowly than geminin upon APC/C-activation in cells. HeLa cells were transfected with geminin or IMUbe2C-geminin and synchronized in prometaphase by thymidine-nocodazole. Cells were released into fresh medium to activate APC/C, and samples were taken at different times. The levels of geminin and IMUbe2C-geminin were monitored by **α-**geminin-Western. Exit from mitosis was followed by Western blot against phosphorylated histone H3Ser10. **(H)** IMUbe2C-geminin is less sensitive than geminin to APC/C-activation. 293T cells were transfected with geminin, IMUbe2C-geminin and NUbe2C-geminin (as a mimic of **Δ**TEK). As indicated, cells were co-transfected with Cdh1 to activate the APC/C. The levels of geminin were monitored by Western blot using specific **α-**geminin antibodies.

Figure S5: PAF15 is a novel APC/C-substrate that depends on its initiation motif for degradation

(A) Schematic overview of PAF15, showing its APC/C-binding sites (D-, KENbox); its chain initiation motif (IM); and its PCNA-binding site (PIP-box). The sequences below show the conservation of these motifs in mice, rats, and humans. **(B)** PAF-levels decrease upon APC/C-activation by Emi1-depletion. Emi1 was depleted from HeLa cells using characterized siRNAs (Williamson et al., 2009). The levels of PAF and two well characterized APC/C-substrates, cyclin A and cyclin B, were analyzed by Western blot. **(C)** PAF is degraded upon APC/C-activation during mitotic exit. HeLa cells were synchronized in prometaphase by thymidine-nocodazole, and then released into fresh medium to activate the APC/C. The levels of PAF and two well-characterized APC/C substrates, cyclin B1 and Ube2C, were measured by Western blot. Exit from mitosis was monitored by analyzing the phosphorylation of Cdc27, a core APC/C-subunit, also by Western blot. **(D)** PAF is absent from quiescent cells, similar to most other known APC/C substrates. T24 cells were synchronized in quiescence by serum-starvation. The cells were then allowed to re-enter the cell cycle by transfer into serum-containing medium. The levels of PAF, cyclin B1, Ube2C, and p27 (used as a marker for quiescence), were measured by Western blot. **(E)** PAF depends on an initiation motif for efficient chain initiation. 35S-PAF mutants were synthesized as ZZ/TEV-tagged proteins by IVT, bound to IgG sepharose, eluted by TEV-cleavage, and incubated with APC/C^{Cdh1}, E1, Ube2C, and methylubiquitin. Reaction products were analyzed by autoradiography.

Figure S6: PAF binds PCNA and Cdh1 through independent sequence motifs

35SCdh1 was synthesized by IVT/T and incubated with Gst, GstPAF, or Gst-tagged PAF mutants. The binding reactions were extensively washed, eluted by gel loading buffer, and analyzed by autoradiography or Coomassie staining.

Figure S7: Expression of stable PAF does not result in apparent cell cycle phenotypes

(A) FACS analysis after propidium iodine staining in HeLa cells that stably express FLAGPAF, FLAGPAF**Δ**PIP, FLAGPAF**Δ**D**Δ**KEN, or FLAGPAF**Δ**D**Δ**KEN**Δ**PIP. Shown is the percentage of cells in G1, S, or G2/M. **(B)** BrdU-staining of the same cell lines to determine the number of cells actively undergoing replication.

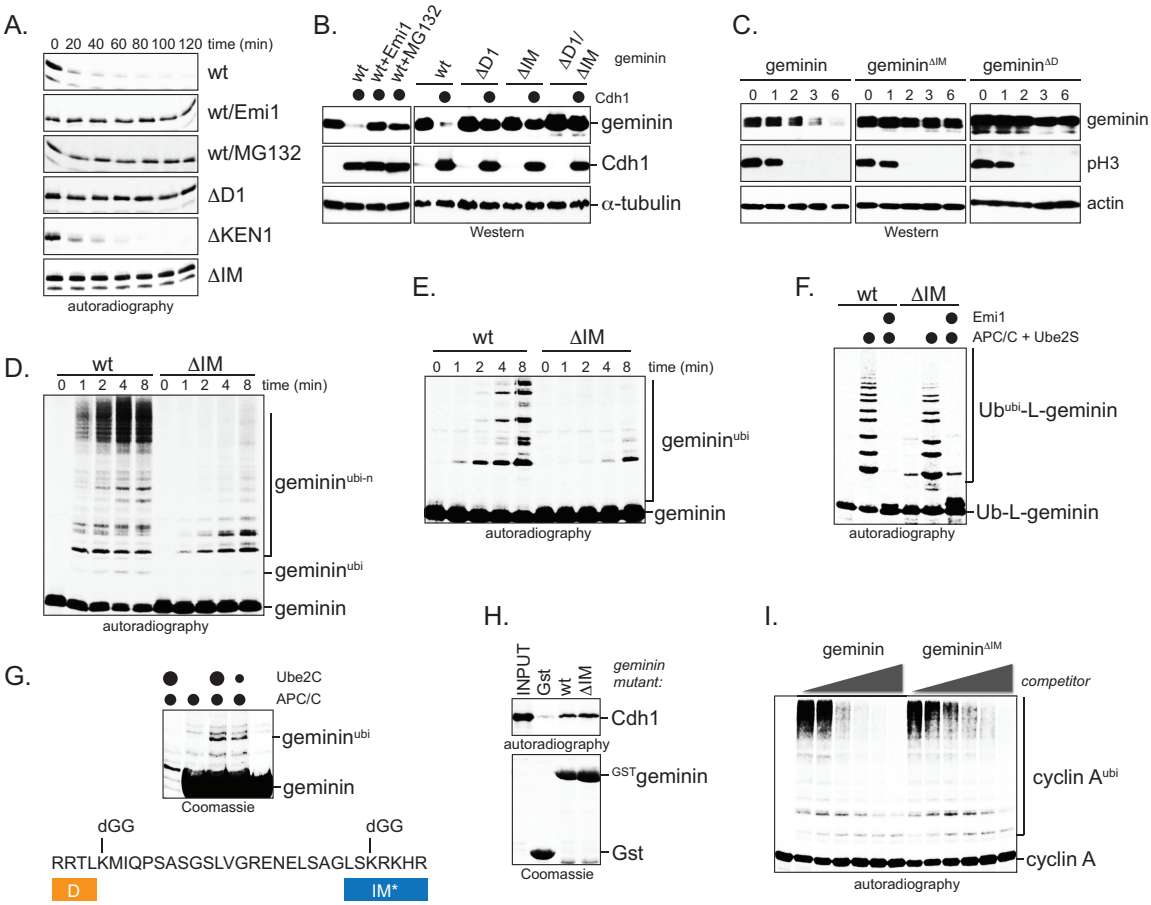
A.
0 20 40 60 80 100 120 time (min)
wt
wt/Emi1
wt/MG132
ΔD1
ΔKEN1
ΔIM
autoradiography
B.
wt
wt+Emi1
wt+MG132
wt
ΔD1
ΔIM
ΔD1/ ΔIM
geminin
Cdh1
geminin
Cdh1
α-tubulin
Western
C.
geminin
geminin^ΔIM
geminin^ΔD
0 1 2 3 6
0 1 2 3 6
0 1 2 3 6
geminin
pH3
actin
Western
D.
wt
ΔIM
0 1 2 4 8 0 1 2 4 8 time (min)
geminin^ubi-n
geminin^ubi
geminin
autoradiography
E.
wt
ΔIM
0 1 2 4 8 0 1 2 4 8 time (min)
geminin^ubi
geminin
autoradiography
F.
wt
ΔIM
Emi1
APC/C + Ube2S
Ub^ubi-L-geminin
Ub-L-geminin
autoradiography
G.
Ube2C
APC/C
geminin^ubi
geminin
Coomassie
dGG
dGG
RRTLKMIQPSASGSLVGRENELSAGLSKRKHR
D
IM*
H.
INPUT
Gst
wt
ΔIM
geminin mutant:
Cdh1
autoradiography
GSTgeminin
Gst
Coomassie
I.
geminin
geminin^ΔIM
competitor
cyclin A^ubi
cyclin A
autoradiography

Figure 1

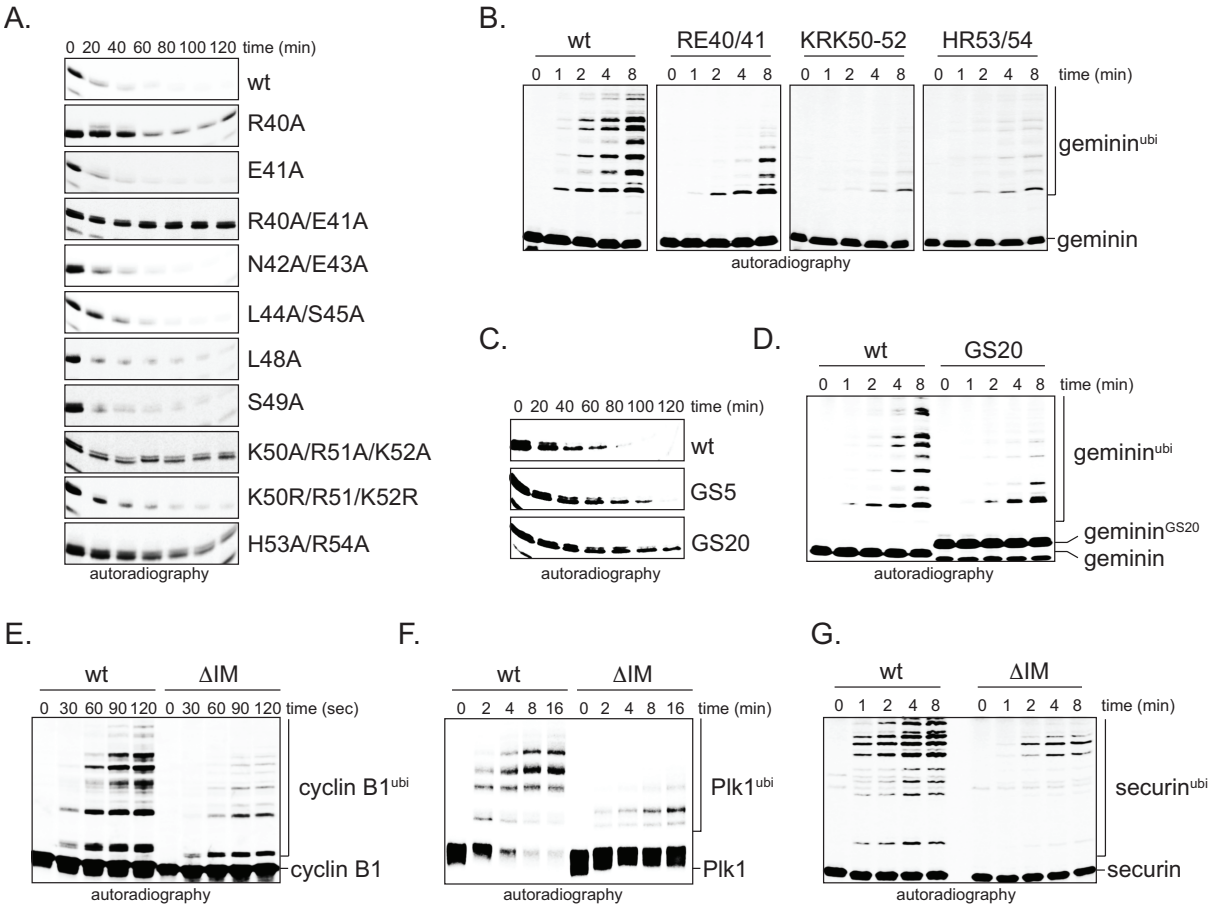
A.
0 20 40 60 80 100 120 time (min)
wt
R40A
E41A
R40A/E41A
N42A/E43A
L44A/S45A
L48A
S49A
K50A/R51A/K52A
K50R/R51/K52R
H53A/R54A
autoradiography
B.
wt
RE40/41
KRK50-52
HR53/54
0 1 2 4 8
time (min)
geminin^ubi
geminin
autoradiography
C.
0 20 40 60 80 100 120 time (min)
wt
GS5
GS20
autoradiography
D.
wt
GS20
0 1 2 4 8
time (min)
geminin^ubi
geminin^GS20
geminin
autoradiography
E.
wt
ΔIM
0 30 60 90 120 time (sec)
cyclin B1^ubi
cyclin B1
autoradiography
F.
wt
ΔIM
0 2 4 8 16
time (min)
Plk1^ubi
Plk1
autoradiography
G.
wt
ΔIM
0 1 2 4 8
time (min)
securin^ubi
securin
autoradiography

Figure 2

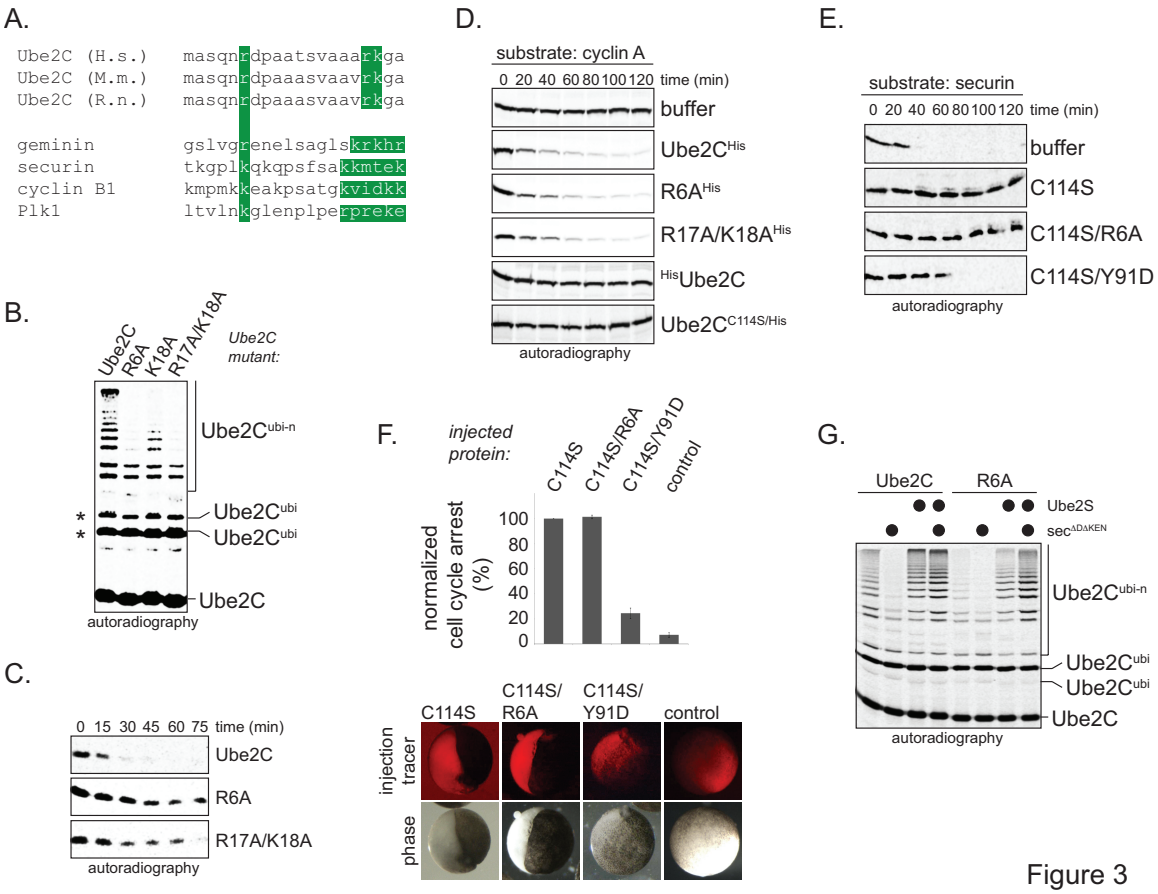
A.
Ube2C (H.s.) masqnrdpaatsvaaarkga
Ube2C (M.m.) masqnrdpaaasvaavrkga
Ube2C (R.n.) masqnrdpaaasvaavrkga
geminin gslvgrenelsaglskrkhr
securin tkgplkqkqpsfsakkmtek
cyclin B1 kmpmkkeakpsatgkvidkk
Plk1 ltvlnkglenplperpreke
B.
Ube2C
R6A
K18A
R17A/K18A
Ube2C mutant:
Ube2C^ubi-n
Ube2C^ubi
Ube2C^ubi
Ube2C
autoradiography
C.
0 15 30 45 60 75 time (min)
Ube2C
R6A
R17A/K18A
autoradiography
D.
substrate: cyclin A
0 20 40 60 80 100 120 time (min)
buffer
Ube2C^His
R6A^His
R17A/K18A^His
^His Ube2C
Ube2C^C114S/His
autoradiography
E.
substrate: securin
0 20 40 60 80 100 120 time (min)
buffer
C114S
C114S/R6A
C114S/Y91D
autoradiography
F.
injected protein:
C114S
C114S/R6A
C114S/Y91D
control
normalized cell cycle arrest (%)
100
80
60
40
20
0
C114S
C114S/ R6A
C114S/ Y91D
control
injection tracer
phase
G.
Ube2C
R6A
Ube2S
sec^ΔDΔKEN
Ube2C^ubi-n
Ube2C^ubi
Ube2C^ubi
Ube2C
autoradiography

Figure 3

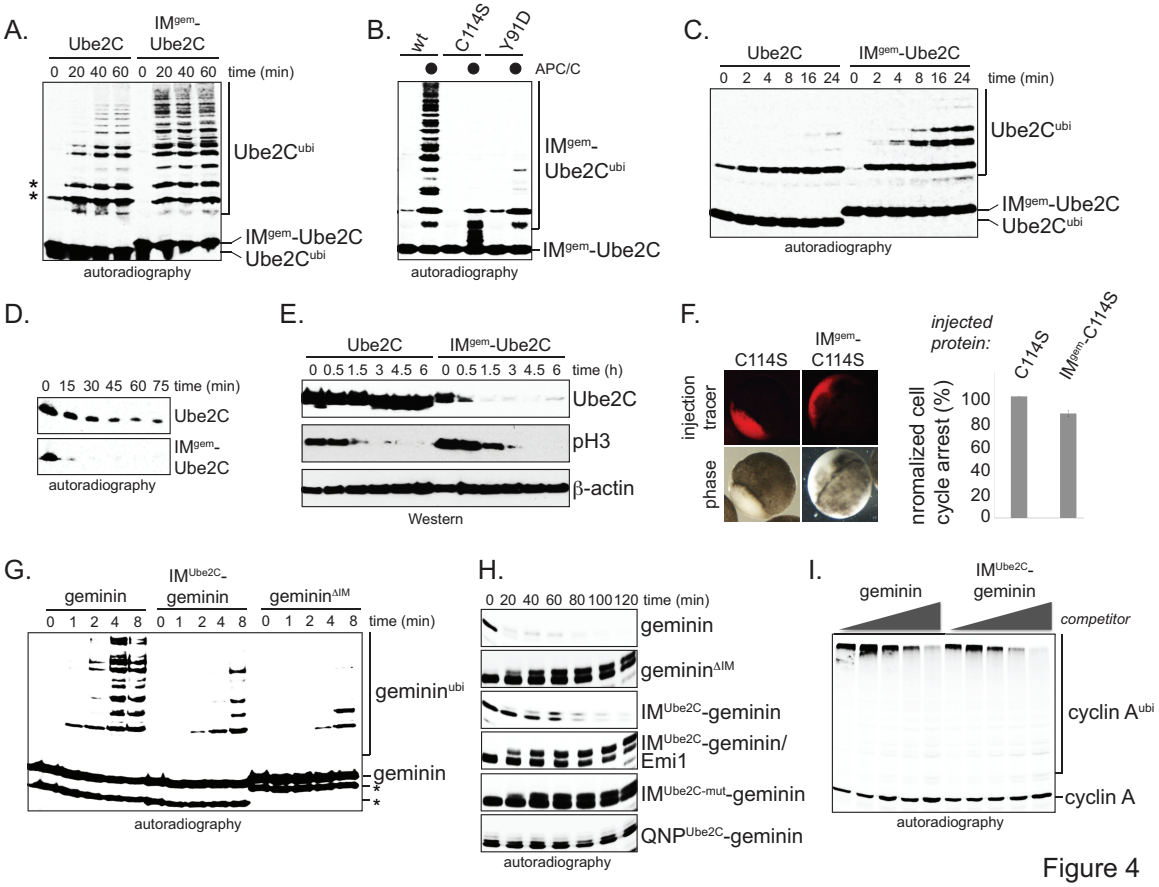
A.
Ube2C
IMgem-Ube2C
0 20 40 60 0 20 40 60 time (min)
Ube2Cubi
IMgem-Ube2C
Ube2Cubi
autoradiography
B.
wt
C114S
Y91D
APC/C
IMgem-Ube2Cubi
IMgem-Ube2C
autoradiography
C.
Ube2C
IMgem-Ube2C
0 2 4 8 16 24 0 2 4 8 16 24 time (min)
Ube2Cubi
IMgem-Ube2C
Ube2Cubi
autoradiography
D.
0 15 30 45 60 75 time (min)
Ube2C
IMgem-Ube2C
autoradiography
E.
Ube2C
IMgem-Ube2C
0 0.5 1.5 3 4.5 6 0 0.5 1.5 3 4.5 6 time (h)
Ube2C
pH3
β-actin
Western
F.
C114S
IMgem-C114S
injection tracer
phase
injected protein:
C114S
IMgem-C114S
normalized cell cycle arrest (%)
100
80
60
40
20
0
G.
geminin
IMUbe2C-geminin
geminΔIM
0 1 2 4 8 0 1 2 4 8 0 1 2 4 8 time (min)
geminubi
geminin
autoradiography
H.
0 20 40 60 80 100 120 time (min)
geminin
geminΔIM
IMUbe2C-geminin
IMUbe2C-geminin/ Emi1
IMUbe2C-mut-geminin
QNPUbe2C-geminin
autoradiography
I.
geminin
IMUbe2C-geminin
competitor
cyclin Aubi
cyclin A
autoradiography

Figure 4

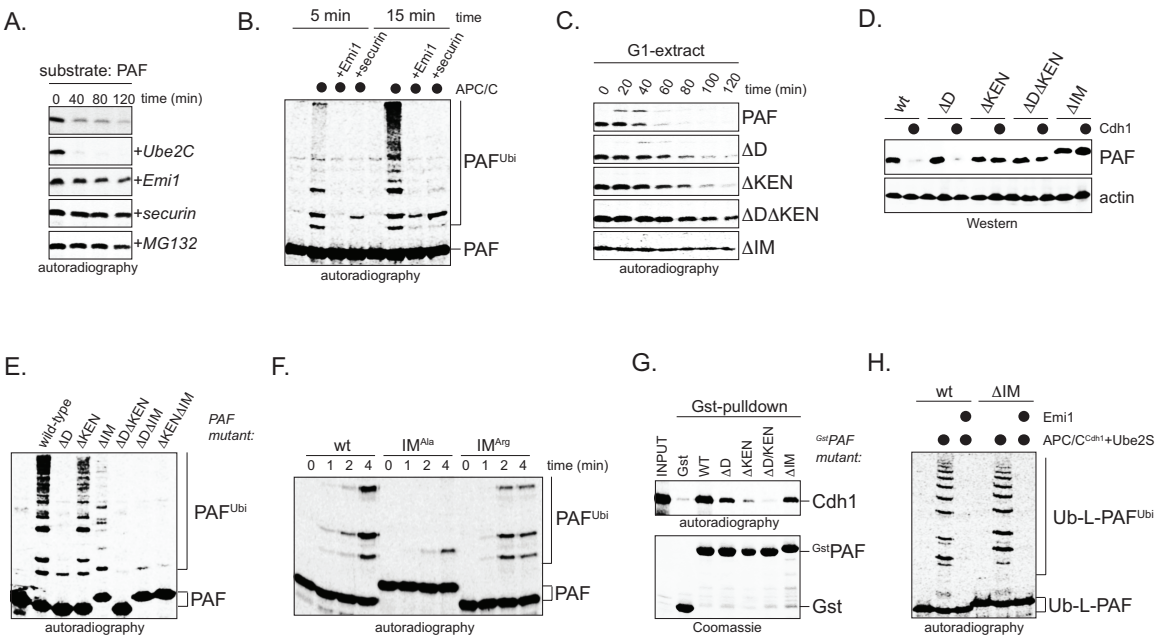
A.
substrate: PAF
0 40 80 120 time (min)
+Ube2C
+Emi1
+securin
+MG132
autoradiography
B.
5 min
15 min
time
+Emi1
+securin
+Emi1
+securin
APC/C
PAFUbi
PAF
autoradiography
C.
G1-extract
0 20 40 60 80 100 120 time (min)
PAF
ΔD
ΔKEN
ΔDΔKEN
ΔIM
autoradiography
D.
wt
ΔD
ΔKEN
ΔDΔKEN
ΔIM
Cdh1
PAF
actin
Western
E.
wild-type
ΔD
ΔKEN
ΔIM
ΔDΔKEN
ΔDΔIM
ΔKENΔIM
PAF mutant:
PAFUbi
PAF
autoradiography
F.
wt
IMAla
IMArg
0 1 2 4 0 1 2 4 0 1 2 4 time (min)
PAFUbi
PAF
autoradiography
G.
Gst-pulldown
INPUT
Gst
WT
ΔD
ΔKEN
ΔD/KEN
ΔIM
GstPAF mutant:
Cdh1
autoradiography
GstPAF
Gst
Coomassie
H.
wt
ΔIM
Emi1
APC/CCdh1+Ube2S
Ub-L-PAFUbi
Ub-L-PAF
autoradiography

Figure 5

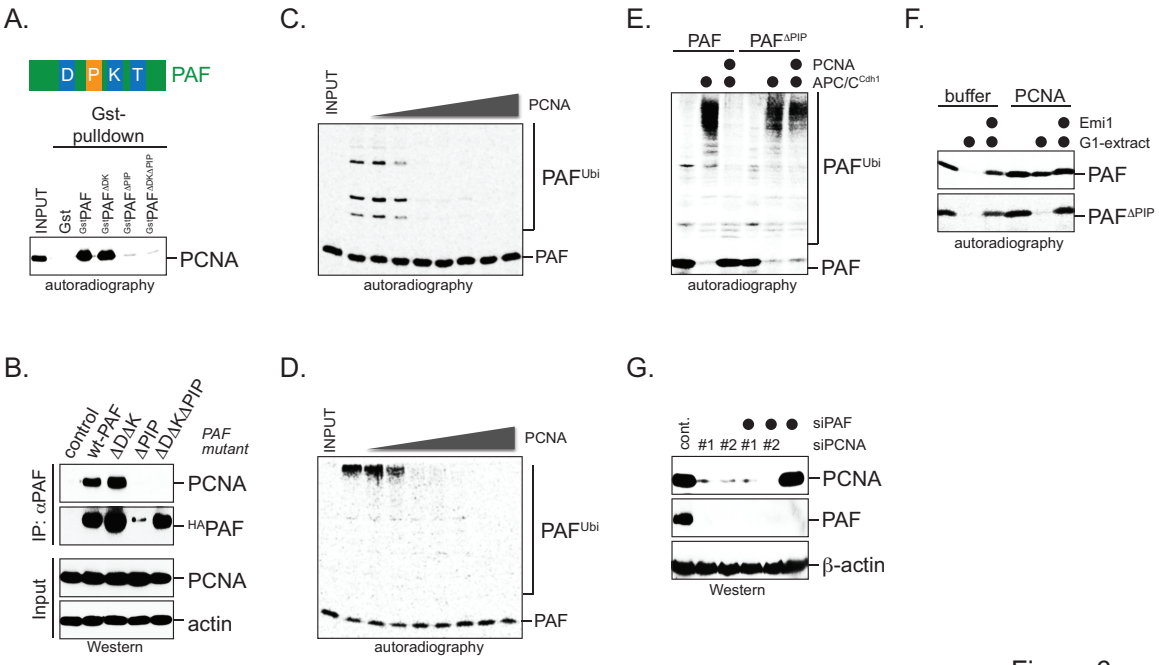
A.
D P K T
PAF
Gst-
pulldown
INPUT
Gst
GstPAF
GstPAFΔDK
GstPAFΔPIP
GstPAFΔDKΔPIP
PCNA
autoradiography
B.
control
wt-PAF
ΔDΔK
ΔPIP
ΔDΔKΔPIP
PAF mutant
IP: αPAF
PCNA
HAPAF
Input
PCNA
actin
Western
C.
INPUT
PCNA
PAFUbi
PAF
autoradiography
D.
INPUT
PCNA
PAFUbi
PAF
autoradiography
E.
PAF
PAFΔPIP
PCNA
APC/CCdh1
PAFUbi
PAF
autoradiography
F.
buffer
PCNA
Emi1
G1-extract
PAF
PAFΔPIP
autoradiography
G.
cont.
#1 #2 #1 #2
siPAF
siPCNA
PCNA
PAF
β-actin
Western

Figure 6

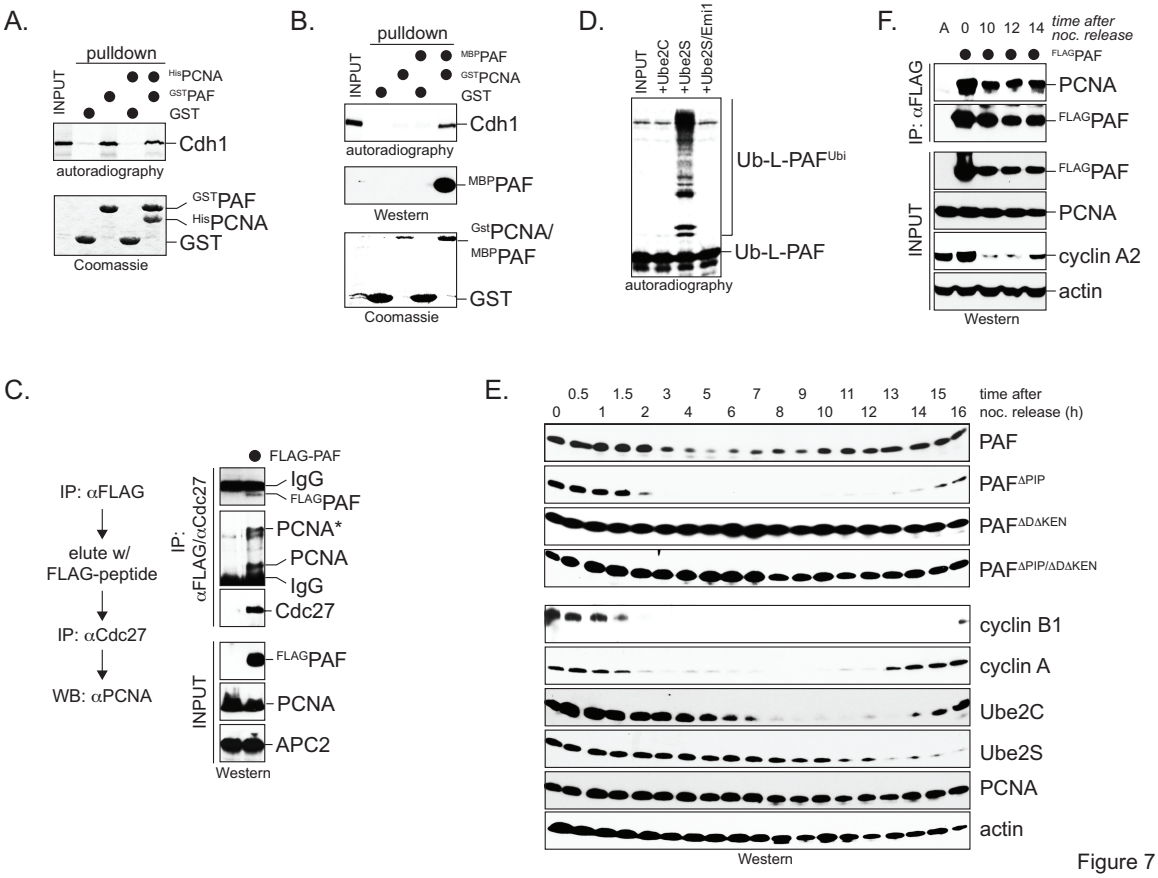
A.
pulldown
INPUT
HisPCNA
GSTPAF
GST
Cdh1
autoradiography
GSTPAF
HisPCNA
GST
Coomassie
B.
pulldown
INPUT
MBPPAF
GSTPCNA
GST
Cdh1
autoradiography
MBPPAF
Western
GstPCNA/
MBPPAF
GST
Coomassie
D.
INPUT
+Ube2C
+Ube2S
+Ube2S/Emi1
Ub-L-PAFUbi
Ub-L-PAF
autoradiography
F.
A 0 10 12 14 time after noc. release
FLAGPAF
IP: αFLAG
PCNA
FLAGPAF
INPUT
FLAGPAF
PCNA
cyclin A2
actin
Western
C.
IP: αFLAG
elute w/ FLAG-peptide
IP: αCdc27
WB: αPCNA
FLAG-PAF
IP: αFLAG/αCdc27
IgG
FLAGPAF
PCNA*
PCNA
IgG
Cdc27
INPUT
FLAGPAF
PCNA
APC2
Western
E.
0.5 1.5 3 5 7 9 11 13 15 time after
0 1 2 4 6 8 10 12 14 16 noc. release (h)
PAF
PAFΔPIP
PAFΔDΔKEN
PAFΔPIP/ΔDΔKEN
cyclin B1
cyclin A
Ube2C
Ube2S
PCNA
actin
Western

Figure 7

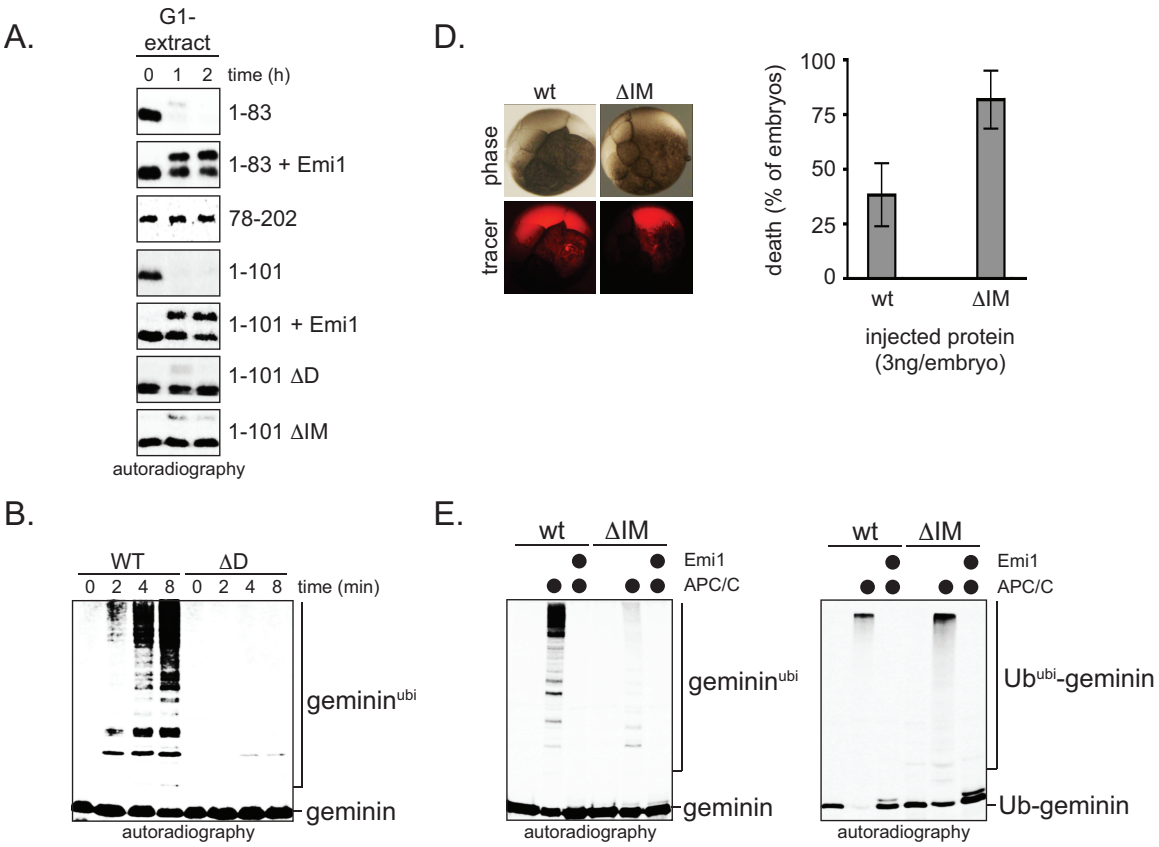
A.
G1-extract
0 1 2 time (h)
1-83
1-83 + Emi1
78-202
1-101
1-101 + Emi1
1-101 ΔD
1-101 ΔIM
autoradiography
D.
wt
ΔIM
phase
tracer
death (% of embryos)
100
75
50
25
0
wt
ΔIM
injected protein
(3ng/embryo)
B.
WT
ΔD
0 2 4 8 0 2 4 8 time (min)
geminin^ubi
geminin
autoradiography
E.
wt
ΔIM
Emi1
APC/C
geminin^ubi
geminin
autoradiography
wt
ΔIM
Emi1
APC/C
Ub^ubi-geminin
Ub-geminin
autoradiography
C.
geminin (h.s.) rrtl -x13- renelsaglskrk-hr
securin (H.s.) rkal -x17- kqkqpsfsa-kkmtek
**** +* * +* *

Figure S1

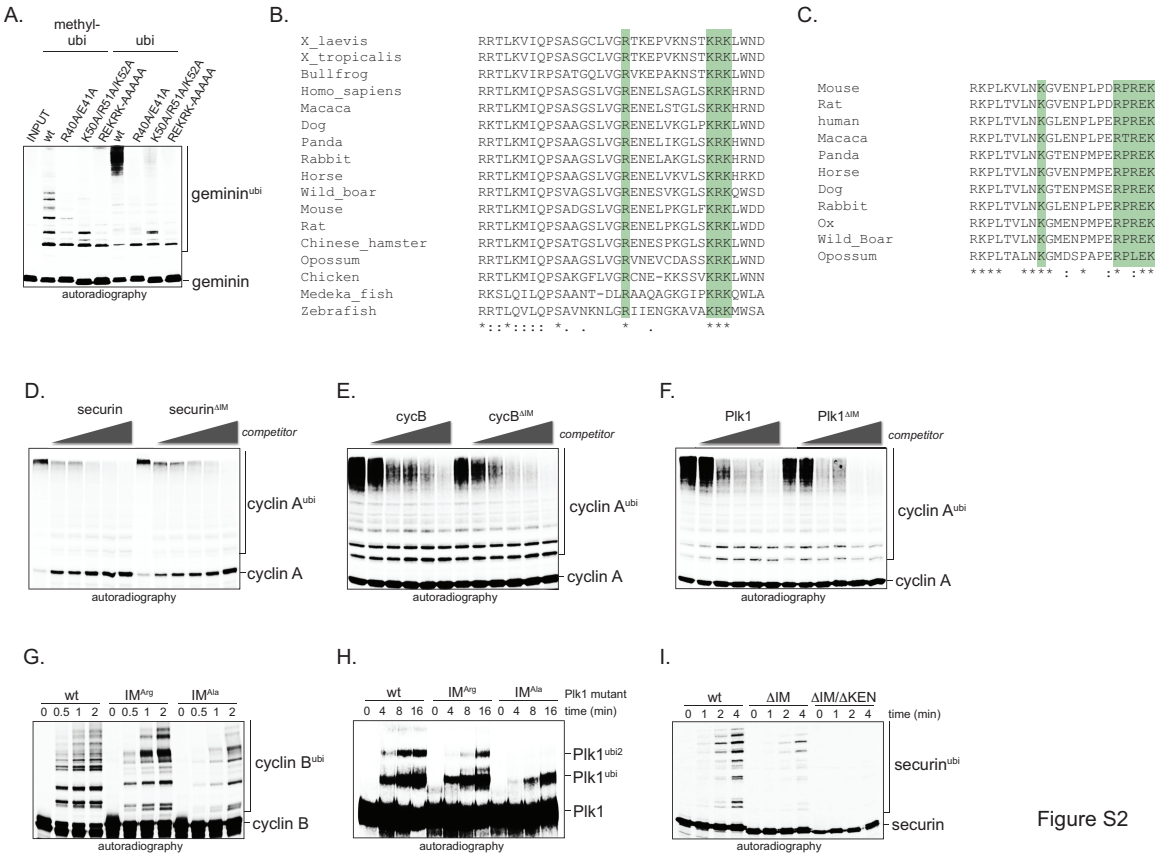
A.
methyl-ubi
ubi
INPUT
wt
R40A/E41A
K50A/R51A/K52A
REKRK-AAAAA
geminin^ubi
geminin
autoradiography
B.
X_laevis RRTLKVIQPSASGCLVGRTKEPVKNSTKRKLWND
X_tropicalis RRTLKVIQPSASGCLVGRTKEPVKNSTKRKLWND
Bullfrog RRTLKVIRPSATGQLVGRVKEPAKNSTKRKLWND
Homo_sapiens RRTLKMIQPSASGSLVGRENELSAGLSKRKHRND
Macaca RRTLKMIQPSASGSLVGRENELSTGLSKRKHRND
Dog RKTLKMIQPSAAGSLVGRENELVKGLPKRKLWND
Panda RRTLKMIQPSAAGSLVGRENELIKGLSKRKHWND
Rabbit RRTLKMIQPSAAGSLVGRENELAKGLSKRKHRND
Horse RRTLKMIQPSAAGSLVGRENELVKVLSKRKHRKD
Wild_boar RRTLKMIQPSVAGSLVGRENESVKGLSKRKQWSD
Mouse RRTLKMIQPSADGSLVGRENELPKGLFKRKLWDD
Rat RRTLKMIQPSAAGSLVGRENELPKGLSKRKLWDD
Chinese_hamster RRTLKMIQPSATGSLVGRENESPKGLSKRKLWND
Opossum RRTLKMIQPSAAGSLVGRVNEVCDASSKRKLWND
Chicken RRTLKMIQPSAKGFLVGRCNE-KKSSVKRKLWNN
Medeka_fish RKSLQILQPSAANT-DLRAAQAGKGIPKRKQWLA
Zebrafish RRTLQVLQPSAVNKNLGRIIENGKAVAKRKMWSA
:::::: *. . * . ***
C.
Mouse RKPLKVLNKGVENPLPDRPREK
Rat RKPLTVLNKGVENPLPDRPREK
human RKPLTVLNKGLENPLPERPREK
Macaca RKPLTVLNKGLENPLPERTREK
Panda RKPLTVLNKGTENPMPERPREK
Horse RKPLTVLNKGVENPMPERPREK
Dog RKPLTVLNKGTENPMSERPREK
Rabbit RKPLTVLNKGLENPLPERPREK
Ox RKPLTVLNKGMENPMPERPREK
Wild_Boar RKPLTVLNKGMENPMPERPREK
Opossum RKPLTALNKGMDSPAPERPLEK
**** **** : * :* :**
D.
securin
securin^ΔIM
competitor
cyclin A^ubi
cyclin A
autoradiography
E.
cycB
cycB^ΔIM
competitor
cyclin A^ubi
cyclin A
autoradiography
F.
Plk1
Plk1^ΔIM
competitor
cyclin A^ubi
cyclin A
autoradiography
G.
wt
IM^Arg
IM^Ala
0 0.5 1 2 0 0.5 1 2 0 0.5 1 2
cyclin B^ubi
cyclin B
autoradiography
H.
wt
IM^Arg
IM^Ala
Plk1 mutant
0 4 8 16 0 4 8 16 0 4 8 16
time (min)
Plk1^ubi2
Plk1^ubi
Plk1
autoradiography
I.
wt
ΔIM
ΔIM/ΔKEN
0 1 2 4 0 1 2 4 0 1 2 4
time (min)
securin^ubi
securin
autoradiography

Figure S2

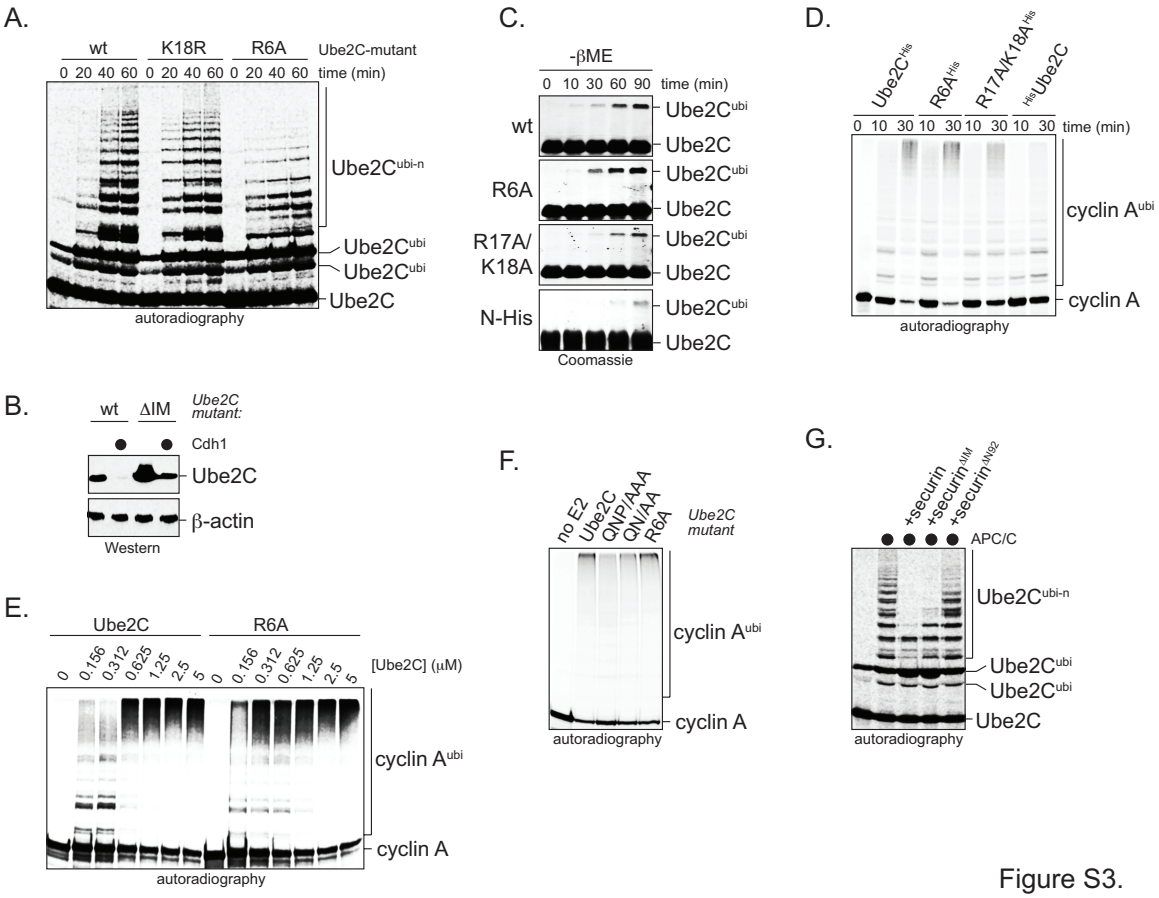
A.
wt
K18R
R6A
Ube2C-mutant
0 20 40 60 0 20 40 60 0 20 40 60
time (min)
Ube2C^ubi-n
Ube2C^ubi
Ube2C^ubi
Ube2C
autoradiography
B.
wt
ΔIM
Ube2C mutant:
Cdh1
Ube2C
β-actin
Western
C.
-βME
0 10 30 60 90
time (min)
wt
R6A
R17A/ K18A
N-His
Ube2C^ubi
Ube2C
Coomassie
D.
Ube2C^His
R6A^His
R17A/K18A^His Ube2C
0 10 30 10 30 10 30 10 30
time (min)
cyclin A^ubi
cyclin A
autoradiography
E.
Ube2C
R6A
0 0.156 0.312 0.625 1.25 2.5 5
[Ube2C] (μM)
cyclin A^ubi
cyclin A
autoradiography
F.
no E2
Ube2C
QNP/AAA
QN/AA
R6A
Ube2C mutant
cyclin A^ubi
cyclin A
autoradiography
G.
+securin
+securin^ΔIM
+securin^ΔN82
APC/C
Ube2C^ubi-n
Ube2C^ubi
Ube2C^ubi
Ube2C
autoradiography

Figure S3.

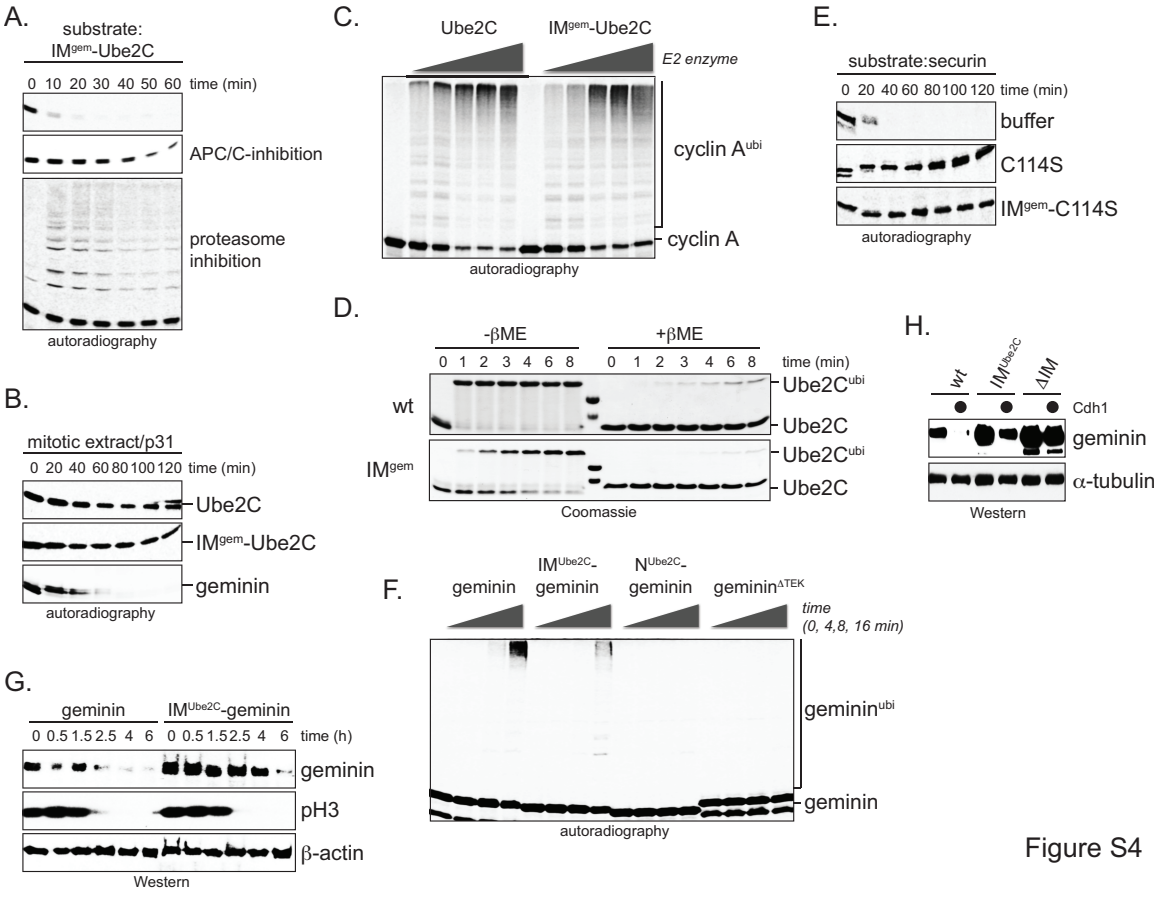
A.
substrate:
IMgem-Ube2C
0 10 20 30 40 50 60 time (min)
APC/C-inhibition
proteasome
inhibition
autoradiography
B.
mitotic extract/p31
0 20 40 60 80 100 120 time (min)
Ube2C
IMgem-Ube2C
geminin
autoradiography
C.
Ube2C
IMgem-Ube2C
E2 enzyme
cyclin Aubi
cyclin A
autoradiography
D.
-βME
+βME
0 1 2 3 4 6 8
0 1 2 3 4 6 8
time (min)
wt
IMgem
Ube2Cubi
Ube2C
Ube2Cubi
Ube2C
Coomassie
E.
substrate:securin
0 20 40 60 80 100 120 time (min)
buffer
C114S
IMgem-C114S
autoradiography
F.
geminin
IMUbe2C-
geminin
NUbe2C-
geminin
geminΔTEK
time
(0, 4,8, 16 min)
geminubi
geminin
autoradiography
G.
geminin
IMUbe2C-geminin
0 0.5 1.5 2.5 4 6 0 0.5 1.5 2.5 4 6 time (h)
geminin
pH3
β-actin
Western
H.
wt
IMUbe2C
ΔIM
Cdh1
geminin
α-tubulin
Western

Figure S4

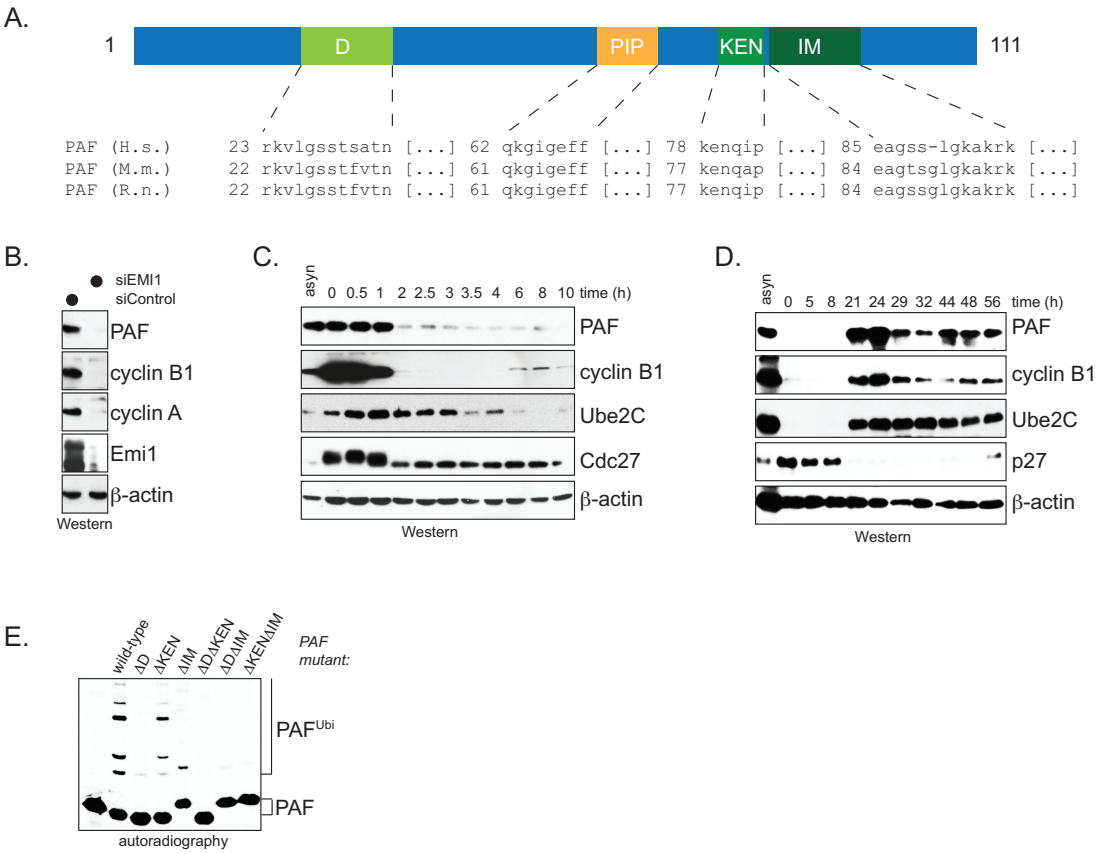
A.
1
D
PIP
KEN
IM
111
PAF (H.s.) 23 rkvlgsstsatn [...] 62 qkgigeff [...] 78 kenqip [...] 85 eagss-lgkakrk [...]
PAF (M.m.) 22 rkvlgsstfvtn [...] 61 qkgigeff [...] 77 kenqap [...] 84 eagtsglgkakrk [...]
PAF (R.n.) 22 rkvlgsstfvtn [...] 61 qkgigeff [...] 77 kenqip [...] 84 eagssglgkakrk [...]
B.
siEMI1
siControl
PAF
cyclin B1
cyclin A
Emi1
β-actin
Western
C.
asyn
0 0.5 1 2 2.5 3 3.5 4 6 8 10 time (h)
PAF
cyclin B1
Ube2C
Cdc27
β-actin
Western
D.
asyn
0 5 8 21 24 29 32 44 48 56 time (h)
PAF
cyclin B1
Ube2C
p27
β-actin
Western
E.
wild-type
ΔD
ΔKEN
ΔIM
ΔDΔKEN
ΔDΔIM
ΔKENΔIM
PAF mutant:
PAFUbi
PAF
autoradiography

Figure S5

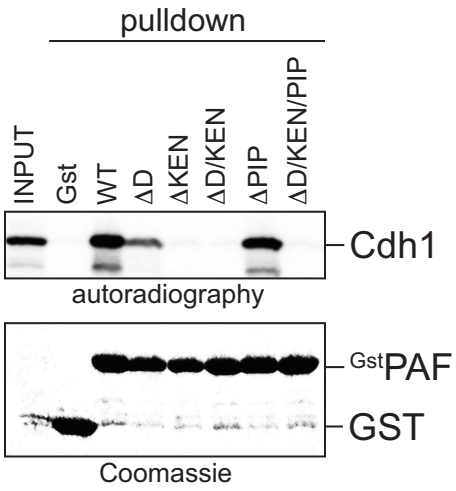

Figure S6

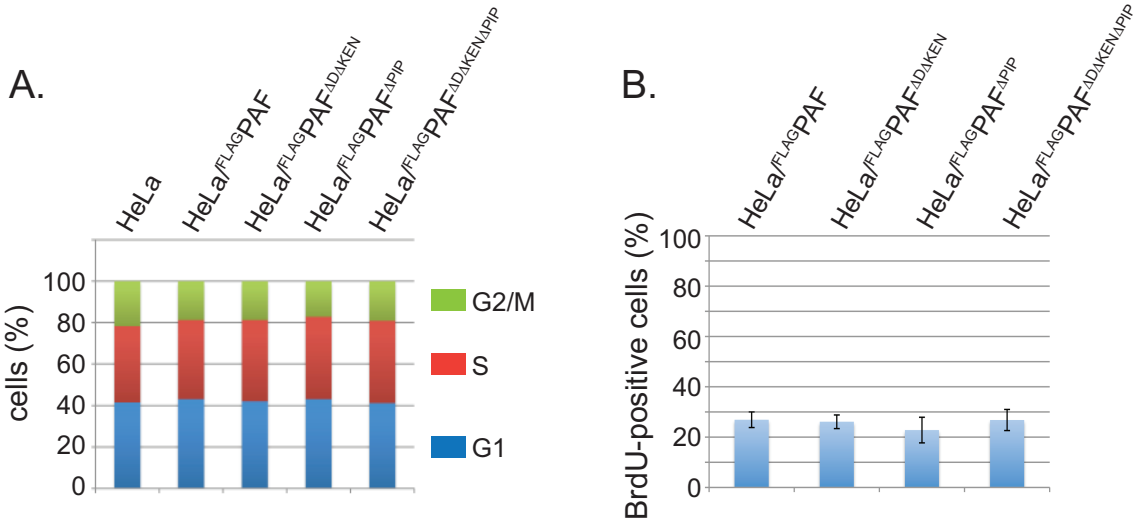

Figure S7

Chapter 4

Identification of a Physiological E2 Module for the Human Anaphase-Promoting Complex

Adam Williamson*, Katherine E. Wickliffe*, Barbara G. Mellone, Ling Song, Gary H. Karpen, and Michael Rape

Proceedings of the National Academy of Sciences (2009) *106*, 18213-18218

* equal contribution

Summary

Ubiquitylation by the anaphase-promoting complex (APC/C) is essential for proliferation in all eukaryotes. The human APC/C promotes the degradation of mitotic regulators by assembling K11-linked ubiquitin chains, the formation of which is initiated by its E2 UbcH10. Here, we identify the conserved Ube2S as a K11-specific chain elongating E2 for human and *Drosophila* APC/C. Ube2S depends on the cell cycle-dependent association with the APC/C activators Cdc20 and Cdh1 for its activity. While depletion of Ube2S inhibits APC/C in cells, the loss of the complete UbcH10/Ube2S-module leads to dramatic stabilization of APC/C substrates, severe spindle defects, and a strong mitotic delay. Ube2S and UbcH10 are tightly co-regulated in the cell cycle by APC/C-dependent degradation. We conclude that UbcH10 and Ube2S constitute a physiological E2-module for APC/C, the activity of which is required for spindle assembly and cell division.

Introduction

The proteasomal degradation of proteins is essential for cell division in all eukaryotes. Proteins are targeted to the proteasome by modification with ubiquitin chains, whose assembly depends on a cascade of E1, E2, and E3 enzymes (Dye and Schulman, 2007; Kerscher et al., 2006). E3s containing a RING-domain recruit substrates and ubiquitin-charged E2s, and promote the transfer of ubiquitin from the E2 active site to a substrate lysine. The E2-E3 pair then switches to modifying one of the seven Lys residues in ubiquitin, which results in chain elongation. E2s with dedicated roles in elongating K48- (Ube2K/E2-25K) or K63-linked chains (Ube2N-UEV1a) have been described (Eddins et al., 2006; Rodrigo-Brenni and Morgan, 2007).

The essential RING-E3 anaphase-promoting complex (APC/C) is a key regulator of cell division in eukaryotes (Peters, 2006). Loss of APC/C activity arrests cells at metaphase and results in severe aberrations in the structure of the mitotic spindle (Goshima et al., 2007; Somma et al., 2008; Tugendreich et al., 1995). Human APC/C regulates progression through mitosis by modifying a large family of substrates with K11-linked ubiquitin chains, which triggers their degradation by the proteasome (Jin et al., 2008; Kirkpatrick et al., 2006; Xu et al., 2009). Its specific E2, Ube2C/UbcH10, initiates chain formation by recognizing a substrate motif, the TEK-box, which is homologous to residues around K11 in ubiquitin (Jin et al., 2008). However, depletion of UbcH10 stabilizes APC/C substrates to a lesser extent than inhibition of APC/C or mutation of K11 in ubiquitin (Jin et al., 2008; Xu et al., 2009), suggesting that additional K11-specific E2s operate with human APC/C.

As expected from its central role in proliferation, the capacity of the APC/C to assemble ubiquitin chains is tightly regulated. When cells enter mitosis, the APC/C is partially activated through phosphorylation of core subunits and binding of the WD40-repeat protein Cdc20 (Kimata et al., 2008; Kraft et al., 2005; Yu, 2007). The APC/C becomes fully active after all chromosomes have achieved bipolar attachment to the mitotic spindle, which results in silencing of the spindle checkpoint and dissociation of Cdc20 from its inhibitors Mad2 and BubR1 (Yu, 2007). Soon after anaphase onset, Cdc20 is degraded and replaced by Cdh1, which maintains ACP/C activity during late

mitosis and early G1 (Pfleger and Kirschner, 2000; Visintin et al., 1997). Accordingly, inactivation of the APC/C before S phase involves phosphorylation and degradation of Cdh1 and binding of the Cdh1-inhibitor Emi1 (Peters, 2006). Cdc20 and Cdh1 recruit substrates to the APC/C (Burton et al., 2005; Kraft et al., 2005), but also increase the catalytic activity of the APC/C by a poorly understood mechanism.

Here, we identify the highly conserved Ube2S as a regulator of human and *Drosophila* APC/C. Ube2S functions as a K11-specific chain elongating E2 of APC/C, which depends on chain initiation by Ube2C. Together, UbcH10 and Ube2S are required for the degradation of all APC/C substrates tested so far, spindle formation, and progression of cells through mitosis. Ube2S and UbcH10 are tightly co-regulated during the cell cycle, and APC/C itself promotes their ubiquitylation and degradation. Our data suggest that UbcH10 and Ube2S constitute the physiological E2-module of human APC/C during mitosis.

Results

Ube2S Promotes the Assembly of K11-Linked Ubiquitin Chains by the APC/C

The human APC/C triggers the proteasomal degradation of its substrates by modifying them with K11-linked ubiquitin chains (Jin et al., 2008; Kirkpatrick et al., 2006). Its specific E2, UbcH10, initiates chain formation by recognizing TEK-boxes in substrates and ubiquitin (Jin et al., 2008). UbcH10 is the only known APC/C-E2 with K11-specificity, but its depletion from extracts fails to completely stabilize the APC/C substrate securin (Rape and Kirschner, 2004). Thus, an unidentified E2 must be able to catalyze the formation of K11-linked ubiquitin chains by the APC/C.

To isolate the unknown E2, we purified human E2 enzymes and measured their activity in catalyzing ubiquitylation by the APC/C. Using this approach we identified the conserved E2 Ube2S, which dramatically promotes the formation of ubiquitin chains, when added together with the APC/C-specific E2 UbcH10 (Figure 1A and 1B). Albeit less efficiently, Ube2S also cooperates with the non-specific E2 UbcH5c (Figure S1E). Ube2S functions with both APC/C^{Cdc20} and APC/C^{Cdh1} (Figure 1D), while it is inactive with other E3s tested (Figure S1F).

Ube2S does not modify substrate Lys residues itself (Figure 1A and 1B), and as seen in reactions with methylubiquitin, does not promote additional chain initiation by UbcH10.

The addition of recombinant ubiquitin mutants revealed that chains assembled by Ube2S and APC/C are strictly linked through K11 of ubiquitin, independently of whether UbcH10 or UbcH5c are used to initiate chain formation (Figure 1E and Figures S1A-C and 1G-I). In promoting chain elongation, Ube2S is reminiscent of E2-25K and Ube2N-UEV1a, which extend K48- or K63-linked ubiquitin chains, respectively (Dye and Schulman, 2007). However, E2-25K and Ube2N-UEV1a do not cooperate with UbcH10 in catalyzing chain formation on APC/C substrates (Figure S1I).

Ube2S contains a UBC-domain and a conserved C-terminal extension. Mutation of the catalytic Cys of Ube2S (Ube2SC95S) or deletion of the C terminus (Ube2SΔC) abrogates its activity towards APC/C substrates (Figure 1F). In a similar manner, addition of a peptide comprising the C terminus of Ube2S (CTP) blocks the activity of Ube2S on

APC/C. Ube2S catalyzes the formation of K11-linked ubiquitin-dimers independently of APC/C (Baboshina and Haas, 1996). This activity depends on the active-site Cys of Ube2S, but is not affected by deletion of its C terminus (Figure 1G), indicating that the C terminus of Ube2S is specifically required for APC/C-dependent chain formation.

To determine whether Ube2S depends on UbcH10 or APC/C during chain elongation, we separated chain initiation from elongation. We briefly incubated the APC/C substrate cyclin A with APC/C and UbcH10, which results in short ubiquitin chains on cyclin A (Figure 1H and 1I). In one experiment, we then added Ube2S together with an excess of inactive UbcH10C114S to block further UbcH10-activity. Under these conditions, Ube2S still elongates ubiquitin chains on cyclin A, indicating that it does not require UbcH10 for chain extension (Figure 1H). In a parallel experiment, we added Ube2S and the APC/C inhibitor Emi1 or an excess of a competitor APC/C substrate to displace preubiquitylated cyclin A from APC/C. This treatment interferes with chain-extension chains on APC/C substrates. Together, these experiments point to Ube2S as a K11-specific chain-elongating E2 of human APC/C.

Ube2S Binds APC/C and APC/C Activators

To test whether Ube2S cooperates with APC/C in cells, we precipitated endogenous Ube2S from synchronized HeLa cells and detected co-purifying proteins by Western analysis. We find a strong association between Ube2S and the APC/C activator Cdc20, which occurs specifically during mitosis (Figure 2A). This interaction is also observed when ^{FLAG}Ube2S or endogenous Cdc20 are immunoprecipiated from mitotic cells (Figure 2B and Figure S2A). During late mitosis and early G1, APC/C is activated by Cdh1, and at this cell cycle stage, Ube2S-precipitates only contain Cdh1, and at this cell cycle stage, Ube2S-precipiates contain only Cdc1, and no Cdc20. FLAGUbe2S also associates with Cdh1 (Figure 2C), and the reverse affinity-purification of Cdh1 recovers high levels of Ube2S (Figure 2D). Thus, Ube2S interacts with both APC/C activators Cdc20 and Cdh1 in a cell cycle-dependent manner.

To determine whether Ube2S directly binds Cdc20 or Cdh1, we performed pulldown-assays using MBPUbe2S. In these experiments, we focused on Cdh1, which does not require mitotic phosphorylation for activity. As expected for a direct interaction, MBPUbe2S efficiently binds Cdh1 from G1 extracts (Figure 2E), Cdh1 synthesized by IVT/T (Figure 2F), and ^{His}Cdh1 purified to homogeneity from insect cells (Figure 2G). The interaction between Ube2S and Cdh1 in vitro as well as in 293T cells requires the WD40-domain of Cdh1 (Figure 2D and Figure S2B). Although the WD40-domain of Cdh1 recognizes APC/C substrates (Burton et al., 2005; Kraft et al., 2005), an excess of APC/C substrates does not block the Cdh1/Ube2S interaction (Figures 2E and Figure S2C), and binding studies show that Cdh1 binds substrates at the same time (Figure S2D). The association of Ube2S with Cdh1 depends on the C terminus of Ube2S and is blocked by the C-terminal Ube2S-peptide (Figure 2F and Figure S2E)). Accordingly, Ube2SΔC fails to interact with Cdh1 in cells (Figure 2H). We conclude that Ube2S directly binds Cdh1 using it C-terminal tail, which is also required for the activity of Ube2S toward APC/C.

In addition to its interaction with Cdc20 and Cdh1, Ube2S binds core APC/C, as Ube2S-precipliates from late G1 and S phase contain the APC/C subunit Cdc27, but little

Cdc20 or Cdh1 (Figure 2A). Indeed, FLAGUbe2S affinity purified from stably transfected 293T cells efficiently precipitates core APC/C subunits, as determined by mass spectrometry. Surprisingly, the levels of Cdc27 co-purifying with Ube2S are reduced in mitosis and G1, which we attribute to a low efficiency of our antibody to precipitate Ube2S*APC/C*Cdc20/Cdh1-complexes. This hypothesis is supported by the reciprocal purification of APC/C using Cdc27-antibodies, which leads to co-purification of Ube2S during mitosis and G1 (Figure S3A); by purification of FLAGUbe2S from stably transfected, mitotic 293T cells, which co-precipitates Cdc27 (Figure S3B); and by co-fractionation of Ube2S with core APC/C in sucrose gradient centrifugations of mitotic and G1-extracts (Figures S3C and S3D). The regulated interaction between Ube2S and APC/C and its activators demonstrates that Ube2S is a component of the APC/C machinery in cells.

Ube2S is Crucial for APC/C Activity In Vivo

To determine whether Ube2S functions with APC/C in vivo, we depleted Ube2S and/or UbcH10 in human HeLa and U2OS and in *Drosophila* S2 and Kc cells. The fly Ube2S cooperates with the UbcH10 homolog Vihar in catalyzing chain formation on APC/C substrates (Figure S4A). If loss of Ube2S and/or UbcH10 abrogates APC/C activity, cells should be delayed in mitosis due to defects in spindle formation, which activate the spindle checkpoint (Goshima et al., 2007; Somma et al., 2008; Tugendreich et al., 1995); failure to disassemble spindle checkpoint complexes (Reddy et al., 2007; Stegmeier et al., 2007; Summers et al., 2008); and stabilization of APC/C substrates, which interferes with mitotic exit (Peters, 2006; Tugendreich et al., 1995); and stabilization of APC/C substrates, which interferes with mitotic exit (Peters, 2006; Tugendreich et al., 1995).

We depleted Ube2S in *Drosophila* S2 cells stably expressing GFP-tagged histone 2B and mCherry-tagged α-tubulin and analyzed progression through mitosis by time-lapse microscopy. As a control, we depleted *Drosophila* UbcH10/Vihar, which is known to activate APC/C in flies (Mathe et al., 2004). Importantly, the depletion of either Ube2S or UbcH10 results in a strong delay in a metaphase-like state (Figure 3A and Figure S4B; t>3h, compared to ~10min in control cells). This suggests that like UbcH10/Vihar, *Drosophila* Ube2S is important for progression through mitosis.

We then depleted Ube2S and/or UbcH10 in asynchronous cells and determined the number of mitotic cells in the population. We used five siRNAs against human Ube2S, and three siRNAs against human UbcH10, all of which effectively knock down the respective protein and result in identical phenotypes (compare Figure 3B and Figure S4C). In both human and fly cells, reducing Ube2S levels does not strongly affect the mitotic distribution (Figure 3B and Figure S4C and S4D), and depletion of UbcH10 results in a weak increase in the mitotic index (Figure 3B), as reported previously (Mathe et al., 2004; Rape and Kirschner, 2004). This is consistent with experiments showing that siRNA-dependent depletion of Cdc20, Cdh1, or single APC/C subunits trigger negligible increases in the mitotic index (Baumgarten et al., 2009; Kittler et al., 2004; Wei et al., 2004). Importantly, the co-depletion of Ube2S and UBcH10 strongly increases the mitotic index of human and *Drosophila* cells (Figure 3B and Figures S4C and S4D). By contrast, co-depleting UbcH10 and all UbcH5 homologs does not strongly impact

progression through mitosis (Figure 3C). The effects on mitosis caused by UbcH10/Ube2S depletion are among the most dramatic seen by siRNA against APC/C, underscoring the importance of UbcH10 and Ube2S in APC/C-dependent chain formation.

We next determined whether co-depletion of Ube2S and UbcH10 results in aberrations in spindle structure and function (Figure S5). Using immunofluorescence and time-lapse microscopy, we observed detachment of spindle poles (Figures S5A and S5D) and spindle elongation (Figure S5F). Chromosome missegregation (Figure S5C), defects in chromosome congression in early mitosis, and an inability to maintain a metaphase plate were evident in experiments performed by time lapse microscopy. All of these phenotypes had been reported after APC/C inactivation (Ban et al., 2007; Gimenez-Abian et al., 2005; Goshima et al., 2007; Somma et al., 2008). To test whether this leads to checkpoint activation, we concurrently depleted Mad2, which abrogates spindle checkpoint function even in the presence of nocodazole or taxol. Switching off the checkpoint partially rescues the mitotic delay caused by UbcH10/Ube2S depletion (Figure 3B and Figure S4D), indicating that the checkpoint had been activated. However, cells co-depleted of Ube2S, UbcH10, and Mad2 are still delayed in progression through mitosis, as seen by time-lapse microscopy in *Drosophilia* S2 cells (Figure 3A), and by accumulation of human cells in prometaphase and metaphase (Figure S5E). Thus, as expected for inhibition of APC/C, loss of Ube2S and UbcH10 results in spindle defects, activation of the spindle checkpoint, and in mitotic delay independent of the checkpoint.

Next, we tested for a role of Ube2S in APC/C-dependent spindle checkpoint silencing by analyzing genetic interactions with p31comet and Usp44. p31comet cooperates with UbcH10 and APC/C to promote checkpoint silencing (Reddy et al., 2007; Summers et al., 2008), which is counteracted by the deubiquitylating enzyme Usp44 (Kim et al., 2009; Stegmeier et al., 2007). Accordingly, the depletion of both UbcH10 and p31comet results in synthetic mitotic arrest, and depletion of UbcH10 inhibits spindle checkpoint bypass caused by siRNA against Usp44 (Figures 3D and 3E). In a similar manner, Ube2S- and p31comet-siRNA strongly synergize in increasing the mitotic index (Figure 3D), and loss of Ube2S recues the defective checkpoint response observed after Usp44 depletion (Figure 3E), showing that Ube2S contributes to APC/C-dependent spindle checkpoint silencing.

Finally, we tested whether Ube2S triggers the degradation of APC/C substrates in vivo. When Ube2S/UbcH10-depleted human cells are released from mitotic arrest, the degradation of several APC/C substrates is strongly delayed (Figure 4A). When analyzed by fluorescence microscopy, multiple APC/C substrates are stabilized in siRNA-treated cells, including cyclin A, cyclin B, and Tpx2 (Figure 4B and 4C and Figure S6A). Tpx2-levels remain high in siRNA-treated cells even in G1, with Tpx2 accumulating at remnants of the spindle midzone (Figure 4C). Tpx2 is also stabilized in G1 if only Ube2S is depleted (Figure S6C). As observed by time-lapse microscopy, the depletion of Ube2S in *Drosophila* S2 cells stably expressing GFP-tagged cyclin B leads to strong stabilization of cyclin B on the spindle pole (Figure 4D). Thus, Ube2S plays a critical role in driving the degradation of APC/C substrates in cells.

Several lines of evidence indicate that depletion of Ube2S and UbcH10 directly affect APC/C activity, and not only indirectly through activation of the spindle checkpoint: first, cyclin A is stabilized by UbcH10/Ube2S depletion (Figure 4B),

although it is not regulated by the checkpoint (Geley et al., 2001); second, Tpbx2 is stabilized at mitotic stages in which the checkpoint is inactive (Figure 4C); third, fly GFP-cyclin B1 is stable in Ube2S/Mad2-depeleted S2 cells as monitored by time-lapse microscopy (Figure 4D); and fourth, depletion of Ube2S also stabilizes APC/C substrates during interphase (Figure S6B). Together, our experiments demonstrate a key role for Ube2S in activating APC/C. The phenotypes of co-depleting Ube2S and UbcH10 are very similar to complete APC/C inhibition: mitotic arrest, spindle defects, prolonged activation of the checkpoint, and stabilization of all tested APC/C substrates.

Ube2S Is Regulated by APC/C-Dependent Degradation

Overexpression of Ube2S transforms cells in culture and promotes tumor growth in mice (Jung et al., 2006; Tedesco et al., 2007). This suggests that Ube2S levels have to be regulated, and indeed, Ube2S is degraded during G1 (Figure 5A). The proteolysis of Ube2S occurs at similar times as the degradation of UbcH10, but is delayed compared to APC/C substrates. Ube2S is undetectable in cells arrested in quiescence (Figure S7A) and synthesized in parallel with UbcH10 when cells re-enter the cell cycle upon stimulation with serum.

Because Ube2S is co-regulated with UbcH10, its levels might indeed be controlled by APC/C itself, as reported for UbcH10 (Rape and Kirschner, 2004). Indeed, APC/C activation, accomplished by depleting its inhibitor Emi1, leads to a dramatic decrease in the concentration of Ube2S, which is also observed for APC/C substrates (Figure 5B). Conversely, co-depletion of Apc2 and UbcH10 results in a strong increase in Ube2S (Figure 5C and Figure S7B).

Consistent with Ube2S being an APC/C substrate, APC/C^{Cdh1} catalyzes the ubiquitylation of Ube2S in vitro, which can be blocked by the APC/C inhibitor Emi1 (Figure 5D). This reaction requires UbcH5 or UbcH10 to promote the attachment of the first ubiquitin to Ube2S. Although substrates do not compete with Ube2S binding to Cdh1 or APC/C, they interfere with the APC/C-dependent ubiquitylation of Ube2S (Figure S7C). Interestingly, ubiquitylation of Ube2S by the APC/C is strongly increased by microtubules (Figure 5E and Figures S7D and S7E), which is consistent with the known spindle binding of APC/C (Peters, 2006). This efficient ubiquitylation of Ube2S depends on its active-site Cys and on its C-terminal tail (Figure 5E), and the ubiquitin chains attached to Ube2S are specifically linked through Kl1 (Figure S7E). 26S proteasomes trigger the degradation of ubiquitylated Ube2S, which is blocked by the addition of the proteasome inhibitor MG132 (Figure 5F). These findings indicated the APC/C promotes the ubiquitylation and degradation of both Ube2S and UbcH10 (Rape and Kirschner, 2004), resulting in the tight co-regulation of these E2 enzymes.

Discussion

The APC/C is essential for cell cycle progression on all eukaryotes (Peters, 2006). The human APC/C modifies substrates with K11-linked ubiquitin chains to trigger their proteasomal degradation (Jin et al., 2008). The formation of K11-linked chains is initiated by its E2 UbcH10, which recognizes TEK boxes in substrates and ubiquitin (Jin et al., 2008). Here, we identify the conserved Ube2S as a K11-specific chain elongating

E2 for human and *Drosophila* APC/C. Together, UbcH10 and Ube2S promote the efficient degradation of APC/C substrates, spindle assembly, and progression through mitosis. We propose that UbcH10 and Ube2S constitute the physiological E2 module of human APC/C during mitosis.

The cooperation between Ube2S and UbcH10 is reminiscent of yeast APC/C, which uses a chain-initiating E2, Ubc4, and a chain elongating E2, Ubc1 (Rodrigo-Brenni and Morgan, 2007). However, Ubc4 and Ubc1 function sequentially to assemble K48-linked ubiquitin chains, whereas human UbcH10 and Ube2S most likely bind APC/C at the same time. This hypothesis is supported by competition studies, in which a large excess of UBcH10 does not block the binding of Ube2S to Cdh1 or APC/C, and by ubiquitylation assays, in which Ube2S and UbcH10 promote the APC/C-dependent ubiquitylation of each other. By binding to different sites on the APC/C, UbcH10 and Ube2S can truly cooperate in the assembly of K11-linked ubiquitin chains, allowing them to promote the degradation of the extended family of human APC/C substrates.

UbcH10 binds the RING subunit Apc11 and the cullin subunit Apc2 (Summers et al., 2008; Tang et al., 2001). Consistent with a different mode of APC/C interaction, Ube2S directly binds the APC/C activators Cdc20 and Cdh1. The deletion of C-terminal amino acids of Ube2S ablates its binding to Cdh1 and abrogates its activity toward APC/C, which implies that the association between Ube2S and Cdh1 is required for Ube2S activity. The interaction between Ube2S and Cdc20/Cdh1 is cell-cycle regulated and occurs only at times when Cdc20 and Cdh1 activate APC/C. We propose that recruitment of Ube2S in part explains the capability of Cdc20 and Cdh1 to increase the catalytic activity of the APC/C.

The strongest effects on cell cycle progression are observed if Ube2S and UbcH10 are co-depleted from cells. This indicates that APC/C ubiquitylates at least some substrates if one E2 is present at low concentrations. It is possible that other E2s partially compensate for loss of either UbcH10 or Ube2S. Such E2s are unlikely to include Ube2D/UbcH5 or Ube2K/E2-25K, which neither assemble K11-linked chains (Jin et al., 2008), nor target APC/C substrates for degradation in extracts (Jin et al., 2008), nor show genetic interactions with UbcH10. We believe it is more likely that even low levels of UBcH10 support initiation of short chains, which could then be extended by Ube2S. In support of this notion, mutation of UbcH10 in flies or its efficient depletion in several human cell lines lead to cyclin B stabilization and a delay in mitosis (Berlingieri et al., 2007; Fujita et al., 2009; Mathe et al., 2004; Rape and Kirschner, 2004; Reddy et al., 2007; Wagner et al., 2004), while incomplete depletion of UbcH10 does not produce these phenotypes (Walker et al., 2008)

Consistent with their close cooperation in modifying APC/C substrates, UbcH10 and Ube2S are tightly co-regulated in cells. Both E2s are degraded during G1, which is promoted by APC/C-dependent ubiquitylation. The APC/C turns against its own E2s only after most, if not all, APC/C substrates have been degraded. As co-depletion of UBcH10 and Ube2S inactivates APC/C during mitosis, it can be assumed that the degradation of both E2s during G1 also shuts off the APC/C, as previously proposed (Rape and Kirschner, 2004).

The identification of a K11-specific E2 for the APC/C underscores the importance of K11-linked ubiquitin chains for cell cycle control (Jin et al., 2008). The phenotypes observed after co-depletion of Ube2S and UbcH10 are reminiscent of a strong mitotic

delay caused by injection of a K11-deficient ubiquitin mutant into *Xenopus* embryos (Jin et al., 2008). A proteomic analysis revealed that p97/Cdc48, whose depletion causes mitotic arrest in HeLa cells (Wojcik et al., 2006), efficiently binds K11-linked ubiquitin chains (Alexandru et al., 2008). K11-linked ubiquitin chains also accumulate in disease with impaired proteasome activity, such as Huntington's or Alzheimer's (Bennett et al., 2007), and they are abundant in normally dividing cells (Xu et al., 2009). Together, these findings point to K11-linked chains as critical, if not essential, regulators of proteasomal degradation and cell cycle progression in higher eukaryotes.

In conclusion, we have identified the highly conserved Ube2S as a chain-elongating E2 of human and *Drosophila* APC/C. UbcH10 and Ube2S likely constitute the physiological E2 module for the APC/C during mitosis, in which UbcH10 initiates Ube2S elongates K11-linked ubiquitin chains. The inhibition of mitotic APC/C is an attractive goal for chemotherapy, as shown here, could be accomplished by small molecules targeting both UbcH10 and Ube2S.

Methods

Detailed materials and methods can be found in the Supplementary Information. Ube2S was purified as an N-terminal MBP fusion protein, and the MBP-tag was cleaved off by TEV protease before Ube2S was used in assays. UbcH10 and UbcH5c were purified from *E. coli*, while E1 and ^{His}Cdh1 were purified from Sf9 cells. In vitro ubiquitylations were performed as described, with APC/C being obtained from human HeLa S3 cells (Jin et al., 2008). Immunofluorescence analysis was performed in HeLa cells in described (Rape and Kirschner, 2004). siRNAs were obtained from Dharmacon (for sequences see Supplementary Information). Ube2S-binding partners were identified by MudPIT-mass spectrometry performed by the UCB Proteomics/Mass Spectrometry Laboratory (P/MSL). Supplemental Information is available at:

http://www.pnas.org/content/106/43/18213/suppl/DCSupplemental

Acknowledgments

We thank Deborah Zajchowski and Rick Feldman for providing antibodies against Ube2S, Eric Griffis and Ron Vale for S2 cells expressing cyclin B1*GFP, Claudio Sunkel (IMBC, Portugal) for Mad2 antibody, Chris Fromme for help with sucrose gradients, Isaac Oderberg for technical help, the Drubin/Barnes laboratory for help with microscopy, and Julia Schaletzky for discussions and critically reading the manuscript. This work was supported by National Institutes of Health Grants RO1 GM066272 (to G.H.K.) and RO1 GM083064 (to M.R.) and a National Institutes of Health Director New Innovator Award (to M.R.). M.R. is a Pew fellow.

Figure Legends

Figure 1: Ube2S Promotes Formation of K11-Linked Ubiquitin Chains on APC/C Substrates

(A) Ube2S promotes chain formation on cyclin A. 35S-cyclin A was incubated with APC/C^{Cdh1}, E1, ubiquitin, and UbcH10, and/or Ube2S. Reaction products were analyzed by autoradiography. **(B)** Ube2S promotes chain formation on Plk1. The ubiquitylation of 35S-Plk1 was analyzed as described for cyclin A. **(C)** Ube2S does not promote chain initiation. 35S-cyclin A and 35S-Plk1 were incubated with APC/C^{Cdh1} and methylubiquitin, as described above. **(D)** Ube2S cooperates with APC/C^{Cdc20}. APC/C^{Cdc20} was activated as described (Reddy et al., 2007), and used to ubiquitinate endogenous Cdc20, as detected by Western blot. **(E)** Ube2S assembles K11-linked chains on APC/C substrates. The ubiquitylation of 35S-cyclin A by APC/C^{Cdh1} and Ube2S was analyzed in the presence of ubiquitin mutants, as indicated. "K6" describes ubiquitin containing Lys-6, "R6" is ubiquitin in which K6 has been exchanged to Arg. **(F)** Ube2S requires its catalytic Cys and its C terminus for APC/C-dependent chain formation. Ubiquitylation of 35S-cyclin A was analyzed in the presence of APC/C^{Cdh1}, Ube2S, Ube2SC95S, or Ube2S1-196/Ube2SΔC. In addition, the activity of Ube2S was competed by a C-terminal peptide encompassing the last 26 amino acids of Ube2S (Ube2S+pep). **(G)** Ube2S catalyzes formation of K11-linked ubiquitin dimers independently of an E3. ube2S and indicated mutants were incubated with E1 and ubiquitin or ubi-R11, and the formation of ubiquitin dimers (ubi-ubi) was detected by Coomassie staining. **(H)** Ube2S does not require UbcH10 during chain elongation. 35S-cyclin A was briefly incubated with APC/C^{Cdh1} and UbcH10, before UbcH10 was inactivated by adding a 100-fold excess of UbcH10C114S. Then, Ube2S was added alone or together with the APC/C inhibitor Emi1. **(I)** Ube2S depends on the APC/C for activity. 35S-cyclin A was briefly incubated with APC/C^{Cdh1} and UbcH10, and then Ube2S alone or Ube2S together with the APC/C inhibitor Emi1 or an excess of the APC/C substrate securin were added.

Figure 2: Ube2S Interacts with APC/C

(A) Ube2S binds Cdc20 and Cdh1 in a cell-cycle dependent manner. Ube2S was precipitated from extracts of synchronized HeLa cells, and co-purifying proteins were detected by Western blot. **(B)** Cdc20 binds Ube2S in mitosis. Cdc20 was precipitated from mitotic HeLa S3 cells. Co-purifying Ube2S and Mad2 were detected by Western blot. **(C)** Ube2S binds Cdh1. FLAGUbe2S was precipitated from 293T cells, and co-purifying Ube2S was detected by Western blot. **(D)** Cdh1 binds Ube2S. HACdh1 or HACdh1ΔWD40 were precipitated from 293T cells, and co-purifying Ube2S was detected by Western blot. **(E)** Ube2S binds Cdh1 from G1 extracts. Immobilized MBP or MBPUbe2S were incubated with HeLa S3 extracts. Recombinant securin or UbcH10 (~100x excess over Cdh1) were added as indicated. Bound Cdh1 was detected by Western blot. **(F)** Ube2S binds Cdh1. 35S-Cdh1 was incubated with immobilized MBPUbe2S or the indicated truncation mutants. Bound Cdh1 was detected by autoradiography. **(G)** Ube2S directly binds Cdh1. ^{His}Cdh1 purified to homogeneity was incubated with MBP and MBPUbe2S. Bound Cdh1 was detected by Western blot. **(H)** The C terminus of ubiquitin is required for its interaction with Cdh1. FLAGUbe2S or

FLAGUbe2SΔC were precipitated from 293T cells, and bound HACdh1 was analyzed by Western blot.

Figure 3: Ube2S Regulates Progression of Cells Through Mitosis

(A) *Drosophila* Ube2S is required for mitosis. S2 cells stably expressing histone H2B-GFP and α-tubulin-mCherry were transfected with RNAi and filmed by time-lapse microscopy. **(B)** Ube2S and UbcH10 cooperate to promote progression through mitosis. HeLa cells were transfected with the indicated siRNAs, and scored for mitotic cells. Error bars, SEM derived from at least seven independent frames of different experiments, counting at least 1000 cells in each frame. The right panel shows the depletion efficiency of Western blot. **(C)** UbcH10 shows genetic interactions with Ube2S, but not UbcH5. UbcH10 was depleted by siRNA alone, together with all four UbcH5-homologs, or with Ube2S, and the mitotic index of the cell population was determined. The right panel shows the depletion efficiency, as detected by Western blot. **(D)** Ube2S contributes to APC/C-dependent spindle checkpoint silencing. HeLa cells were transfected with the indicated siRNA and scored for cells arresting in mitosis. **(E)** Ube2S counteracts the DUB Usp44. HeLa cells were transfected with indicated siRNA, and treated with taxol to activate the spindle checkpoint. The number of cells arrested in mitosis were counted.

Figure 4: Ube2S and UbcH10 promote the degradation of APC/C substrates in cells

(A) Depletion of Ube2S and UbcH10 strongly stabilizes APC/C substrates. Mitotic HeLa cells transfected with siRNA against UbcH10 and Ube2S were released into G1, and the levels of several APC/C substrates were measured by Western blot. **(B)** The UbcH10/Ube2S module drives degradation of cyclin A. HeLa cells were transfected with control or UbcH10/Ube2S siRNA, and cyclin A was detected by immunofluorescence (green). The spindle was visualized by antibodies against α-tubulin (red) and DNA was stained with DAPI (blue). (Scale bar 10 μm.) **(C)** Accumulation of Tpx2 in postmitotic HeLa cells after depletion of Ube2S and UbcH10. Tpx2 was detected in HeLa cells transfected with the indicated siRNAs by immunofluorescence. Cells in early G1 were identified, and representative images are shown. (Scale bar 10 μm.) The right panel shows a quantification of Tpx2 levels in HeLa cells in G1. **(D)** Ube2S is required for degradation of cyclin B in *Drosophila*. S2 cells stably expressing cyclin B-GFP were transfected with the RNAi, and imaged by timelapse microscopy. Depletion of Ube2S stabilizes cyclin B-GFP on the spindle pole (arrow) independently of spindle checkpoint activation.

Figure 5: Ube2S is Regulated by the APC/C

(A) Ube2S is degraded during G1. Mitotic HeLa cells were released into fresh medium to allow mitotic exit, and the indicated proteins were detected by Western blot. **(B)** Ube2S levels decrease upon activation of the APC/C. HeLa cells were treated with siRNA against the APC/C inhibitor Emi1, and the indicated proteins were detected by Western blot. **(C)** Ube2S-levels increase after depletion of APC/C subunits. HeLa cells were treated with the indicated siRNAs, and the levels of Ube2S were determined by Western

blotting. **(D)** Ube2S is ubiquitylated by APC/C^{Cdh1}. Affinity-purified APC/C^{Cdh1} was incubated with 35S-Ube2S in the absence or presence of UbcH5c, UbcH10, or Emi1. Reaction products were detected by autoradiography. **(E)** Microtubules promote the ubiquitylation of Ube2S. APC/C^{Cdh1} was incubated with taxol-stabilized microtubules, UbcH5c, and 35S-Ube2S, 35S-Ube2SC95S, 35S-Ube2SΔC, or 35S-Ube2S, and the C-terminal Ube2S peptide. Reaction products were detected by autoradiography. **(F)** Ubiquitylated Ube2S is degraded by the 26S proteasome. 35S-Ube2S was ubiquitylated by APC/C^{Cdh1} in the presence of microtubules. Subsequent to the ubiquitylation, purified 26S proteasomes were added. MG132 was added as indicated. The reaction products were visualized by autoradiography.

Fig. S1. Ube2S extends K11-linked ubiquitin chains on APC/C substrates

(A) Ube2S extends K11-linked ubiquitin chains on cyclin B1. APC/C^{Cdh1} and UbcH10/Ube2S were used to ubiquitinate ^{35}S-cyclin B1. The reactions were performed in the presence of ubiquitin or ubi-R11, and reaction products were detected by autoradiography. **(B)** Ube2S extends K11-linked ubiquitin chains on geminin. The ubiquitylation of ^{35}S-geminin by APC/C^{Cdh1} in the presence of ubiquitin and ubi-R11 was performed as described above. **(C)** Ube2S extends K11-linked ubiquitin chains on Tpx2. The ubiquitylation of ^{35}S-Tpx2 by APC/C^{Cdh1} in the presence of ubiquitin and ubi-R11 was performed as described above. **(D)** Ube2S extends ubiquitin chains beyond the length achieved by UbcH10 and APC/C alone. APC/C^{Cdh1} and increasing concentrations of UbcH10 ([UbcH10] from 10–50 nM) were used to promote ubiquitylation of ^{35}S-cyclin A. Ube2S or Ube2SC95S were added where indicated. The reaction products were separated on long 5–15% SDS gradient gels, and visualized by autoradiography. **(E)** Ube2S can extend ubiquitin chains formed by APC/C and UbcH5c. APC/C^{Cdh1} was used to promote the ubiquitylation of ^{35}S-cyclin A. Ube2S and UbcH5c were added when indicated. This reaction contained an increased concentration of ^{35}S-cyclin A, including more reticulocyte lysate. E2 enzymes present in reticulocyte lysate are responsible for weak chain initiation observed in the reaction containing only Ube2S. Reaction products were separated on long 5–15% SDS gradient gels and analyzed by autoradiography. **(F)** Ube2S does not extend ubiquitin chains formed by Brca1. ^{35}S-Brca1 was incubated with E1, UbcH5c, and ubiquitin in the presence of buffer or Ube2S, and the time course of ubiquitylation at 16 °C was analyzed after autoradiography. Addition of Ube2S has no effect on chain length. **(G)** Ube2S is unable to extend ubiquitin chains nucleated by UbcH5c, if ubi-R11 is present. The ubiquitylation of ^{35}S-cyclin A by APC/C^{Cdh1} was analyzed in the presence of ubi-R11. **(H)** Ube2S extends K11-linked ubiquitin chains with APC/C^{Cdc20}. The ubiquitylation of Cdc20 was analyzed after APC/C^{Cdc20} was precipitated from mitotic extracts and incubated with E1, p31comet, and UbcH10/Ube2S. The reaction was performed in the presence of wt-ubiquitin or ubi-R11. Ubiquitylated Cdc20 was detected by Western blotting. **(I)** The chain elongating E2 enzymes E2–25K and Ube2N/Uev1A do not cooperate with UbcH10 and APC/C^{Cdh1} in promoting chain assembly. The ubiquitylation of ^{35}S-Plk1 by APC/C^{Cdh1} was initiated by incubation with UbcH10, and chain elongation was catalyzed by addition of Ube2S, E2–25K, or Ube2N/Uev1A. The reactions were performed in the presence of wt-ubiquitin and ubi-

R11, and products were detected by autoradiography.

Figure S2. Ube2S interacts with APC/C-activators

(A) ^{FLAG}Ube2S binds Cdc20 and core APC/C in mitosis. 293T cells were transfected with FLAGUbe2S and synchronized in mitosis. FLAGUbe2S was precipitated on FLAG-agarose, and co-purifying proteins were detected by Western blotting. **(B)** The interaction between Ube2S and ^{35}S-Cdh1 is mediated by the WD40-repeat domain of Cdh1. MBP or MBPUbe2S were coupled to amylose resin and incubated with the indicated Cdh1-truncation mutants. Bound proteins were detected by autoradiography. **(C)** APC/C substrates do not compete for binding of Ube2S to Cdh1. MBP or MBPUbe2S were immobilized on amylose resin and incubated with ^{35}S-Cdh1 either alone or in presence of an approximate 100-fold excess of the unlabeled APC/C substrate securin. Beads were extensively washed, eluted, and bound proteins were analyzed by autoradiography. **(D)** Cdh1 can bind substrates and Ube2S at the same time. MBP or MBPUbe2S were incubated with the APC/C substrate ^{35}S-cyclin A alone, or with ^{35}S-cyclin A and recombinant ^{His}Cdh1. The reaction products were analyzed by Coomassie staining and autoradiography. The substrate cyclin A is found in Ube2S complexes only in the presence of ^{His}Cdh1, indicating that Cdh1 can bind to Ube2S and substrate at the same time. **(E)** The C terminus of Ube2S is a binding element for Cdh1. ^{35}S-Cdh1 was incubated with the C-terminal Ube2S peptide and then added to MBP or MBPUbe2S-beads. Bound proteins were detected by autoradiography.

Fig. S3. Ube2S associates with APC/C during mitosis and G1

(A) Ube2S binds APC/C. The core APC/C-subunit Cdc27 was precipitated from extracts of synchronized HeLa cells using monoclonal αCdc27-antibodies, and bound Ube2S and Cdc20 were detected by Western blotting. **(B)** Ube2S binds core APC/C during mitosis. 293T cells stably expressing FLAGUbe2S were arrested in mitosis. FLAGUbe2S was precipitated, and co-purifying Cdc27 and Cdc20 were detected by Western blotting. Cdc20 runs very closely to IgG, explaining the background in the control reaction. (C and D*)* Ube2S co-fractionates with APC/C in extracts of HeLa S3 cells in mitosis **(C)** and G1 **(D)**, as detected by sucrose gradient centrifugation. Sucrose gradient centrifugations of mitotic or G1 extracts were fractionated, proteins were precipitated with TCA, and the indicated proteins were detected by Western blotting using specific antibodies. The signal intensity of the Western blots was quantified using Quantity One; it shows that the peaks of the Ube2S, Cdc20/Cdh1, and APC/C blots overlap.

Fig. S4. Effects of Ube2S-depletion

(A) *Drosophila* Vihar/UbcH10 and Ube2S catalyze ubiquitin chain formation by APC/C. ^{35}S-cyclin A was incubated with human APC/C^{Cdh1} and recombinant *Drosophila* Vihar/UbcH10 and *Drosophila* Ube2S. The reaction products were detected by autoradiography. **(B)** The depletion of UbcH10/Vihar by RNAi in S2 cells stably expressing histone H2B-GFP and α-tubulin-mCherry causes a mitotic arrest, which is

rescued by co-depletion of Mad2. If Ube2S is depleted in addition to Vihar, Mad2 does not rescue the mitotic arrest, and cells slip into G1 without chromosome segregation. **(C)** The co-depletion of Ube2S and UbcH10 causes mitotic arrest. HeLa cells were treated with the indicated siRNAs. The number of mitotic cells in the bulk population was determined 48 h later. The siRNA against Ube2S is different from the siRNA used for Fig. 5. The right panel shows the efficiency of depletion, as determined by Western analysis. **(D)** The co-depletion of Ube2S and UbcH10/Vihar by RNAi causes a pronounced mitotic arrest in S2 cells, as scored by pH3 staining. The right panel shows depletion of Mad2 in both Kc and S2 cells, as detected by Western blotting.

Fig. S5. Depletion of Ube2S and UbcH10 causes widespread spindle defects

(A) Ube2S-depletion leads to spindle pole detachment. *Drosophila* S2 cells stably expressing H2B-GFP and α-tubulin-mCherry were treated with RNAi against Ube2S, and imaged by time-lapse microscopy. The arrow indicates a spindle pole, which detaches from the spindle in the RNAi-treated cells. **(B)** Quantification of spindle defects in *Drosophila* Kc cells treated with the indicated siRNA and analyzed by fluorescence microscopy against tubulin. **(C)** Quantification of chromosome missegregation events in postmetaphase Kc cells treated with RNAi as described above. **(D)** Quantification of centrosome defects in RNAi-treated Kc cells measured by immunofluorescence with anti-centrosomin (Cnn) antibodies. **(E)** Depletion of Ube2S and UbcH10 delays mitosis in HeLa cells even in the absence of Mad2. Mitotic cells in metaphase or anaphase were counted after depletion of Mad2, Ube2S/UbcH10, or Mad/Ube2S/UbcH10 by specific siRNA. **(F)** Ube2S and UbcH10 are required for proper spindle formation. Depletion of Ube2S and UbcH10 from HeLa cells results in spindle elongation, chromosome congression defects, and spindle pole abnormalities. Representative figures are shown, in which DNA is detected by DAPI (blue), and the spindle is visualized by immunofluorescence against α-tubulin (red). The length of multiple spindles was measured in control and depleted cells, which is shown in the right panel.

Fig. S6. Ube2S is crucial for APC/C-activity in vivo

(A) Loss of Ube2S and UbcH10 stabilizes cyclin B1 and Tpx2 on the spindle. HeLa cells were transfected with the indicated siRNA, and stained with antibodies against cyclin B1 (red) and Tpx2 (green). DNA was detected by DAPI-staining (blue). Representative images of all mitotic stages are shown. (Scale bar, 10 μm.) Co-depletion of Ube2S and UbcH10 results in strong stabilization of cyclin B1 and Tpx2. **(B)** Ube2S is required for APC/C^{Cdh1} activity in interphase. HeLa cells were treated with control siRNA or specific siRNAs against Emi1 (to activate APC/C and degrade APC/C substrates), Ube2S, or both. The indicated proteins were detected by Western blots. **(C)** Ube2S is required for Tpx2-degradation in cells. HeLa cells were stained for endogenous Tpx2 by immunofluorescence. The fluorescence intensity in G1 cells was measured and plotted for approximately 100 cells per experiment.

Figure S7. APC/C-dependent ubiquitylation and degradation of Ube2S

(A) Ube2S is co-regulated with UbcH10 during quiescence. T24 cells were synchronized

in quiescence by serum starvation, and allowed to reenter the cell cycle by serum stimulation. The levels of the indicated proteins, including Ube2S, were measured by Western blotting. **(B)** Ube2S levels increase after APC/C^{Cdh1}-inhibition in vivo. HeLa cells were treated with the indicated siRNAs, and the levels of Ube2S, Cdh1, UbcH10, and α-actin were determined by Western blotting. The asterisk marks a cross-reactive band of the Cdh1-antibody. **(C)** APC/C substrates inhibit ubiquitylation of Ube2S by APC/C^{Cdh1}. APC/C^{Cdh1} was incubated with the recombinant APC/C substrate securin or the indicated securin mutants and tested for its capability to ubiquitinate ^{35}S-Ube2S. UbcH5c was added as E2. Reaction products were detected by autoradiography. **(D)** The ubiquitylation of Ube2S by APC/C^{Cdh1} is stimulated by microtubules, proceeds by formation of K11-linked ubiquitin chains, and results in Ube2S degradation. ^{35}S-Ube2S was incubated with APC/C^{Cdh1} and UbcH5c in the presence taxol-stabilized microtubules and ubiquitin or ubi-R11. Purified 26S proteasomes were added when indicated. The reaction products were detected by autoradiography.

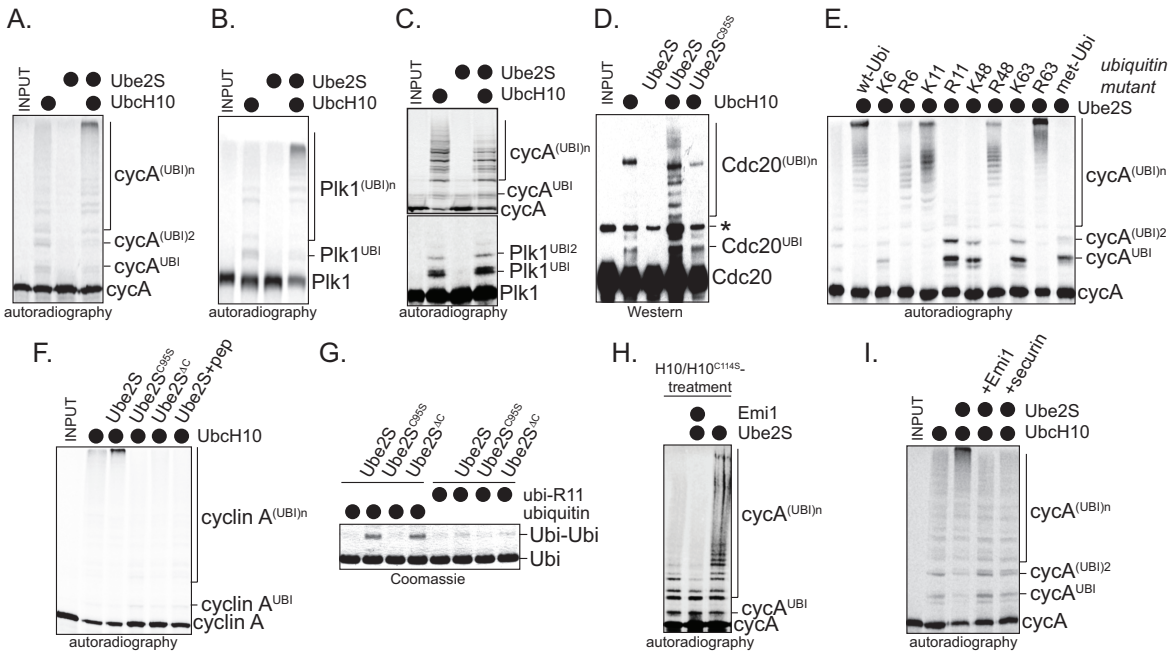
A.
INPUT
Ube2S
UbcH10
cycA(UBI)n
cycA(UBI)2
cycA UBI
cycA
autoradiography
B.
INPUT
Ube2S
UbcH10
Plk1(UBI)n
Plk1 UBI
Plk1
autoradiography
C.
INPUT
Ube2S
UbcH10
cycA(UBI)n
cycA UBI
cycA
Plk1 UBI2
Plk1 UBI
Plk1
autoradiography
D.
INPUT
Ube2S
Ube2S
Ube2S C95S
UbcH10
Cdc20(UBI)n
*
Cdc20 UBI
Cdc20
Western
E.
wt-Ubi
K6
R6
K11
R11
K48
R48
K63
R63
met-Ubi
ubiquitin mutant
Ube2S
cycA(UBI)n
cycA(UBI)2
cycA UBI
cycA
autoradiography
F.
INPUT
Ube2S
Ube2S C95S
Ube2S ΔC
Ube2S+pep
UbcH10
cyclin A(UBI)n
cyclin A UBI
cyclin A
autoradiography
G.
Ube2S
Ube2S C95S
Ube2S ΔC
Ube2S
Ube2S C95S
Ube2S ΔC
ubi-R11
ubiquitin
Ubi-Ubi
Ubi
Coomassie
H.
H10/H10 C114S-
treatment
Emi1
Ube2S
cycA(UBI)n
cycA UBI
cycA
autoradiography
I.
+Emi1
+securin
INPUT
Ube2S
UbcH10
cycA(UBI)n
cycA(UBI)2
cycA UBI
cycA
autoradiography

Figure 1

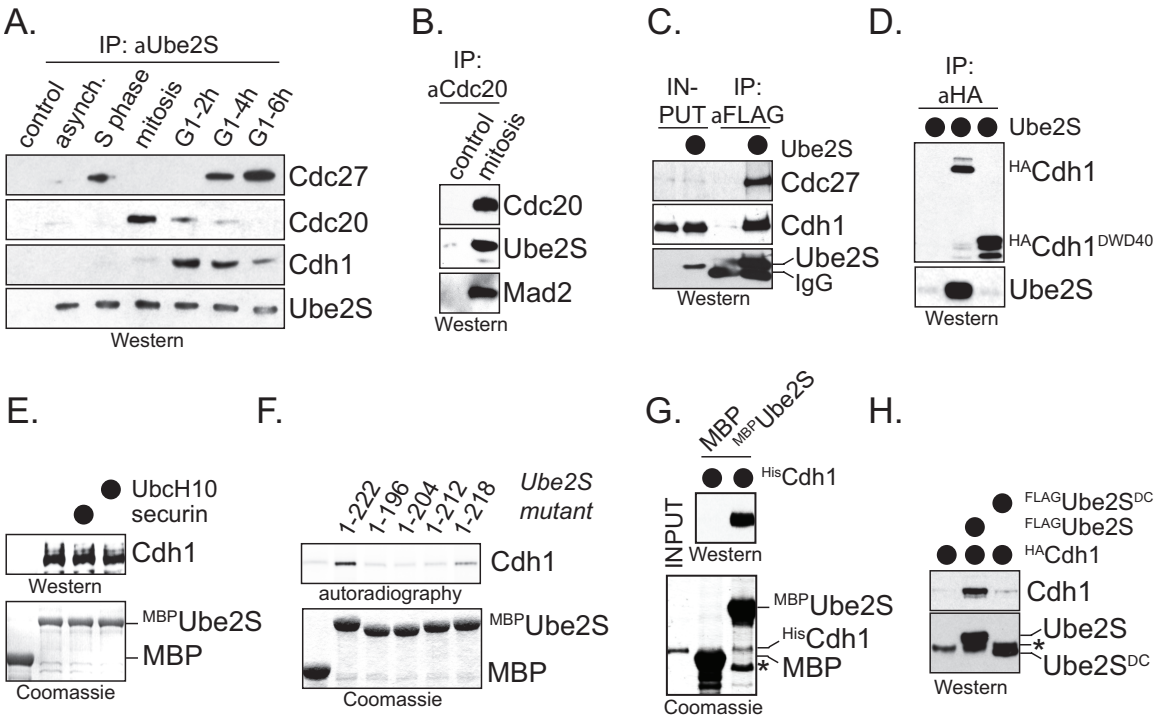
A.
IP: aUbe2S
control
asynch.
S phase
mitosis
G1-2h
G1-4h
G1-6h
Cdc27
Cdc20
Cdh1
Ube2S
Western
B.
IP:
aCdc20
control
mitosis
Cdc20
Ube2S
Mad2
Western
C.
IN-
PUT
IP:
aFLAG
Ube2S
Cdc27
Cdh1
Ube2S
IgG
Western
D.
IP:
aHA
Ube2S
HACdh1
HACdh1DWD40
Ube2S
Western
E.
UbcH10
securin
Cdh1
Western
MBPUbe2S
MBP
Coomassie
F.
1-222
1-196
1-204
1-212
1-218
Ube2S
mutant
Cdh1
autoradiography
MBPUbe2S
MBP
Coomassie
G.
MBP
MBPUbe2S
HisCdh1
INPUT
Western
MBPUbe2S
HisCdh1
MBP
Coomassie
H.
FLAGUbe2SDC
FLAGUbe2S
HACdh1
Cdh1
Ube2S
Ube2SDC
Western

Figure 2

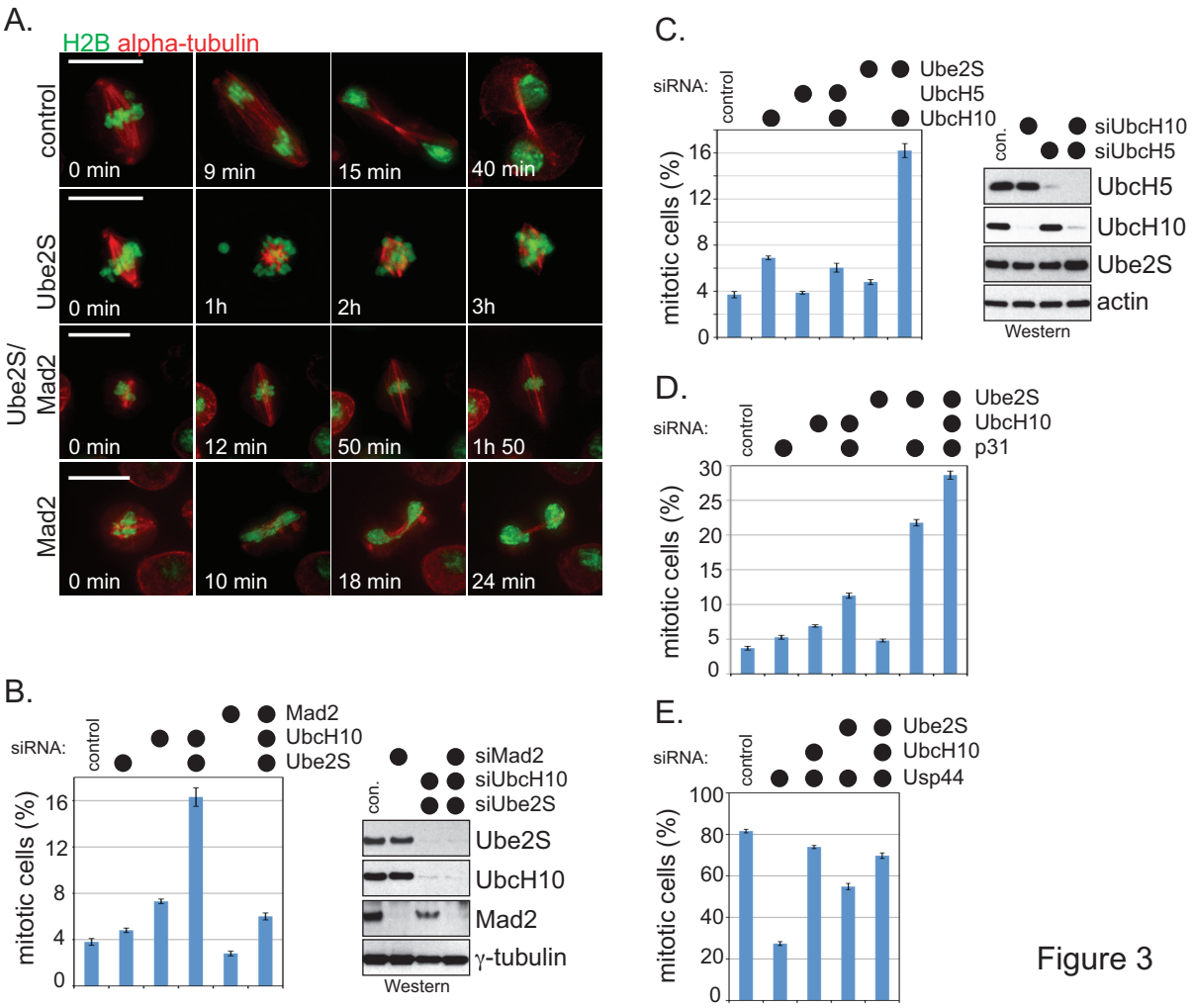
A.
H2B alpha-tubulin
control
Ube2S
Ube2S/ Mad2
Mad2
0 min
9 min
15 min
40 min
1h
2h
3h
12 min
50 min
1h 50
10 min
18 min
24 min
B.
siRNA:
control
Mad2
UbcH10
Ube2S
mitotic cells (%)
con.
siMad2
siUbcH10
siUbe2S
Ube2S
UbcH10
Mad2
γ-tubulin
Western
C.
Ube2S
UbcH5
UbcH10
siUbcH10
siUbcH5
actin
D.
p31
E.
Usp44

Figure 3

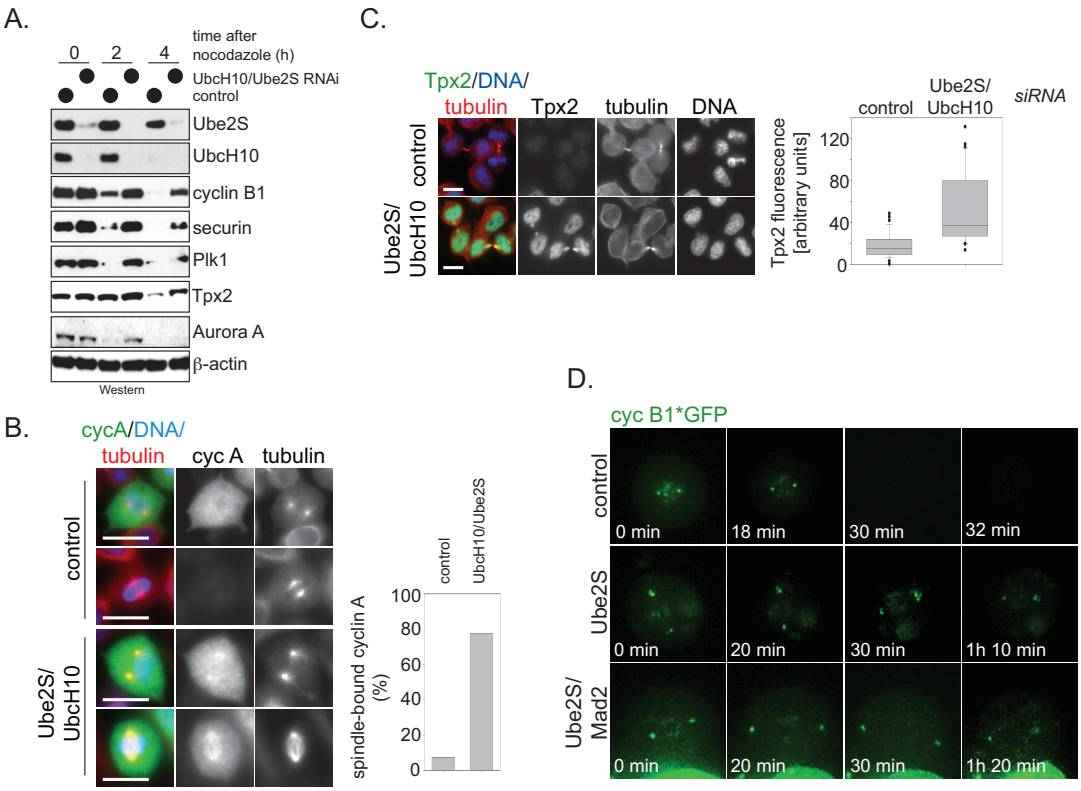
A.
time after nocodazole (h)
0
2
4
UbcH10/Ube2S RNAi
control
Ube2S
UbcH10
cyclin B1
securin
Plk1
Tpx2
Aurora A
β-actin
Western
B.
cycA/DNA/
tubulin
cyc A
tubulin
control
Ube2S/ UbcH10
spindle-bound cyclin A (%)
control
UbcH10/Ube2S
C.
Tpx2/DNA/
tubulin
Tpx2
tubulin
DNA
control
Ube2S/ UbcH10
Tpx2 fluorescence [arbitrary units]
control
Ube2S/ UbcH10
siRNA
D.
cyc B1*GFP
control
Ube2S
Ube2S/ Mad2
0 min
18 min
30 min
32 min
20 min
1h 10 min
1h 20 min

Figure 4

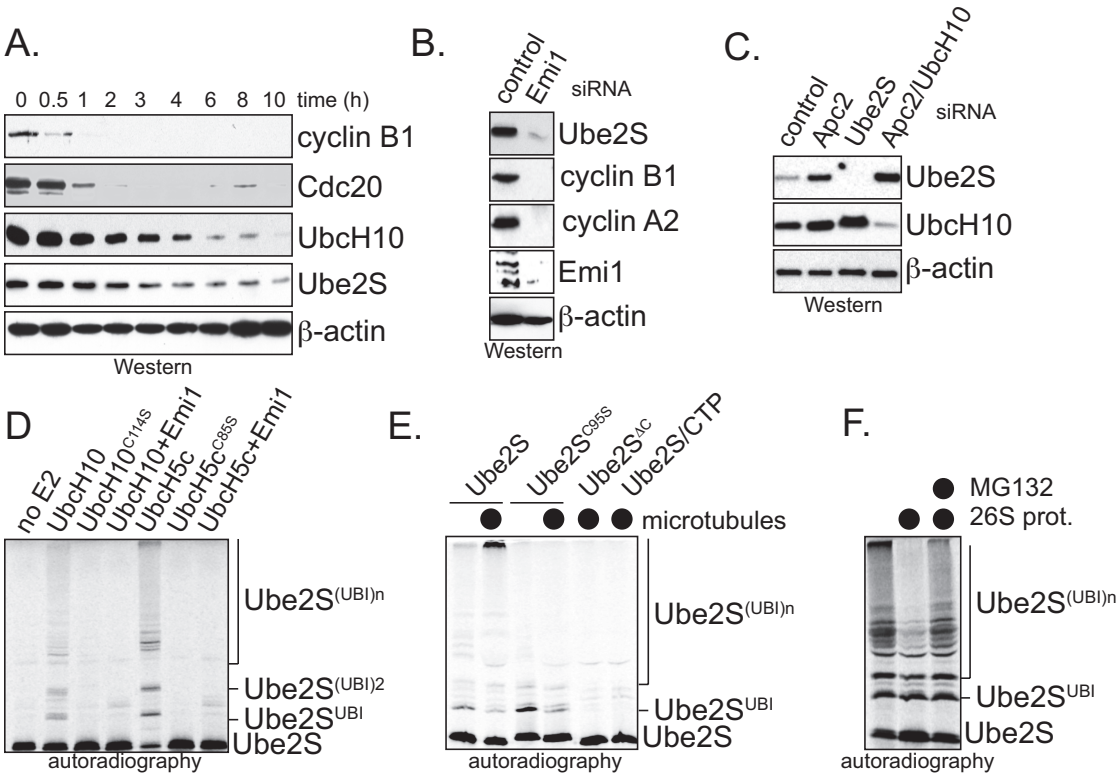
A.
0 0.5 1 2 3 4 6 8 10 time (h)
cyclin B1
Cdc20
UbcH10
Ube2S
β-actin
Western
B.
control
Emi1
siRNA
Ube2S
cyclin B1
cyclin A2
Emi1
β-actin
Western
C.
control
Apc2
Ube2S
Apc2/UbcH10
siRNA
Ube2S
UbcH10
β-actin
Western
D
no E2
UbcH10
UbcH10C114S
UbcH10+Emi1
UbcH5c
UbcH5cC85S
UbcH5c+Emi1
Ube2S(UBI)n
Ube2S(UBI)2
Ube2SUBI
Ube2S
autoradiography
E.
Ube2S
Ube2SC95S
Ube2SΔC
Ube2S/CTP
microtubules
Ube2S(UBI)n
Ube2SUBI
Ube2S
autoradiography
F.
MG132
26S prot.
Ube2S(UBI)n
Ube2SUBI
Ube2S
autoradiography

Figure 5

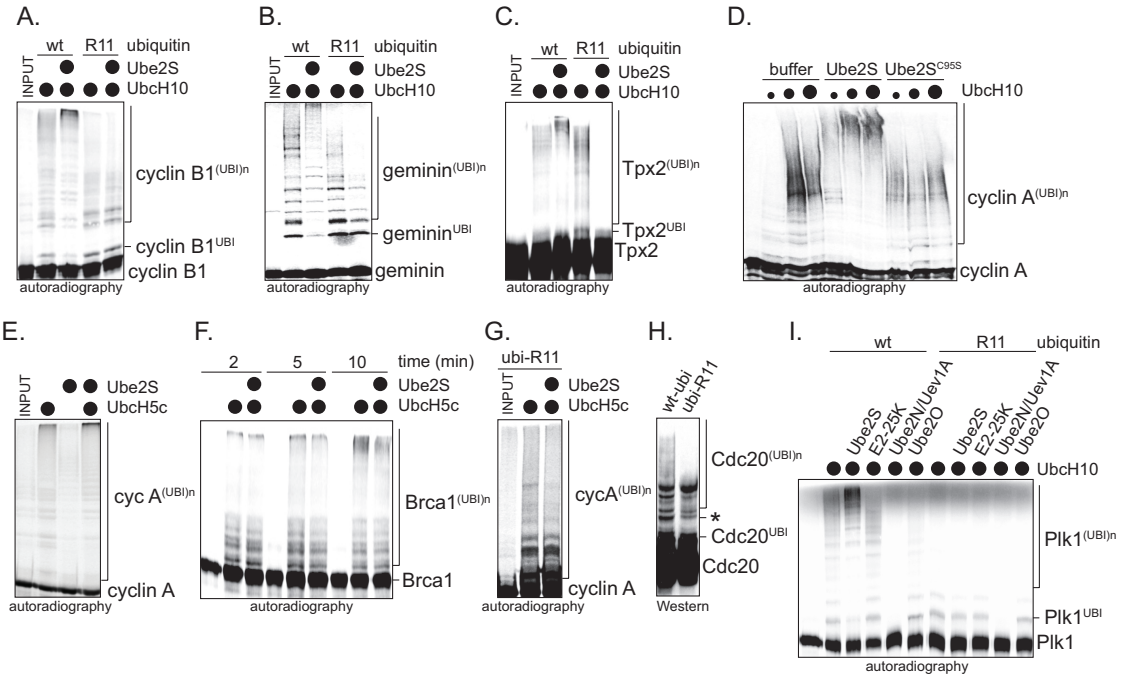
A.
wt
R11
ubiquitin
INPUT
Ube2S
UbcH10
cyclin B1(UBI)n
cyclin B1UBI
cyclin B1
autoradiography
B.
geminin(UBI)n
gemininUBI
geminin
C.
Tpx2(UBI)n
Tpx2UBI
Tpx2
D.
buffer
Ube2S
Ube2SC95S
cyclin A(UBI)n
cyclin A
E.
UbcH5c
cyc A(UBI)n
F.
2
5
10
time (min)
Brca1(UBI)n
Brca1
G.
ubi-R11
cycA(UBI)n
H.
wt-ubi
ubi-R11
Cdc20(UBI)n
*
Cdc20UBI
Cdc20
Western
I.
Ube2S
E2-25K
Ube2N/Uev1A
Ube2O
Plk1(UBI)n
Plk1UBI
Plk1

Figure S1

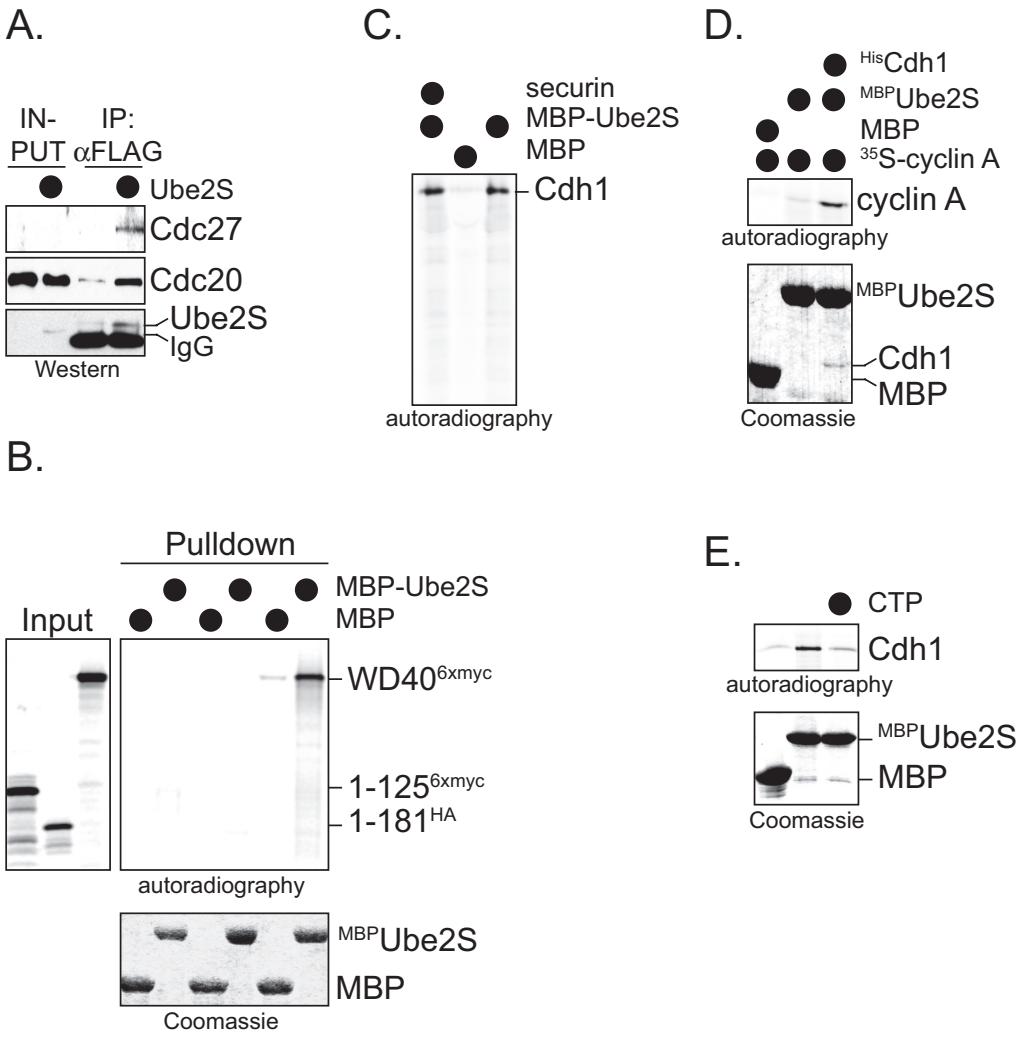
A.
IN-PUT
IP: αFLAG
Ube2S
Cdc27
Cdc20
Ube2S
IgG
Western
C.
securin
MBP-Ube2S
MBP
Cdh1
autoradiography
D.
HisCdh1
MBPUbe2S
MBP
35S-cyclin A
cyclin A
autoradiography
MBPUbe2S
Cdh1
MBP
Coomassie
B.
Pulldown
Input
MBP-Ube2S
MBP
WD406xmyc
1-1256xmyc
1-181HA
autoradiography
MBPUbe2S
MBP
Coomassie
E.
CTP
Cdh1
autoradiography
MBPUbe2S
MBP
Coomassie

Figure S2

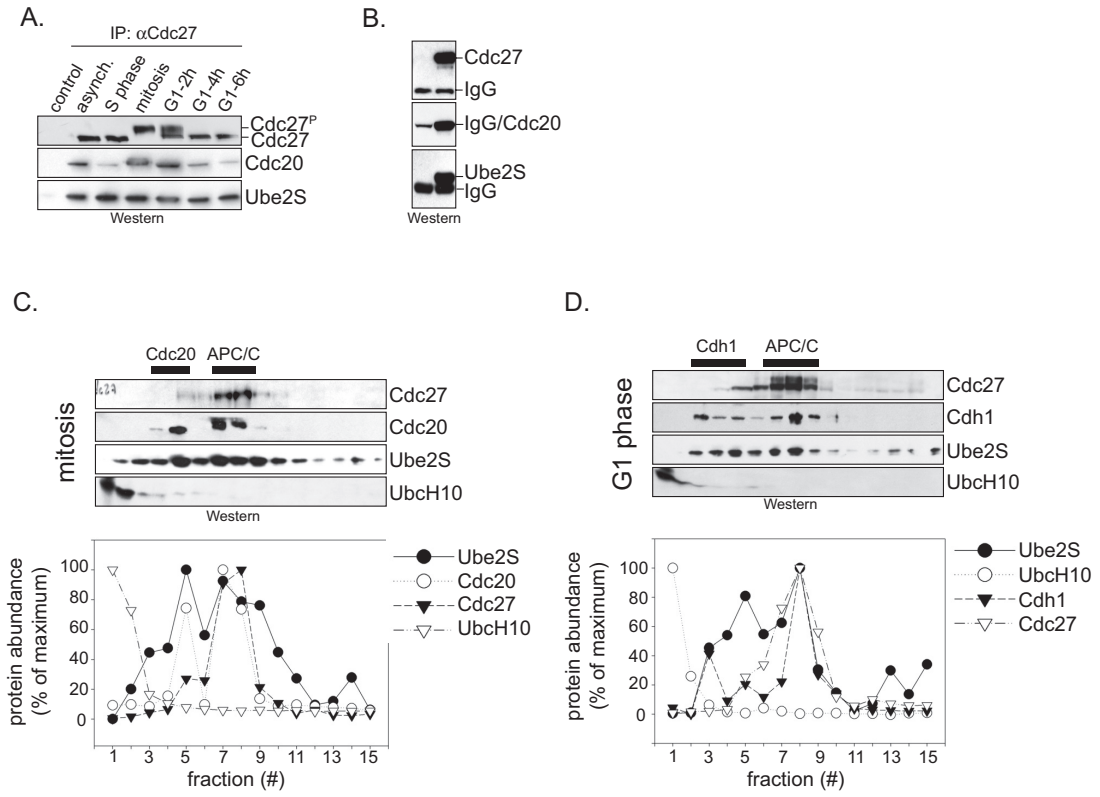
A.
IP: αCdc27
control
asynch.
S phase
mitosis
G1-2h
G1-4h
G1-6h
Cdc27P
Cdc27
Cdc20
Ube2S
Western
B.
Cdc27
IgG
IgG/Cdc20
Ube2S
IgG
Western
C.
Cdc20
APC/C
mitosis
Cdc27
Cdc20
Ube2S
UbcH10
Western
protein abundance (% of maximum)
fraction (#)
Ube2S
Cdc20
Cdc27
UbcH10
D.
Cdh1
APC/C
G1 phase
Cdc27
Cdh1
Ube2S
UbcH10
Western
protein abundance (% of maximum)
fraction (#)
Ube2S
UbcH10
Cdh1
Cdc27

Figure S3

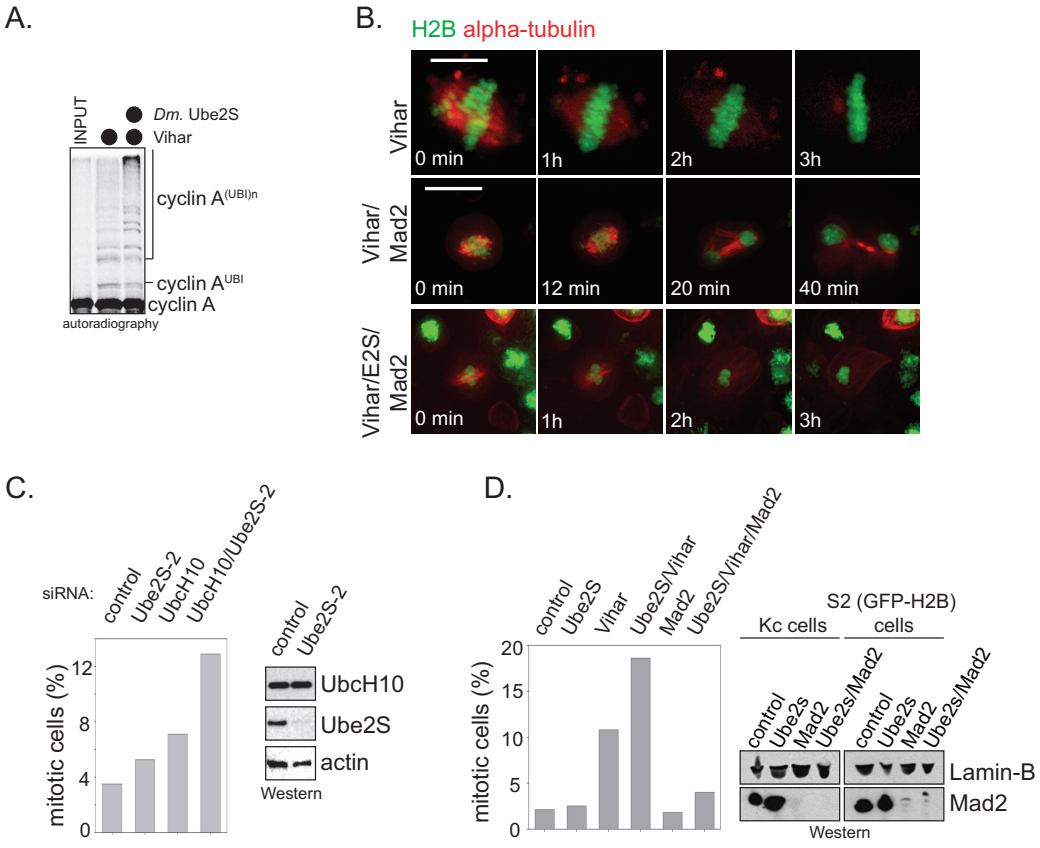
A.
INPUT
Dm. Ube2S
Vihar
cyclin A(UBI)n
cyclin AUBI
cyclin A
autoradiography
B.
H2B alpha-tubulin
Vihar
Vihar/ Mad2
Vihar/E2S/ Mad2
0 min
1h
2h
3h
12 min
20 min
40 min
C.
siRNA:
control
Ube2S-2
UbcH10
UbcH10/Ube2S-2
mitotic cells (%)
UbcH10
Ube2S
actin
Western
D.
control
Ube2S
Vihar
Ube2S/Vihar
Mad2
Ube2S/Vihar/Mad2
mitotic cells (%)
S2 (GFP-H2B) cells
Kc cells
Ube2s
Ube2s/Mad2
Lamin-B
Mad2
Western

Figure S4

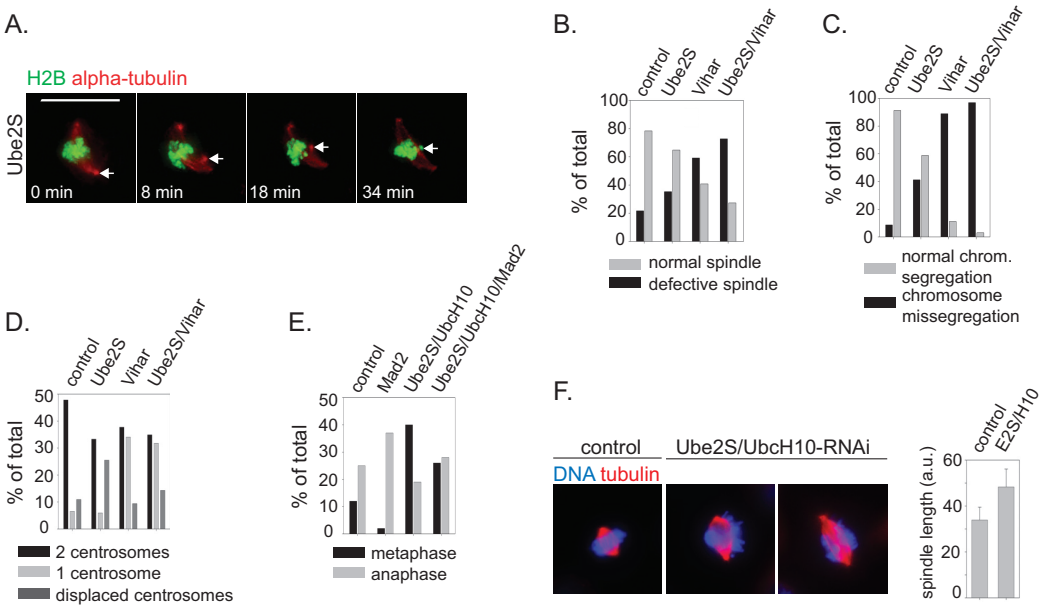
A.
H2B alpha-tubulin
Ube2S
0 min
8 min
18 min
34 min
B.
control
Ube2S
Vihar
Ube2S/Vihar
% of total
normal spindle
defective spindle
C.
normal chrom. segregation
chromosome missegregation
D.
2 centrosomes
1 centrosome
displaced centrosomes
E.
control
Mad2
Ube2S/UbcH10
Ube2S/UbcH10/Mad2
metaphase
anaphase
F.
control
Ube2S/UbcH10-RNAi
DNA tubulin
spindle length (a.u.)
E2S/H10

Figure S5

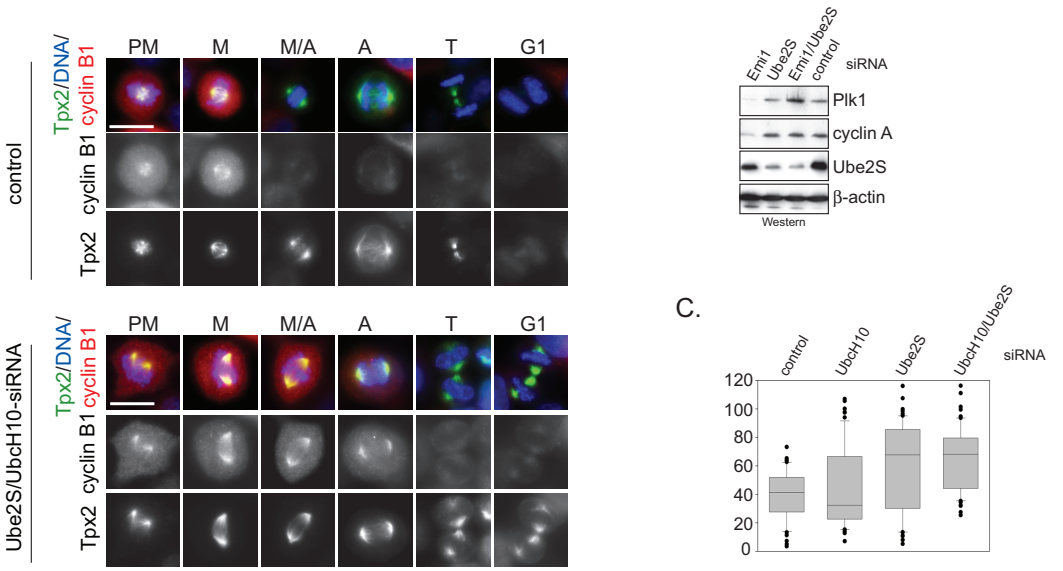
A.
B.
C.
PM
M
M/A
A
T
G1
Tpx2/DNA/cyclin B1
cyclin B1
Tpx2
control
Ube2S/UbcH10-siRNA
Emi1
Ube2S
Emi1/Ube2S
control
siRNA
Plk1
cyclin A
Ube2S
β-actin
Western
UbcH10
UbcH10/Ube2S
120
100
80
60
40
20
0

Figure S6

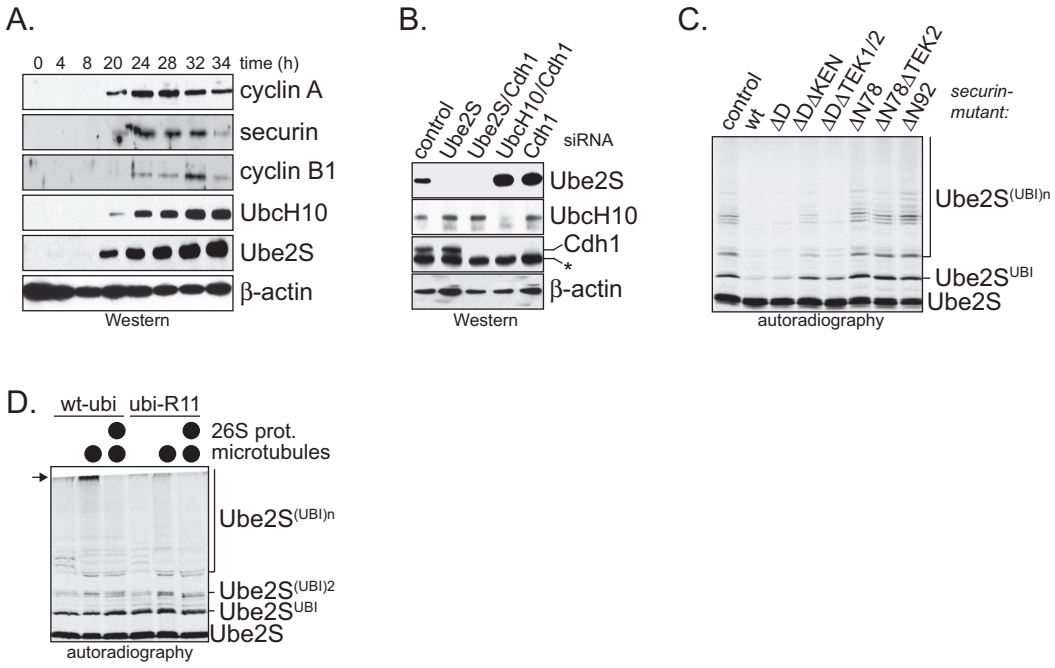
A.
0 4 8 20 24 28 32 34 time (h)
cyclin A
securin
cyclin B1
UbcH10
Ube2S
β-actin
Western
B.
control
Ube2S
Ube2S/Cdh1
UbcH10/Cdh1
Cdh1
siRNA
Ube2S
UbcH10
Cdh1
*
β-actin
Western
C.
control
wt
ΔD
ΔDΔKEN
ΔDΔTEK1/2
ΔN78
ΔN78ΔTEK2
ΔN92
securin-mutant:
Ube2S(UBI)n
Ube2SUBI
Ube2S
autoradiography
D.
wt-ubi
ubi-R11
26S prot.
microtubules
Ube2S(UBI)n
Ube2S(UBI)2
Ube2SUBI
Ube2S
autoradiography

Figure S7

Chapter 5

Conclusions and Outlook

Conclusions

In the Chapters above, I presented our discoveries that 1. The human APC/C forms ubiquitin chains on its substrates linked through K11 on ubiquitin and that K11-linkages are essential for cell division (Chapter 2), 2. Chain initiation is the regulated, rate-limiting step for APC/C substrate degradation and that conserved initiation motifs are essential for efficient attachment of the first ubiquitin to APC/C substrates (Chapter 3), and 3. Ubiquitin chain elongation is accomplished by a dedicated E2 enzyme, Ube2S, that does not itself modify substrate lysine residues but instead cooperates with Ube2C to elongate ubiquitin chains (Chapter 4). Study of the human APC/C as a model E3 has uncovered novel mechanisms to regulate the degradation of its many substrates and has revealed parallels between APC/C-dependent ubiquitylation and other processive reactions.

Current Work

The work presented in my dissertation opened at least as many questions as it answered. Studies from our lab and other groups have been essential in helping to understand the many remaining mysteries of APC/C function and the ubiquitin code.

Development and characterization of a linkage specific antibody has been instrumental for visualizing K11-linked chains during mitosis (Matsumoto et al., 2010). Using Ube2S to make K11-linked ubiquitin dimers, our lab collaborated with Vishva Dixit's group to show that K11-linked ubiquitin chains show a spectacular spike during mitosis, while K48-linkages remain relatively constant. Formation of K11-linked chains was abolished when APC/C was compromised or its E2s were knocked down, showing that APC/C is the major engine of K11-linked chains during division. The linkage specific-antibodies have been instrumental in learning about the ubiquitin code, but only recognize a single ubiquitin-ubiquitin linkage. The next generations of mass spectrometry instrumentation promise "top-down" approaches that will allow us to learn about the fidelity of long ubiquitin chains and hopefully understand not only their dynamics during mitosis, but also in ubiquitylation-related human diseases such as Huntington's disease, where buildup of ubiquitylated proteins has been described (Bennett et al., 2007). The question of "why K11- rather than K48-linkages?" remains an exciting, open, and intensely studied one.

The work on Ube2S reporting its initial discovery and cooperation with APC/C in Chapter 4 has since been greatly expanded upon. Our lab collaborated with John Kuriyan's group to understand the mechanism of K11-specificity of Ube2S using a combination of structural and biochemical approaches to show that Ube2S forms K11-linked chains by a novel and elegant mechanism involving a previously-overlooked non-covalent binding site between E2 and ubiquitin (Wickliffe et al., 2011).

Much has also been learned about the structure of APC/C during my time in the lab. It has been exciting to follow as the resolution of available structures has improved. A high resolution structure of yeast APC/C revealed that substrate binding is coordinated between two subunits, Apc10 and Cdh1, not just on the co-activator as previously thought (da Fonseca et al., 2011), changing our perception of how the APC/C co-

activators Cdh1 and Cdc20 function. There was also a mystery concerning the placement of APC/C degradation motifs - KEN-boxes often occur upstream of D-boxes in APC/C substrates and the directionality of the motifs is important for degradation. Furthermore, KEN-boxes that are important for substrate degradation often have a Pro residue just downstream. Based on a structure of yeast APC/C inhibited by the mitotic checkpoint complex (MCC) we can begin to see why: the KEN-box binds on the top of the co-activator, in this case Cdc20, and if present the Pro kinks the remainder of the degradation motif. The D-box receptor is on the edge of Cdc20, coordinating the substrate with the RING-finger where E2 binds (Chao et al., 2012). This structure also hints as to why the spacing between the D-box and initiation motif might be important, as we reported (Chapter 3; (Williamson et al., 2011)). The D-box receptor allows unstructured regions of the substrate to thread through a channel near the RING-finger of the yeast APC/C, positioning the substrate for efficient ubiquitylation.

It will be fascinating to learn how the human APC/C, structures forthcoming, is both similar and different than yeast APC/C. As yeast do not possess a Ube2S homolog and form K48- rather than K11-linked ubiquin chains (Rodrigo-Brenni and Morgan, 2007), the differences will likely inform models of Ube2S function with the human APC/C.

Opportunities to characterize functions of other ubiquitylation enzymes have come from unexpected places during our research on the human APC/C. In Chapter 4, I presented our finding that depletion of either Ubc2C or Ube2S by siRNA did not produce a strong phenotype in human cultured cells, but simultaneous knockdown of both factors produced a strong mitotic arrest. We expanded the discovery of Ube2C/Ube2S synthetic lethality into a screening platform to discover ubiquitin ligases other than APC/C that are important for cell proliferation. By sensitizing human tissue culture cells using "query" siRNAs that perturb the assembly of the mitotic spindle, strengthen the mitotic checkpoint, or hinder the activity of APC/C, we created sensitized isogenic backgrounds that modeled conditions seen in many tumors. We then interrogated these backgrounds using an siRNA library comprising the human ubiquitin/proteasome system and discovered factors essential in each background. These projects are ongoing.

Discovery and characterization of ubiquitin ligases that are relevant for human disease will be essential: currently the only ubiquitylation-related approved therapies are inhibitors of Nedd8-E1 that activates SCF ubiquitin ligases or inhibitors of the 26S proteasome. Targeting the apex (E1) or outcome of all ubiquitin-dependent protein degradation (26S proteasome) results in pleiotropic side effects. By identifying and understanding the mechanisms of E2s and E3s we will greatly increase the specificity of treatments that result from perturbations of the ubiquitin system. Truly fruitful approaches to drugging the ubiquitylation system will combine the identification of essential factors with a mechanistic understanding of their function.

References

Alexandru, G., Graumann, J., Smith, G.T., Kolawa, N.J., Fang, R., and Deshaies, R.J. (2008). UBXD7 binds multiple ubiquitin ligases and implicates p97 in HIF1alpha turnover. Cell *134*, 804-816.

Amir, R., Ciechanover, A., and Cohen, S. (2001). [The ubiquitin-proteasome system: the relationship between protein degradation and human diseases]. Harefuah *140*, 1172-1176, 1229.

Ang, X.L., and Harper, J.W. (2005). SCF-mediated protein degradation and cell cycle control. Oncogene *24*, 2860-2870.

Baboshina, O.V., and Haas, A.L. (1996). Novel multiubiquitin chain linkages catalyzed by the conjugating enzymes E2EPF and RAD6 are recognized by 26 S proteasome subunit 5. The Journal of biological chemistry *271*, 2823-2831.

Ban, K.H., Torres, J.Z., Miller, J.J., Mikhailov, A., Nachury, M.V., Tung, J.J., Rieder, C.L., and Jackson, P.K. (2007). The END network couples spindle pole assembly to inhibition of the anaphase-promoting complex/cyclosome in early mitosis. Developmental cell *13*, 29-42.

Barford, D. (2011a). Structural insights into anaphase-promoting complex function and mechanism. Philosophical transactions of the Royal Society of London Series B, Biological sciences *366*, 3605-3624.

Barford, D. (2011b). Structure, function and mechanism of the anaphase promoting complex (APC/C). Quarterly reviews of biophysics *44*, 153-190.

Baumgarten, A.J., Felthaus, J., and Wasch, R. (2009). Strong inducible knockdown of APC/CCdc20 does not cause mitotic arrest in human somatic cells. Cell Cycle *8*, 643-646.

Bennett, E.J., Shaler, T.A., Woodman, B., Ryu, K.Y., Zaitseva, T.S., Becker, C.H., Bates, G.P., Schulman, H., and Kopito, R.R. (2007). Global changes to the ubiquitin system in Huntington's disease. Nature *448*, 704-708.

Berlingieri, M.T., Pallante, P., Sboner, A., Barbareschi, M., Bianco, M., Ferraro, A., Mansueto, G., Borbone, E., Guerriero, E., Troncone, G., *et al*. (2007). UbcH10 is overexpressed in malignant breast carcinomas. Eur J Cancer *43*, 2729-2735.

Bernier-Villamor, V., Sampson, D.A., Matunis, M.J., and Lima, C.D. (2002). Structural basis for E2-mediated SUMO conjugation revealed by a complex between ubiquitin-conjugating enzyme Ubc9 and RanGAP1. Cell *108*, 345-356.

Burton, J.L., and Solomon, M.J. (2001). D box and KEN box motifs in budding yeast Hsl1p are required for APC-mediated degradation and direct binding to Cdc20p and Cdh1p. Genes & development *15*, 2381-2395.

Burton, J.L., Tsakraklides, V., and Solomon, M.J. (2005). Assembly of an APC-Cdh1-substrate complex is stimulated by engagement of a destruction box. Molecular cell *18*, 533-542.

Carroll, C.W., and Morgan, D.O. (2002). The Doc1 subunit is a processivity factor for the anaphase-promoting complex. Nature cell biology *4*, 880-887.

Chao, W.C., Kulkarni, K., Zhang, Z., Kong, E.H., and Barford, D. (2012). Structure of the mitotic checkpoint complex. Nature *484*, 208-213.

Christensen, D.E., Brzovic, P.S., and Klevit, R.E. (2007). E2-BRCA1 RING interactions dictate synthesis of mono- or specific polyubiquitin chain linkages. Nature structural & molecular biology *14*, 941-948.

da Fonseca, P.C., Kong, E.H., Zhang, Z., Schreiber, A., Williams, M.A., Morris, E.P., and Barford, D. (2011). Structures of APC/C(Cdh1) with substrates identify Cdh1 and Apc10 as the D-box co-receptor. Nature *470*, 274-278.

Dikic, I., Wakatsuki, S., and Walters, K.J. (2009). Ubiquitin-binding domains - from structures to functions. Nature reviews Molecular cell biology *10*, 659-671.

Dube, P., Herzog, F., Gieffers, C., Sander, B., Riedel, D., Muller, S.A., Engel, A., Peters, J.M., and Stark, H. (2005). Localization of the coactivator Cdh1 and the cullin subunit Apc2 in a cryo-electron microscopy model of vertebrate APC/C. Molecular cell *20*, 867-879.

Dye, B.T., and Schulman, B.A. (2007). Structural mechanisms underlying posttranslational modification by ubiquitin-like proteins. In Annual review of biophysics and biomolecular structure (Palo Alto: Annual Reviews), pp. 131-150.

Eddins, M.J., Carlile, C.M., Gomez, K.M., Pickart, C.M., and Wolberger, C. (2006). Mms2-Ubc13 covalently bound to ubiquitin reveals the structural basis of linkage-specific polyubiquitin chain formation. Nature structural & molecular biology *13*, 915-920.

Eletr, Z.M., Huang, D.T., Duda, D.M., Schulman, B.A., and Kuhlman, B. (2005). E2 conjugating enzymes must disengage from their E1 enzymes before E3-dependent ubiquitin and ubiquitin-like transfer. Nature structural & molecular biology *12*, 933-934.

Finley, D. (2009). Recognition and processing of ubiquitin-protein conjugates by the proteasome. Annual review of biochemistry *78*, 477-513.

Fujita, T., Ikeda, H., Taira, N., Hatoh, S., Naito, M., and Doihara, H. (2009). Overexpression of UbcH10 alternates the cell cycle profile and accelerate the tumor proliferation in colon cancer. BMC cancer *9*, 87.

Garnett, M.J., Mansfeld, J., Godwin, C., Matsusaka, T., Wu, J., Russell, P., Pines, J., and Venkitaraman, A.R. (2009). UBE2S elongates ubiquitin chains on APC/C substrates to promote mitotic exit. Nature cell biology *11*, 1363-1369.

Geley, S., Kramer, E., Gieffers, C., Gannon, J., Peters, J.M., and Hunt, T. (2001). Anaphase-promoting complex/cyclosome-dependent proteolysis of human cyclin A starts at the beginning of mitosis and is not subject to the spindle assembly checkpoint. The Journal of cell biology *153*, 137-148.

Gimenez-Abian, J.F., Diaz-Martinez, L.A., Wirth, K.G., Andrews, C.A., Gimenez-Martin, G., and Clarke, D.J. (2005). Regulated separation of sister centromeres depends on the spindle assembly checkpoint but not on the anaphase promoting complex/cyclosome. Cell Cycle *4*, 1561-1575.

Glotzer, M., Murray, A.W., and Kirschner, M.W. (1991). Cyclin is degraded by the ubiquitin pathway. Nature *349*, 132-138.

Goshima, G., Wollman, R., Goodwin, S.S., Zhang, N., Scholey, J.M., Vale, R.D., and Stuurman, N. (2007). Genes required for mitotic spindle assembly in Drosophila S2 cells. Science *316*, 417-421.

Haglund, K., Sigismund, S., Polo, S., Szymkiewicz, I., Di Fiore, P.P., and Dikic, I. (2003). Multiple monoubiquitination of RTKs is sufficient for their endocytosis and degradation. Nature cell biology *5*, 461-466.

Hartwell, L.H., Culotti, J., Pringle, J.R., and Reid, B.J. (1974). Genetic control of the cell division cycle in yeast. Science *183*, 46-51.

Havens, C.G., and Walter, J.C. (2009). Docking of a specialized PIP Box onto chromatin-bound PCNA creates a degron for the ubiquitin ligase CRL4Cdt2. Molecular cell *35*, 93-104.

Hicke, L., Schubert, H.L., and Hill, C.P. (2005). Ubiquitin-binding domains. Nature reviews Molecular cell biology *6*, 610-621.

Hoege, C., Pfander, B., Moldovan, G.L., Pyrowolakis, G., and Jentsch, S. (2002). RAD6-dependent DNA repair is linked to modification of PCNA by ubiquitin and SUMO. Nature *419*, 135-141.

Hosokawa, M., Takehara, A., Matsuda, K., Eguchi, H., Ohigashi, H., Ishikawa, O., Shinomura, Y., Imai, K., Nakamura, Y., and Nakagawa, H. (2007). Oncogenic role of KIAA0101 interacting with proliferating cell nuclear antigen in pancreatic cancer. Cancer research *67*, 2568-2576.

Huang, D.T., Zhuang, M., Ayrault, O., and Schulman, B.A. (2008). Identification of conjugation specificity determinants unmasks vestigial preference for ubiquitin within the NEDD8 E2. Nature structural & molecular biology *15*, 280-287.

Jin, L., Williamson, A., Banerjee, S., Philipp, I., and Rape, M. (2008). Mechanism of ubiquitin-chain formation by the human anaphase-promoting complex. Cell *133*, 653-665.

Jung, C.R., Hwang, K.S., Yoo, J., Cho, W.K., Kim, J.M., Kim, W.H., and Im, D.S. (2006). E2-EPF UCP targets pVHL for degradation and associates with tumor growth and metastasis. Nature medicine *12*, 809-816.

Kerscher, O., Felberbaum, R., and Hochstrasser, M. (2006). Modification of proteins by ubiquitin and ubiquitin-like proteins. Annual review of cell and developmental biology *22*, 159-180.

Kim, A.H., Puram, S.V., Bilimoria, P.M., Ikeuchi, Y., Keough, S., Wong, M., Rowitch, D., and Bonni, A. (2009). A centrosomal Cdc20-APC pathway controls dendrite morphogenesis in postmitotic neurons. Cell *136*, 322-336.

Kimata, Y., Baxter, J.E., Fry, A.M., and Yamano, H. (2008). A role for the Fizzy/Cdc20 family of proteins in activation of the APC/C distinct from substrate recruitment. Molecular cell *32*, 576-583.

King, R.W., Glotzer, M., and Kirschner, M.W. (1996). Mutagenic analysis of the destruction signal of mitotic cyclins and structural characterization of ubiquitinated intermediates. Molecular biology of the cell *7*, 1343-1357.

Kirkpatrick, D.S., Hathaway, N.A., Hanna, J., Elsasser, S., Rush, J., Finley, D., King, R.W., and Gygi, S.P. (2006). Quantitative analysis of in vitro ubiquitinated cyclin B1 reveals complex chain topology. Nature cell biology *8*, 700-710.

Kittler, R., Putz, G., Pelletier, L., Poser, I., Heninger, A.K., Drechsel, D., Fischer, S., Konstantinova, I., Habermann, B., Grabner, H., *et al*. (2004). An endoribonuclease-prepared siRNA screen in human cells identifies genes essential for cell division. Nature *432*, 1036-1040.

Koegl, M., Hoppe, T., Schlenker, S., Ulrich, H.D., Mayer, T.U., and Jentsch, S. (1999). A novel ubiquitination factor, E4, is involved in multiubiquitin chain assembly. Cell *96*, 635-644.

Komander, D., and Rape, M. (2012). The Ubiquitin Code. Annual review of biochemistry.

Kraft, C., Vodermaier, H.C., Maurer-Stroh, S., Eisenhaber, F., and Peters, J.M. (2005). The WD40 propeller domain of Cdh1 functions as a destruction box receptor for APC/C substrates. Molecular cell *18*, 543-553.

Lasorella, A., Stegmuller, J., Guardavaccaro, D., Liu, G., Carro, M.S., Rothschild, G., de la Torre-Ubieta, L., Pagano, M., Bonni, A., and Iavarone, A. (2006). Degradation of Id2 by the anaphase-promoting complex couples cell cycle exit and axonal growth. Nature *442*, 471-474.

Li, W., Tu, D., Brunger, A.T., and Ye, Y. (2007). A ubiquitin ligase transfers preformed polyubiquitin chains from a conjugating enzyme to a substrate. Nature *446*, 333-337.

Lin, Y., Hwang, W.C., and Basavappa, R. (2002). Structural and functional analysis of the human mitotic-specific ubiquitin-conjugating enzyme, UbcH10. The Journal of biological chemistry *277*, 21913-21921.

Marangos, P., and Carroll, J. (2008). Securin regulates entry into M-phase by modulating the stability of cyclin B. Nature cell biology *10*, 445-451.

Mathe, E., Kraft, C., Giet, R., Deak, P., Peters, J.M., and Glover, D.M. (2004). The E2-C vihar is required for the correct spatiotemporal proteolysis of cyclin B and itself undergoes cyclical degradation. Current biology : CB *14*, 1723-1733.

Matsumoto, M.L., Wickliffe, K.E., Dong, K.C., Yu, C., Bosanac, I., Bustos, D., Phu, L., Kirkpatrick, D.S., Hymowitz, S.G., Rape, M., *et al*. (2010). K11-linked polyubiquitination in cell cycle control revealed by a K11 linkage-specific antibody. Molecular cell *39*, 477-484.

McGarry, T.J., and Kirschner, M.W. (1998). Geminin, an inhibitor of DNA replication, is degraded during mitosis. Cell *93*, 1043-1053.

Meyer, H.J., and Rape, M. (2011). Processive ubiquitin chain formation by the anaphase-promoting complex. Seminars in cell & developmental biology *22*, 544-550.

Mohideen, F., Capili, A.D., Bilimoria, P.M., Yamada, T., Bonni, A., and Lima, C.D. (2009). A molecular basis for phosphorylation-dependent SUMO conjugation by the E2 UBC9. Nature structural & molecular biology *16*, 945-952.

Nijman, S.M., Luna-Vargas, M.P., Velds, A., Brummelkamp, T.R., Dirac, A.M., Sixma, T.K., and Bernards, R. (2005). A genomic and functional inventory of deubiquitinating enzymes. Cell *123*, 773-786.

Peng, J., Schwartz, D., Elias, J.E., Thoreen, C.C., Cheng, D., Marsischky, G., Roelofs, J., Finley, D., and Gygi, S.P. (2003). A proteomics approach to understanding protein ubiquitination. Nat Biotechnol *21*, 921-926.

Peters, J.M. (2006). The anaphase promoting complex/cyclosome: a machine designed to destroy. Nature reviews Molecular cell biology *7*, 644-656.

Petroski, M.D., and Deshaies, R.J. (2005a). Function and regulation of cullin-RING ubiquitin ligases. Nature reviews Molecular cell biology *6*, 9-20.

Petroski, M.D., and Deshaies, R.J. (2005b). Mechanism of lysine 48-linked ubiquitin-chain synthesis by the cullin-RING ubiquitin-ligase complex SCF-Cdc34. Cell *123*, 1107-1120.

Pfleger, C.M., and Kirschner, M.W. (2000). The KEN box: an APC recognition signal distinct from the D box targeted by Cdh1. Genes & development *14*, 655-665.

Pickart, C.M. (2001). Mechanisms underlying ubiquitination. In Annual review of biochemistry, C.C. Richardson, J.N. Abelson, C.R.H. Raetz, and J.W. Thorner, eds. (Annual Reviews {a} , 4139 El Camino Way, Palo Alto, CA, 94303-0139, USA), pp. 503-533.

Pierce, N.W., Kleiger, G., Shan, S.O., and Deshaies, R.J. (2009). Detection of sequential polyubiquitylation on a millisecond timescale. Nature *462*, 615-619.

Rape, M., and Kirschner, M.W. (2004). Autonomous regulation of the anaphase-promoting complex couples mitosis to S-phase entry. Nature *432*, 588-595.

Rape, M., Reddy, S.K., and Kirschner, M.W. (2006). The processivity of multiubiquitination by the APC determines the order of substrate degradation. Cell *124*, 89-103.

Ravid, T., and Hochstrasser, M. (2007). Autoregulation of an E2 enzyme by ubiquitin-chain assembly on its catalytic residue. Nature cell biology *9*, 422-427.

Reddy, S.K., Rape, M., Margansky, W.A., and Kirschner, M.W. (2007). Ubiquitination by the anaphase-promoting complex drives spindle checkpoint inactivation. Nature *446*, 921-925.

Reverter, D., and Lima, C.D. (2004). A basis for SUMO protease specificity provided by analysis of human Senp2 and a Senp2-SUMO complex. Structure *12*, 1519-1531.

Reyes-Turcu, F.E., Ventii, K.H., and Wilkinson, K.D. (2009). Regulation and cellular roles of ubiquitin-specific deubiquitinating enzymes. Annual review of biochemistry *78*, 363-397.

Rodrigo-Brenni, M.C., and Morgan, D.O. (2007). Sequential E2s drive polyubiquitin chain assembly on APC targets. Cell *130*, 127-139.

Sadowski, M., Suryadinata, R., Lai, X., Heierhorst, J., and Sarcevic, B. (2010). Molecular basis for lysine specificity in the yeast ubiquitin-conjugating enzyme Cdc34. Molecular and cellular biology *30*, 2316-2329.

Schulman, B.A., and Harper, J.W. (2009). Ubiquitin-like protein activation by E1 enzymes: the apex for downstream signalling pathways. Nature reviews Molecular cell biology *10*, 319-331.

Somma, M.P., Ceprani, F., Bucciarelli, E., Naim, V., De Arcangelis, V., Piergentili, R., Palena, A., Ciapponi, L., Giansanti, M.G., Pellacani, C., *et al*. (2008). Identification of Drosophila mitotic genes by combining co-expression analysis and RNA interference. PLoS genetics *4*, e1000126.

Sonenberg, N., and Hinnebusch, A.G. (2009). Regulation of translation initiation in eukaryotes: mechanisms and biological targets. Cell *136*, 731-745.

Song, L., and Rape, M. (2010). Regulated degradation of spindle assembly factors by the anaphase-promoting complex. Molecular cell *38*, 369-382.

Stegmeier, F., Rape, M., Draviam, V.M., Nalepa, G., Sowa, M.E., Ang, X.L., McDonald, E.R., 3rd, Li, M.Z., Hannon, G.J., Sorger, P.K., *et al*. (2007). Anaphase initiation is regulated by antagonistic ubiquitination and deubiquitination activities. Nature *446*, 876-881.

Summers, M.K., Pan, B., Mukhyala, K., and Jackson, P.K. (2008). The unique N terminus of the UbcH10 E2 enzyme controls the threshold for APC activation and enhances checkpoint regulation of the APC. Molecular cell *31*, 544-556.

Tang, Z., Li, B., Bharadwaj, R., Zhu, H., Ozkan, E., Hakala, K., Deisenhofer, J., and Yu, H. (2001). APC2 Cullin protein and APC11 RING protein comprise the minimal ubiquitin ligase module of the anaphase-promoting complex. Molecular biology of the cell *12*, 3839-3851.

Tedesco, D., Zhang, J., Trinh, L., Lalehzadeh, G., Meisner, R., Yamaguchi, K.D., Ruderman, D.L., Dinter, H., and Zajchowski, D.A. (2007). The ubiquitin-conjugating enzyme E2-EPF is overexpressed in primary breast cancer and modulates sensitivity to topoisomerase II inhibition. Neoplasia *9*, 601-613.

Thornton, B.R., Ng, T.M., Matyskiela, M.E., Carroll, C.W., Morgan, D.O., and Toczyski, D.P. (2006). An architectural map of the anaphase-promoting complex. Genes & development *20*, 449-460.

Tolbert, B.S., Tajc, S.G., Webb, H., Snyder, J., Nielsen, J.E., Miller, B.L., and Basavappa, R. (2005). The active site cysteine of ubiquitin-conjugating enzymes has a significantly elevated pKa: functional implications. Biochemistry *44*, 16385-16391.

Tugendreich, S., Tomkiel, J., Earnshaw, W., and Hieter, P. (1995). CDC27Hs colocalizes with CDC16Hs to the centrosome and mitotic spindle and is essential for the metaphase to anaphase transition. Cell *81*, 261-268.

Turchi, L., Fareh, M., Aberdam, E., Kitajima, S., Simpson, F., Wicking, C., Aberdam, D., and Virolle, T. (2009). ATF3 and p15PAF are novel gatekeepers of genomic integrity upon UV stress. Cell death and differentiation *16*, 728-737.

Varadan, R., Assfalg, M., Raasi, S., Pickart, C., and Fushman, D. (2005). Structural determinants for selective recognition of a Lys48-linked polyubiquitin chain by a UBA domain. Molecular cell *18*, 687-698.

Verma, R., Chen, S., Feldman, R., Schieltz, D., Yates, J., Dohmen, J., and Deshaies, R.J. (2000). Proteasomal proteomics: identification of nucleotide-sensitive proteasome-interacting proteins by mass spectrometric analysis of affinity-purified proteasomes. Molecular biology of the cell *11*, 3425-3439.

Visintin, R., Prinz, S., and Amon, A. (1997). CDC20 and CDH1: a family of substrate-specific activators of APC-dependent proteolysis. Science *278*, 460-463.

Wagner, K.W., Sapinoso, L.M., El-Rifai, W., Frierson, H.F., Butz, N., Mestan, J., Hofmann, F., Deveraux, Q.L., and Hampton, G.M. (2004). Overexpression, genomic amplification and therapeutic potential of inhibiting the UbcH10 ubiquitin conjugase in human carcinomas of diverse anatomic origin. Oncogene *23*, 6621-6629.

Walker, A., Acquaviva, C., Matsusaka, T., Koop, L., and Pines, J. (2008). UbcH10 has a rate-limiting role in G1 phase but might not act in the spindle checkpoint or as part of an autonomous oscillator. Journal of cell science *121*, 2319-2326.

Wei, W., Ayad, N.G., Wan, Y., Zhang, G.J., Kirschner, M.W., and Kaelin, W.G., Jr. (2004). Degradation of the SCF component Skp2 in cell-cycle phase G1 by the anaphase-promoting complex. Nature *428*, 194-198.

Wickliffe, K.E., Lorenz, S., Wemmer, D.E., Kuriyan, J., and Rape, M. (2011). The mechanism of linkage-specific ubiquitin chain elongation by a single-subunit E2. Cell *144*, 769-781.

Williamson, A., Banerjee, S., Zhu, X., Philipp, I., Iavarone, A.T., and Rape, M. (2011). Regulation of ubiquitin chain initiation to control the timing of substrate degradation. Molecular cell *42*, 744-757.

Williamson, A., Wickliffe, K.E., Mellone, B.G., Song, L., Karpen, G.H., and Rape, M. (2009). Identification of a physiological E2 module for the human anaphase-promoting complex. Proceedings of the National Academy of Sciences of the United States of America *106*, 18213-18218.

Wirth, K.G., Ricci, R., Gimenez-Abian, J.F., Taghybeeglu, S., Kudo, N.R., Jochum, W., Vasseur-Cognet, M., and Nasmyth, K. (2004). Loss of the anaphase-promoting complex in quiescent cells causes unscheduled hepatocyte proliferation. Genes & development *18*, 88-98.

Wojcik, C., Rowicka, M., Kudlicki, A., Nowis, D., McConnell, E., Kujawa, M., and DeMartino, G.N. (2006). Valosin-containing protein (p97) is a regulator of endoplasmic reticulum stress and of the degradation of N-end rule and ubiquitin-fusion degradation pathway substrates in mammalian cells. Molecular biology of the cell *17*, 4606-4618.

Wu, G., Xu, G., Schulman, B.A., Jeffrey, P.D., Harper, J.W., and Pavletich, N.P. (2003). Structure of a beta-TrCP1-Skp1-beta-catenin complex: destruction motif binding and lysine specificity of the SCF(beta-TrCP1) ubiquitin ligase. Molecular cell *11*, 1445-1456.

Wu, T., Merbl, Y., Huo, Y., Gallop, J.L., Tzur, A., and Kirschner, M.W. (2010). UBE2S drives elongation of K11-linked ubiquitin chains by the anaphase-promoting complex. Proceedings of the National Academy of Sciences of the United States of America *107*, 1355-1360.

Xu, P., Duong, D.M., Seyfried, N.T., Cheng, D., Xie, Y., Robert, J., Rush, J., Hochstrasser, M., Finley, D., and Peng, J. (2009). Quantitative proteomics reveals the function of unconventional ubiquitin chains in proteasomal degradation. Cell *137*, 133-145.

Ye, Y., and Rape, M. (2009). Building ubiquitin chains: E2 enzymes at work. Nature reviews Molecular cell biology *10*, 755-764.

Yu, H. (2007). Cdc20: a WD40 activator for a cell cycle degradation machine. Molecular cell *27*, 3-16.

Yu, P., Huang, B., Shen, M., Lau, C., Chan, E., Michel, J., Xiong, Y., Payan, D.G., and Luo, Y. (2001). p15(PAF), a novel PCNA associated factor with increased expression in tumor tissues. Oncogene *20*, 484-489.

Zheng, N., Wang, P., Jeffrey, P.D., and Pavletich, N.P. (2000). Structure of a c-Cbl-UbcH7 complex: RING domain function in ubiquitin-protein ligases. Cell *102*, 533-539.